Title

Paleoecology and Geochemistry of the Upper Kellwasser Black Shale and Extinction Event

Author

Haddad, Emily Elizabeth

Publication Date

2015

UNIVERSITY OF CALIFORNIA
RIVERSIDE

Paleoecology and Geochemistry of the Upper Kellwasser Black Shale and Extinction Event

A Dissertation submitted in partial satisfaction
of the requirements for the degree of

Doctor of Philosophy

in

Geological Sciences

by

Emily Elizabeth Haddad

August 2015

Dissertation Committee:
    Dr. Mary Droser, Chairperson
    Dr. Gordon Love
    Dr. Seth Finnegan

The Dissertation of Emily Elizabeth Haddad is approved:

Committee Chairperson

University of California, Riverside

ACKNOWLEDGMENTS

This doctoral research was supported by an NSF Graduate Research Fellowship and a UCR Graduate Research Mentorship Fellowship, a scholarship from the American Federation of Mineralogical Societies, and grants from the Gulf Coast Section of the Society for Sedimentary Geology, the American Association of Petroleum Geologists, the Paleontological Society, the Society for Sedimentary Geology, and the Geological Society of America. Additional acknowledgment is made to the American Chemical Society Petroleum Research Fund # PRF 50400-UNI8 and National Science Foundation grant NSF-EAR 1348988 for providing funding for this research through my advisors and collaborators. I am deeply indebted to my co-advisors, Mary Droser and Gordon Love, who patiently and expertly directed, supervised, and supported me through this research. I especially thank Diana Boyer and Michael Tuite, my co-authors on the material included herein and Devonian comrades-in-arms, for their expertise, discussions, and encouragement. Fieldwork in western New York was made possible and comfortable through the powerhouse that is Emily Seeger, and by the generosity and hospitality of the Boyers in Oswego and the Seegers in Holland. Immense gratitude to Jeff Over for his invaluable assistance in the field and for his efforts in laying the biostratigraphic groundwork for this dissertation. Assistance with sample preparation and biomarker analyses at UCR came from Rosemarie Bisquera, Carina Lee, Aaron Martinez, James Minor, Mounga Nonu, Megan Rohrssen, and Mark Williams. This research also benefited greatly from the contributions of Mark Riccio at the Cornell Mulitscale CT Facility who prepared the CT scan included in Chapter 1, Anita Pratt and Paul Tomascak

at SUNY Oswego who helped prepare and analyze the trace metals included in Chapters 1 and 3, Sarah de la Rue who provided the Pando X-1 core samples analyzed in Chapter 2, and Timothy Lyons at UCR and Kenneth Williford at NASA JPL who allowed the use of their labs for the generation of some of the following data. Finally, I am grateful to my qualifying and defense committees – Mary, Gordon, Peter Sadler, Nigel Hughes, Michael Allen, and Seth Finnegan – for their constructive criticism, intelligent questions, and helpful advice.

DEDICATION

To Mom and Dad,

for *The Land Before Time,* for *All About Dinosaurs,* for the formative discussions, for the hikes, for the Archosaur anatomy phone calls, for the emotional support, for the financial support, for a lifetime of encouragement, for the nurturing, for the love

and

to my favorite boys, EDH and JBH,

for the sacrifices, for the long commutes, for the late night help, for keeping me sane, for the smiles, for the hugs, for the laughter, for the love.

ABSTRACT OF THE DISSERTATION

Paleoecology and Geochemistry of the Upper Kellwasser Black Shale and Extinction Event

by

Emily Elizabeth Haddad

Doctor of Philosophy, Graduate Program in Geological Sciences
University of California, Riverside, August 2015
Dr. Mary Droser, Chairperson

The deposition of the Upper Kellwasser black shale at the Frasnian-Famennian stage boundary in the Late Devonian coincided with one of the most enigmatic diversity crises and ecological perturbations in the Phanerozoic. Because of the ubiquity of organic-rich sediments deposited in Devonian epeiric seaways, it is commonly assumed that anoxia was the main driver of biological turnover at this time. Little is understood, however, about the actual mechanisms of extrinsically-forced ecological change in the Late Devonian, in part because of an incomplete understanding of the paleoenvironmental conditions of the habitats in which these changes took place. Specifically, the duration and extent of anoxia and euxinia during the deposition of the Upper Kellwasser has not been well-constrained globally. Previous studies have focused on the presence or absence of these conditions, especially in the European type sections, even though it is recognized that organic-rich sediments can capture rapid fluctuations in ocean redox chemistry and that oxygen profiles vary between basins.

Here I present new data integrating trace fossils, lipid biomarkers, trace metals, stable isotopes, and elements which track temporal and spatial changes in the marine redox structure and primary producer assemblages leading up to and through the Upper Kellwasser in the Appalachian Basin, North America and the Madre de Dios Basin, South America. Highly variable dissolved oxygen levels were reconstructed for the Appalachian Basin at an unprecedented high stratigraphic resolution. The ichnological and trace metal data show that environmental perturbation in association with the Frasnian-Famennian extinction event was concurrent with bottom-water oxygen conditions that fluctuated rapidly through suboxia to anoxia preceding and during the deposition of the Upper Kellwasser; lipid biomarker data support this basinal model characterized by neither permanent nor pervasive anoxia and with only sporadic sulfidic conditions in the photic zone. These results challenge the assumption of widespread and persistent anoxia and euxinia at the Frasnian-Famennian boundary. Integrating biomarker parameters with nutrient profiles also facilitated an inter-latitudinal comparison of phytoplanktonic ecology: hopane and sterane ratios suggest eukaryotes, and specifically prasinophytes at high latitudes, thrived during the deposition of the Upper Kellwasser in Laurentia and Gondwana.

Table of Contents

Introduction

Chapter 1: The Last Gasp: Trace Fossils Track De-Oxygenation Leading into the Frasnian-Famennian Extinction Event

Chapter 2: Microbial Ecology of the Late Devonian Frasnian-Famennian Boundary: Comparing the High-Latitude Madre de Dios Basin and the Low-Latitude Appalachian Basin

Chapter 3: Paleoecological Implications of Redox Chemistry During the Upper Kellwasser Event, New York State

Conclusions

List of Figures

List of Tables

INTRODUCTION

The Frasnian-Famennian Biodiversity Crisis

Mass extinction events have fundamentally structured life on Earth, and the unique biotic events during the Late Devonian represented an evolutionary and ecological turning point for marine organisms. The details of the magnitude and duration of diversity loss in the Late Devonian, however, have long proven complicated. Raup and Sepkoski (1982) recognized five Phanerozoic mass extinctions based on abrupt drops in diversity, but singled out the Late Devonian mass extinction as exceptional: the combined series of extinction events in the Givetian, Frasnian, and Famennian display total familial extinction rates above background levels but these extinction rates are not statistically significant because of the protracted duration of the bioevents under consideration (~15 Myr). McGhee (1996) summarized the stratigraphic evidence to date for the time-scale of extinction in the Late Devonian and narrowed the "crisis interval" surrounding the Frasnian-Famennian boundary to ~3.0 Myr. Separating extinction events for various clades by conodont zonation revealed that diversity loss in the Late Devonian occurred as pulsed events, each lasting individually on the order of 10^5 years within the 3.0 Myr span. The most severe pulse in extinction occurred within the *linguiformis* chronozone at the Frasnian-Famennian stage boundary (376.1 +/- 3.6 Ma; Kaufmann, 2006) and was coeval with the global deposition of an organic-rich sedimentary facies known as the Upper Kellwasser.

Many previous investigations have found that, for the Frasnian-Famennian biodiversity crisis, low-latitude and shallow-water marine invertebrates, notably the reef-building stromatoporoids and tabulate and rugose corals, were preferentially depleted. Deep-water cnidarian, poriferan, ammonoid and high-latitude brachiopod species all exhibited differential survival with regards to their shallower and tropical counterparts (McGhee 1996; Oliver and Pedder 1994; Copper 1977). Paleozoic fauna (Sepkoski, 1981) were especially hard hit with respect to their Modern Fauna ecological counterparts. Brachiopods experienced a 75% loss in genera at the Frasnian-Famennian with several major orders disappearing – specifically, the Pentamerida and Atrypida go extinct, with Orthida and Strophomenida suffering major familial losses (Boucot, 1975) – while bivalves, on the other hand, made it through the end-Frasnian extinction comparatively unscathed, losing only two families; Hallam and Miller (1988) assessed the clade to have been relatively unaffected by environmental and ecological perturbations in the Late Devonian. Rode and Lieberman (2004; 2005) determined that geographic range was statistically associated with species survivorship of both brachiopods and bivalves across the Frasnian-Famennian boundary; species with wider geographic ranges (more cosmopolitan) were less susceptible to extinction during the Late Devonian; additionally, invasive species were more likely to survive than non-invasive species. Increased survival advantage was also noted for taxa inhabiting middle-outer platform environments but not for taxa inhabiting open shelf environments (Harnik and Lockwood, 2011). Table 1 details the impact and intraclade selectivity of the Frasnian-Famennian bioevent on the major marine clades.

Table 1. Compilation of marine faunal data with diversity loss and qualitative interclade selectivity information.

Fauna	**Loss in Diversity**	**Intraclade Selectivity**
Foraminiferids	Siliceous families survive, 45% of calcareous families do not (Toomey and Mamet, 1979; Brasier, 1988)	Siliceous vs. calcareous; species w/ advanced septate architectures eliminated
Receptaculitids	Hit hard - presumed total extinction until recently (Nitecki, 1969; Nitecki et al., 2004)	None reported
Stromatoporoids	46% loss in genera at F-F; worse at end-Famennian (Stearn, 1987)	Famennian survivors more primitive, but still reef building
Glass Sponges	None reported	Nonstomatoporoids diversify across F-F, especially in NY (Racki, 1990; Rigby, 1979; Geldsetzer et al., 1993)
Tabulate Corals	80% loss in genera at F-F (Hill, 1981)	Favositids heavily decimated
Rugose Corals	60% loss in genera at F-F (Hill, 1981)	Solitary, nondissepimentate are unaffected at generic level; loss mostly among colonial and large dissepimented forms
Bryozoans	Givetian-Frasnian was a major extinction, but only 3/32 families extinct at F-F (Horowitz and Pachut, 1993; Cuffey and McKinney, 1979)	Solitary forms hardest hit; North American fauna hit worse (Bigey, 1986)
Brachiopods	75% loss in genera; Pentamerida, Atrypida extinct; Orthida and Strophomenida suffer familial loss (Boucot, 1975)	Famennian fauna made of Productellidae, Spiriferida, and Rhynchonellida
Bivalves	2 families: Antipleuridae and Ambonychiidae (Hallam and Miller, 1988)	F-F crisis had negligible effect on bivalves
Gastropods	Only 8 genera extinct at F-F, and only 4 families go extinct in Late Dev (Sepkoski, 1982; McKinney, 1985)	Possibly first invaded fresh/brackish water in Devonian (Dineley, 1984)
Cephalopods	Ammonoids: Only 8 genera survive F-F; Nautiloids: 29/49 genera go extinct (House, 1985; House and Kirchgasser, 1993)	Both ammonoids and nautiloids recover and rapidly rediversify after F-F (Becker et al., 1989; Becker, 1993)
Echinoderms	42% Asterozoan family loss; 32% Crinozoan family loss; (Sepkoski, 1982; McKinney, 1985)	Blastozoa and Echinozoa relatively unaffected
Phyllocarids	68% species loss at F-F; 88% species loss at end-Famennian (McGhee, 1996)	None reported
Trilobites	Steady decline through M and L Devonian, but 42% subfamily loss at end-Frasnian (Alberti, 1979; Briggs et al., 1988)	Scutellidae go extinct; Proetids, brachymetopids, phacopids go extinct in North America but survive in Europe
Ostracodes	Steady decline through M and L Devonian; locally up to 65% species loss at F-F (Casier et al., 1996)	None reported
Conodonts	89% species loss; palmatolepids, ancyrognathids, polygnathids disappear (Aldridge, 1988)	Last of the conodonts with true conoform appartuses disappear
Fishes	Placodermii and Acanthodii: 50% species loss at F-F (Halstead, 1988; Dennison 1978, 1979). Vertebrates experience bottleneck at D-C (Sallan and Coates, 2010)	Agnathan disappearance, but already on decline since the earliest Devonian; Gnathostomes suffer major diversity losses

The ecological significance of the Late Devonian biotic crises was greater even than the End Ordovician extinction event, which by all metrics is still considered one of the great Phanerozoic mass extinctions (Droser et al., 2000; Bambach, 2006). The selective extinction of certain keystone taxa, especially in reefs, resulted in a complete restructuring of many marine ecosystems. The protracted diversity depletion throughout the Devonian Period, and its coincident reef turnover with concentrated losses at the Frasnian-Famennian and the end-Devonian, rival only the End-Permian in severity (Copper, 2002). The Devonian represents a case-in-point that taxonomic severity is only one factor for consideration of the overall impact of extinction. The ecological value of component species in an ecosystem is as important as species diversity in maintaining ecosystem integrity and is therefore an essential metric with which to judge the relative importance of a bioevent (McGhee et al., 2004; McGhee et al., 2013).

The Upper Kellwasser Event

Marine anoxia is widely thought to be an important contributing factor in the Frasnian-Famennian biodiverisity crisis in part because of the pervasiveness of black shale preservation coincident to diversity loss (Joachimski and Buggisch, 1993; Becker and House, 1994; Levman and von Bitter, 2002; Bond et al, 2004); the extinction event is interchangeably referred to as the Kellwasser Event or Crisis (House, 1985; McGhee et al., 1986; Buggisch, 1991) because of the synchronous global deposition of a set of bituminous limestone /black shale beds, associated with the Lower and Upper Kellwasser horizons (first recognized in the Harz Mountains, Germany). The Upper Kellwasser horizon is temporally correlative to the largest drop in diversity at the end-Frasnian, raising the question of a causative mechanism between the low-oxygen conditions which facilitated the deposition of a globally-recognized organic-rich facies and the loss of marine clades at that time. Whether anoxia, or more specifically euxinia (toxic hydrogen sulfide pervading into the water column), can be evoked as a kill mechanism at the Frasnian-Famennian is undetermined, because the duration and extent of marine anoxia during the Upper Kellwasser Event is not well-constrained, but reduced oxygen conditions are generally agreed to be a major environmental characteristic of the Late Devonian period.

“Reduced oxygen conditions,” though useful as a starting point for paleoenvironmental studies, is a crude oversimplification of the environment during the Late Devonian biotic crises. Despite the prevalence of black shales in Devonian-aged deposits, their close association with a well-known extinction, and their economic importance as an abundant hydrocarbon source, they persist in being among the least understood of all sedimentary rock types. While defined as “dark-coloured, fine grained mudrocks having the sedimentological, palaeoecological and geochemical characteristics associated with deposition under oxygen-deficient or oxygen-free bottom waters” (Tyson 1987), there is a growing body of literature suggesting a wide range of possible preservation and/or depositional conditions for black shales, beyond the traditional interpretation of requiring a persistently anoxic water-column (Arthur and Sageman, 1994; Boyer et al., 2011).

Early end-member explanations for the deposition of black shale (i.e. the “preservation” model vs. the “productivity” model) have been displaced in favor of models featuring interdependent roles of sedimentation, primary production, and microbial metabolism (Sageman et al., 2003; Murphy et al., 2000a). There is still much debate over the relative significance of each of these contributors, though these multiple factors appear to have led to an observed diversity in types of black shales. These debates are complicated by seemingly conflicting observations: 1) that most ancient organic-rich deposits appear to have accumulated under low bulk sedimentation rates despite modern data suggesting that organic matter concentration increases with sedimentation, 2) that many epicontinental basin deposits show evidence of intermittent to frequent events of oxygenation even though persistent anoxia would outweigh modulation of concentration by sedimentation effects, and 3) that primary production has frequently been evoked as a control of ancient organic matter burial though this is based on modern observations at continental margins (Sageman et al., 2003). These complications illuminate another major problem: black shale in the Devonian was deposited in epeiric, or epicontinental, seas, an environment for which there is no true modern-day analog (despite continued comparisons to the Black Sea and other silled basins).

Possible Extinction Mechanisms

The most widely cited mechanisms for the Late Devonian extinction are global cooling and anoxia, due to the apparent geographic selectivity in extinction and the ubiquity of preservation of black shale in the rock record (Joachimski and Buggisch, 1993; House, 2002; Bond, et al., 2004). Other potential extinction mechanisms include global warming, rapidly varying climate (irrespective of temperature directionality), reduced habitable space, hypercapnia, and sulfide poisoning (see McGhee, 1996 for an overview of prevailing hypotheses).

Possible trigger scenarios for lethal cooling include glaciation (Caputo, 1985; Caputo and Crowell, 1985; Streel, 1986; Caplan and Bustin, 1999), atmospheric CO_2 drawdown promoted either by the evolution and diversification of land plants (Algeo et al., 1995) or enhanced organic carbon burial (Joachimski et al., 2002), and extraterrestrial impact (McGhee, 1981). There are many proposed environmental triggers for widespread anoxia in the Late Devonian, in more or less complicated scenarios, including marine transgression leading to a shoaling of anoxic bottom waters (Hallam, 1989; Berry and Wilde, 1978; Becker, 1993), increased nutrient delivery to the oceans leading to eutrophication (Johnson et al., 1985; Algeo et al., 1995; Murphy et al., 2000b), enhanced oxygen deficiency as a result of warmer oceans (Joachimski and Buggisch, 1993), oceanic overturn (Wilde and Berry, 1984; 1986), and, again, extraterrestrial impact (Geldsetzer, et al., 1987).

The evidence for global warming is slim, as the world was moving into icehouse conditions at the end of the Devonian, and proponents of a global warming scenario have invoked unspecified “periodic ‘greenhouse’ climatic overheating episodes” (e.g. Becker and House, 1994). Rapid climate change may also result in thermal stress: Fischer and

Arthur (1977) note that the Late Devonian is a period of transition from a hothouse to an icehouse and claim that the highest rate of extinction coincides with the highest rate of climate change; they suggest that rapid climate change, in either direction, and not the extreme environmental conditions resulting from that change, puts the biggest physiological stress on fauna and can result in global ecosystem collapse. Buggisch (1991) proposes a highly oscillatory “autocyclic” climate model driven by organic carbon flux and sea level fluctuations, resulting in detrimental rapid climate perturbation. Sea level fluctuations, specifically regressive cycles due to glaciation, are the invoked trigger mechanisms for a reduction in habitable area on the continental shelves, which would be expected to result in a reduction of marine benthic populations, especially reefs (Johnson, 1974).

Hypercapnia is caused by carbon dioxide toxicity; elevated levels of dissolved CO_2 in the oceans, barring anthropogenic inputs, is most commonly attributed to mass volcanism, the primary suspect for the Permo-Triassic Mass Extinction (Knoll, et al., 2007). The Viluy trap volcanism, a Siberian flood basalt event, has been dated to ~374 Ma, in the Late Devonian (Courtillot, et al., 2010). Finally, euxinic conditions, when hydrogen sulfide is dissolved in the water column, occur in anoxic waters depleted in nitrate via bacterial reduction of sulfate. Sulfide is almost universally toxic to eukaryotes in varying concentrations (Lyons, et al., 2009). The primary trigger mechanisms for euxinia are the same as for anoxia (e.g. stagnation, restriction); however, because euxinia requires specific nutrient conditions (relative concentrations of phosphate, nitrate, and iron; Meyer and Kump, 2008), anoxia does not always lead to euxinic conditions. Euxinia is fairly straightforward to constrain in the rock record through trace metal concentrations and lipid biomarker profiles, however, and euxinic proxies provide evidence for anoxic conditions in the water column when sedimentology and paleontology may only demonstrate oxygen stress in bottom-waters or pore waters.

Scope and Aim of This Research

In this dissertation I will present integrated paleontological and geochemical datasets to provide constraints on ocean chemistry and ecology during the deposition of the Upper Kellwasser black shale in two Devonian epicontinental basins. Chapter 1 closely examines the ichnofabrics, trace fossils, and trace metal content of sediments deposited immediately preceding the Upper Kellwasser in the Appalachian Basin to establish the context of the onset of oxygen stress at the Frasnian-Famennian. Chapter 2 introduces lipid biomarkers as paleoenvironmental and paleoecological proxies, coupled with bulk stable isotopes and nutrient elements, to reconstruct the primary producer assemblages of the Appalachian Basin and the Madre de Dios Basin in a cross-latitudinal study through the Upper Kellwasser. Chapter 3 integrates the methods from the first two chapters to test the assumption of persistent anoxia and pervasive euxinia in the Appalachian Basin during the Upper Kellwasser deposition. Such a multiproxy study examining one basin in fine detail, supplemented by cross-basinal contrast, will provide new insights into the mechanisms of marine diversity crises, ecological turnover, and global environmental perturbation.

CHAPTER 1: THE LAST GASP: TRACE FOSSILS TRACK DE-OXYGENATION LEADING INTO THE FRASNIAN-FAMENNIAN EXTINCTION EVENT

Abstract

The Frasnian-Famennian boundary is correlated with one of several Late Devonian extinction pulses that resulted in a significant decrease in diversity as well as ecological restructuring. This event is recognized within the globally correlated Upper Kellwasser interval that is well-exposed and biostratigraphically well-constrained in shales of western New York State. The ichnological and geochemical signals of the interval stratigraphically below the Upper Kellwasser event at these localities provides insight into the onset of this important extinction event. Detailed analysis of ichnogeneric composition, relative size of burrow populations, amount of bioturbation, and trace metal concentrations vary in concert. Deep-penetrating, pyritized *Skolithos* burrows terminate abruptly at a thin, laminated black shale interval with enriched Mo levels, up to 31 ppm, and are overlain by an interval of gray green bioturbated shales dominated by *Chondrites*. These textural and chemical shifts reveal that bottom water oxygen levels decrease rapidly below the base of the Upper Kellwasser interval. Relative oxygen levels are interpreted to remain low through the *Chondrites* dominated interval, with protracted stressed conditions followed by a gradual decrease to anoxic conditions within the Upper Kellwasser interval. These results suggest that, at least locally in the Appalachian Basin, bottom water oxygen stress and/or fluctuating oxygen conditions were present leading up

to the extinction event. This evidence does not support an instantaneous onset of anoxia as causal mechanism for extinction.

Introduction

The Late Devonian is punctuated by periods of severe diversity reduction correlated with increased extinction rates; the most well-known of these extinction events occurred at the Frasnian-Famennian (F-F) boundary, correlative with the global deposition of the Upper Kellwasser black shale (House, 2002; Bambach et al., 2004; Alroy, 2008). The F-F/Upper Kellwasser depositional event is significant not just in terms of correlative overall faunal diversity loss (Sepkoski, 1986; Jablonski, 1991; McGhee, 1996) but importantly because the resultant community restructuring was ecologically critical (Droser et al., 2000). Despite the distinct impact on marine life, the specific environmental conditions leading up to this event are not well-resolved. While the kill mechanisms implicated in this biotic crisis are still debated, many researchers recognize anoxia as an important environmental factor (Joachimski and Buggisch, 1993; Becker and House, 1994; Levman and von Bitter, 2002; Bond et al., 2004). Outcrop-exposed and biostratigraphically well-constrained black shales that preserve this important interval in western New York State provide the ideal opportunity to examine closely the nature and timing of the onset of oxygen stress that is associated with this extinction event. This study describes in detail the environmental conditions preceding and immediately following the extinction interval, to better resolve the extent to which anoxia contributed to extinction at the F-F boundary.

Details of conditions leading into and out of this event are important to understand better the stimuli for large-scale biotic turnovers. The rate and timing of the onset of environmental stress, rather than just a lack of dissolved oxygen in the water column, may be most significant in the determination of ecological impact on marine communities. Investigations into the dynamics of extinction events in the geologic past are highly applicable for understanding how modern environmental perturbations, in particular eutrophication and other de-oxygenation processes, impact marine ecosystems (e.g. Diaz and Rosenberg, 2008; Vaquer-Sunyer and Duarte, 2008).

Bottom-water oxygen conditions can be well-constrained in the rock record via biological signals preserved as trace fossils (Droser and Bottjer, 1986; Savrda and Bottjer, 1986); burrow size, ichnogeneric diversity, and relative amount of bioturbation have been widely applied to successions throughout the Phanerozoic (Savrda and Bottjer, 1986; Savrda, 1992; Martin, 2004; Rodríguez-Tovar et al., 2009), and specifically in Devonian black shales (Boyer and Droser, 2009, 2011), to successfully infer relative bottom-water oxygen levels and rates of oxygenation and de-oxygenation. Under reduced bottom-water oxygen levels there is a decrease in the diversity, size, and abundance of infaunal organisms, in conjunction with the depth of feeding and residence within the sediment. This biotic response is translated to the rock record as a successive decrease in size of individual burrows and relative amount of bioturbation, in concert with decreasing levels of bottom-water oxygen (Rhoads and Morse, 1971; Thompson et al., 1985; Tyson and Pearson, 1991; Savrda, 1992). Furthermore, the exclusive occurrence of specific ichnogenera, in particular *Chondrites,* has been associated with reduced bottom-water oxygen levels based on their inferred life habits (Bromley, 1996). Because of this sensitivity of marine life to subtle changes in bottom-water chemistry, a detailed understanding of the ichnological signals preserved in the rock record can yield a high precision record of the dynamics of bottom-water oxygen and the onset of anoxia.

Geochemical metrics of depositional redox conditions, in particular trace metal concentrations, provide further support for interpretations of bottom water oxygen levels associated with the Kellwasser interval. Although various trace metals reveal different aspects of depositional redox conditions, Mo is targeted for this study in part because of its utility as an indicator of euxinic and/or persistently anoxic conditions, as enriched values (>100 ppm) are consistent with conditions in which sulfide is concentrated in bottom waters (Arthur and Sageman, 1994; Wignall, 1994; Rimmer, 2004; Scott and Lyons, 2012). Further, slightly enriched values (~2-30 ppm) have been recognized under dysoxic or intermittently euxinic conditions (McManus et al., 2006, Murphy et al., 2000; Lyons et al., 2009). This study uses combined ichnological and geochemical methods to reconstruct bottom water oxygen conditions of the interval immediately preceding the deposition of the Upper Kellwasser black shale, leading into the significant biotic crisis at the F-F boundary.

Geologic Setting

During the Devonian, the Appalachian Basin was a foreland basin associated with the Acadian Orogeny. Strata in western New York State preserve the distal expression of the westward-thinning package of primarily clastic sediment that was sourced from the Acadian Highlands to the east. The latest *linguiformis* Zone and correlative F-F boundary have been well-constrained in these areas (Over, 1997; 2002). Based on these studies, a black shale interval of the Hanover Formation of the Java Group that is well-exposed and easily recognized in western New York has been identified as the Point Gratiot Bed (Over et al., 2013) and represents the Upper Kellwasser equivalent. The three localities investigated for this study include Eighteenmile Creek along New Oregon Road in Eden (N42 37.530, W78 50.289), Irish Gulf along Boston State Road in North Boston (N42 40.651, W78 44.647), and Walnut Creek along County Route 86 in Silver Creek (N42 36.446, W78 30.196) (Fig. 1). The Hanover Formation is exposed at these localities and is comprised of over 35 meters of alternating gray-green mudstones and laminated black shales with nodular carbonate beds, which has been interpreted as an overall shallowing-upward succession, with the black shales representing periodic deepening events (Over, 2002).

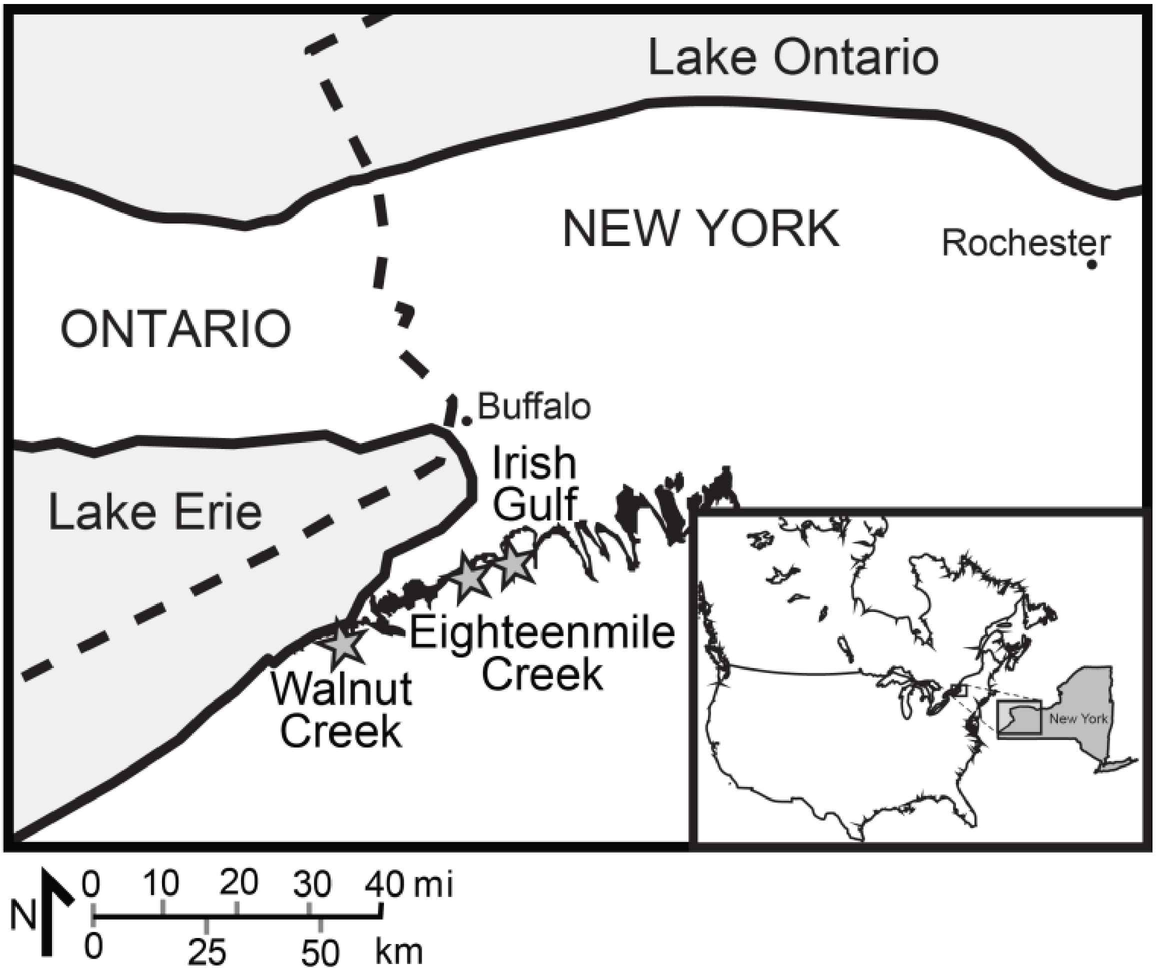

Figure 1. Locality map of the three field localities in western New York State. The dark-shaded area, after Pepper and de Witt (1950), tracks the undifferentiated Hanover Shale and Wiscoy Sandstone in New York, inclusive of the Upper Kellwasser-equivalent black shale unit examined here.

Methods

Samples were collected from approximately 30 cm below, through the black shale of the Upper Kellwasser interval, and 15 cm into the overlying gray silty-mudstone at each locality. Hand samples were cut perpendicular to bedding and polished to reveal ichnofabric, and bedding plane exposures were studied both in the field as exposed in creek beds and in the laboratory. Individual burrows were measured for width, depth of penetration when horizon of origination was exposed, and identified to the ichnogenus when possible. A transitional gray-black shale sample was analyzed at the Cornell Imaging Multiscale CT Facility to capture the three-dimensional aspect of the burrows that is lost through sectioning or bedding plane views. The pyritized preservation of burrows allowed for excellent contrast for this imaging method.

Samples from each of the primary sampled intervals were powdered for whole rock trace metal analysis using the ICP-MS at the Interdisciplinary Elemental Measurement Facility at SUNY Oswego. Measured values fell consistently within 10% of the value of duplicate samples and standards**.** In this study, Mo concentrations are evaluated because detailed studies in modern and ancient settings have identified ranges of values diagnostic of euxinic (persistent and fluctuating), anoxic, dysoxic and oxic depositional conditions (Arthur and Sageman, 1994; Wignall, 1994; Rimmer, 2004; McManus et al., 2006; Scott and Lyons, 2012) and this particular redox proxy has been successfully used in combination with paleontological proxies in other studies (see Boyer et al., 2011).

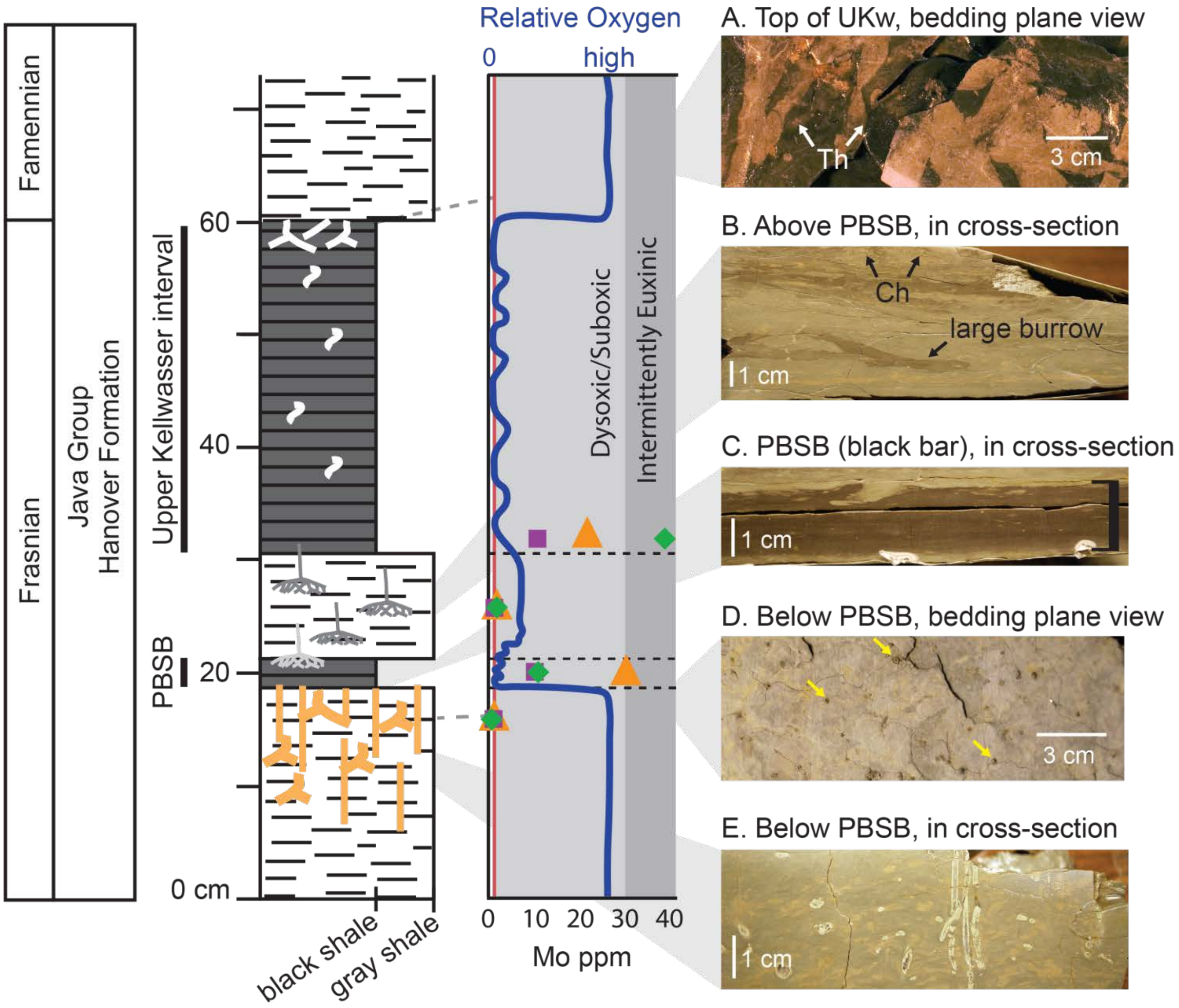
Famennian
Frasnian
Java Group
Hanover Formation
Upper Kellwasser interval
PBSB
60
40
20
0 cm
black shale
gray shale
Relative Oxygen
0
high
Dysoxic/Suboxic
Intermittently Euxinic
0
10
20
30
40
Mo ppm
A. Top of UKw, bedding plane view
Th
3 cm
B. Above PBSB, in cross-section
Ch
large burrow
1 cm
C. PBSB (black bar), in cross-section
1 cm
D. Below PBSB, bedding plane view
3 cm
E. Below PBSB, in cross-section
1 cm

Figure 2. A schematic section showing, from left to right, a composite representation of the generalized stratigraphy, lithology, inferred relative oxygen levels from the three sampled localities (blue line), and Mo values for each stratigraphic horizon at each locality. Red line = average crustal value (ppm Mo). A) Top of Upper Kellwasser, bedding-plane view. *Th* = *Thalassinoides*. B) Above precursor black shale bed (PBSB), in cross section. *Ch* = *Chondrites*. C) PBSB, indicated by black bar, in cross section. D) Below PBSB, bedding-plane view. *Skolithos*-type burrows indicated by arrows. E) Below PBSB, in cross section.

Table 2. Summary of trace fossil and trace metal data. PBSB = precursor black shale boundary; N = number of burrows measured to obtain averages.

	Burrow data				Mo values (ppm)		
Horizon	Max. depth (cm)	Avg. width (mm)	N	Dominant ichnotaxa	Walnut Creek	18 Mile Creek	Irish Gulf
Kellwasser	0.3	N.A.	4	No dominant form	21	9	37
Above PBSB	4	1.47	131	*Chondrites*	3	2	3
PBSB	0.5	1.04	18	No dominant form	31	8	9.5
Below PBSB	>8	1.64	1012	*Skolithos*	2	2	1

Results

The stratigraphic expression and trace fossil signals at all three localities are consistent and varied within only several cm thickness over the approximately 40 km of the study area. Below the distinctive Upper Kellwasser black shale bed at these localities is an interval of bioturbated gray-green shale that is punctuated by a thin (2-3 cm) black shale bed noted as the precursor black shale bed (PBSB; Fig. 2). Based on the measurement and characterization of over 1300 distinct burrows and the overall ichnofabric through these intervals, it is recognized that the PBSB divides strata with two distinct ichnological signals. Table 2 presents burrow data, including maximum depth in cm and the burrow width that is averaged among the three localities for each stratigraphic horizon.

Conspicuous in the beds below the PBSB are abundant pyritized burrows within fully bioturbated mudstones. Vertical *Skolithos*-type burrows are dominant and very abundant, comprising more than 96% of the distinct measurable burrows, with an average burrow density of 45 burrows per 100 cm^2 (Fig. 2D); *Planolites*, *Thalassinoides* and *Chondrites* are also present in this interval but in much lower relative abundance. The *Skolithos*-type burrows were preferentially pyritized, while the other ichnogenera were rarely pyritized. The burrows below the PBSB, dominantly the *Skolithos*-type as other ichnotaxa were difficult to definitively distinguish through this interval, have diameters ranging from 0.4-5.3 mm, with over 99% less than 3.0 mm in diameter, and penetrate up to at least 8 cm in depth. Many of these burrows are sub-vertical or have a horizontal component so their maximum depth is often obscured or not sampled in entirety. The average burrow width through this interval is 1.64 mm (Table 2). Evidence of infaunal activity, including the abundant pyritized vertical burrows, terminates abruptly at the precursor black shale bed as seen clearly from CT images of this boundary; there is no evidence of microscouring at the boundary between the pyritized burrow interval and the PBSB, and no pyritic lags that are commonly associated with sediment starved horizons are observed (Fig. 3). Although pyritized burrows are abundant and densely concentrated just below the PBSB, they decrease in abundance moving progressively down section until they are rare at just 10-12 cm below the PBSB.

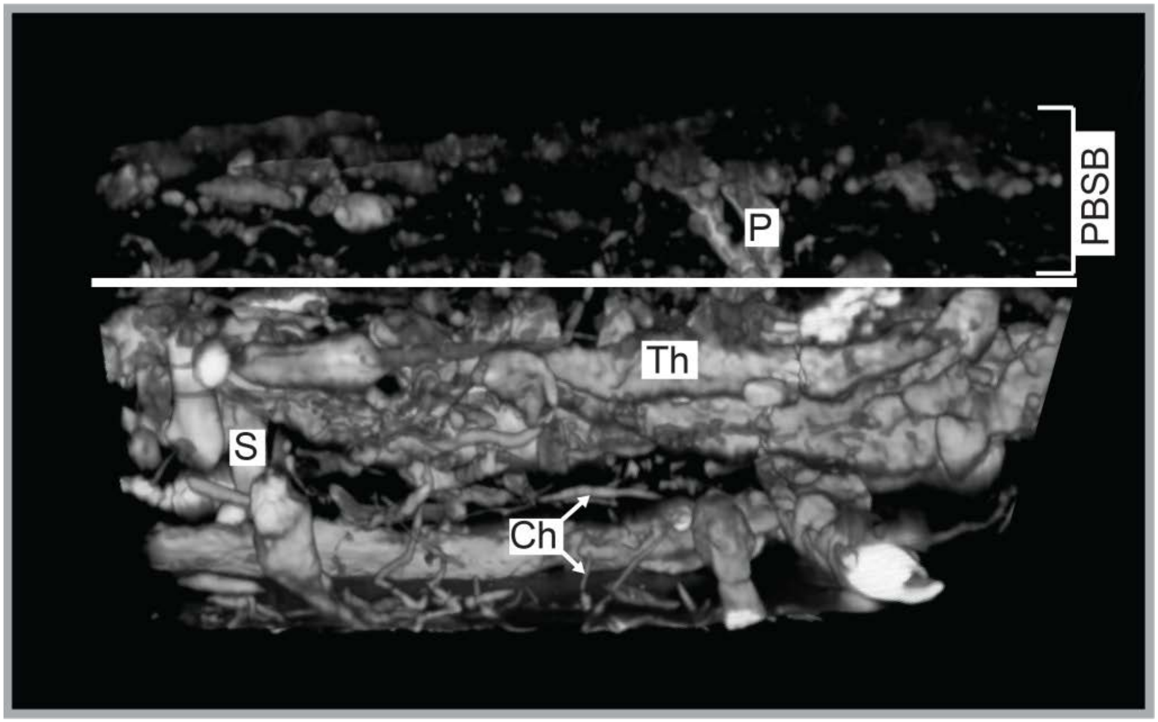

Figure 3. CT scan of interval leading up to the PBSB showing numerous pyritized infilled burrow structures and the dramatic termination of burrows at this boundary. Heavy white line = base of the PBSB. P = Planolites, S = Skolithos, Th = Thalassinoides, and Ch = Chondrites. Field of view is 2.9 cm across.

The thin PBSB is laterally persistent through these localities and preserves thin silt laminations. There is an increase in bioturbation through this interval as breaks in lamination and *Chondrites* are recognized penetrating the black shale and are infilled with lighter colored muds from the overlying sediment (Fig 2C). Burrows are small, consistently less than 0.5 cm in depth and 0.5-2 mm in width, although discrete burrows are rare (Table 2).

The gray shale overlying the PBSB is completely bioturbated and contains rare pyritized burrows. *Chondrites* are more commonly preserved here than in the interval below the PBSB and generally appear as clusters of round to ovate spots and branches that are infilled with lighter colored sediment than the matrix (Fig. 2B). Unlike the interval below the PBSB, *Chondrites* are conspicuous and are therefore the most abundant burrow measured through this interval. Burrow widths are on average 1.47 mm, and large burrows, greater than 0.5 cm in burrow width or penetration depth, are rare through this interval (Table 2). One individual burrow that reached nearly 4 cm in depth was recognized; however, most of the burrows penetrate less than 1 cm in depth. One of the largest preserved burrows in this interval is shown in Figure 2B. There is a gradual lithologic change over less than 10 cm leading into the Upper Kellwasser-equivalent black shale and a corresponding decrease in bioturbation until laminated black shales with punctuated intervals of small and uncommon infaunal activity is preserved.

Through the approximately 20-30 cm of persistent black shale interpreted to be the Upper Kellwasser interval, laminations are common; however, small distinct burrows, likely *Planolites*, and breaks in lamination consistent with biological activity are recognized periodically at these localities. No burrows greater than 2 mm wide and 3 mm in burrow depth were observed. Average burrow width was not calculated through this interval because of the scarcity of burrows.

At the top of the Upper Kellwasser black shale, large *Thalassinoides* burrows >1 cm in burrow width and penetrating up to 5 cm below the overlying gray shale are present at all localities (Fig. 2A). These burrows are infilled with gray mud and are interpreted to originate from the horizon marked by the lithologic shift.

Mo values below the PBSB are of crustal value (1-2 ppm) at all localities (Table 2; Fig. 2). Mo concentrations within the PBSB are consistently enriched, ranging from 8 to 31 ppm across the localities. In the gray shales above the PBSB, Mo values are near crustal values (2-3 ppm). Mo values for the Upper Kellwasser black shale were taken from the base of the interval and range from 9 to 37 ppm.

Discussion

Three distinct ichnofabrics were identified in the interval leading into the Upper Kellwasser black shale: (1) a pyritized, deeply-penetrating *Skolithos*-dominated assemblage in the well-bioturbated gray-green shale below the PBSB; (2) a laminated to weakly-bioturbated ichnofabric in the PBSB; (3) a shallow *Chondrites*-dominated assemblage in the gray-green shale above the PBSB. The fully bioturbated interval below the PBSB, containing abundant pyritized burrows that commonly penetrate several cm into the sediment, is interpreted to represent fully oxygenated conditions (Fig. 2D). A transition from fully oxic to anoxic bottom-water conditions is inferred at the base of the PBSB from the abundant pyritized vertical burrows that terminate abruptly at the base of the laminated black shale, as clearly depicted in the movie of CT scanned images through this interval. The ability to rotate and view these images in a 3D profile allows for a clear depiction of the abrupt boundary between bioturbated and laminated sediments. Although this type of relationship could represent an erosional contact, there is no evidence for scouring at this boundary, and, further, the concentration of pyritized burrows restricted just below the boundary is inconsistent with the contact surface being a purely erosional feature. More likely, this boundary preserves a shift in bottom water chemistry to anoxic conditions that was very rapid; this rapid shift is indicated by the preferential pyritization of the organic matter within *Skolithos*-type burrows and *Thalassinoides* that have a vertical component, as these burrows are expected to have been open at the sediment water interface and the overlying water column.

The PBSB Mo values are enriched when compared with Mo values for the surrounding intervals, but concentrations of 8-31 ppm are lower than those commonly found in anoxic sediments and well below those interpreted to be euxinic (see Scott and Lyons, 2012), and, collected independently of ichnological data, these Mo values might not be interpreted to represent deposition under anoxic bottom waters. The preservation of laminated sediments, however, provides robust evidence for anoxia within this interval. Within and above the PBSB, bottom-water oxygen conditions are interpreted to slowly increase based on breaks in lamination from shallow infaunal activity, followed up-section by the appearance of *Chondrites,* and then a fully bioturbated or mottled ichnofabric moving up-section from the base of the laminated black shale interval (Fig. 2B,C). The fully bioturbated texture through the interval above the PBSB, however, is interpreted to represent persistent or fluctuating dysoxic conditions rather than fully oxygenated conditions, as supported by the lack of ichnogeneric diversity, smaller size of burrows, and abundance of *Chondrites*. Rare larger burrows suggest that there may have been short-lived intervals of relatively higher bottom-water oxygen levels, consistent with fluctuating conditions. What is significant through this interval is the much shallower depth of burrow penetration (<0.5cm) compared to the interval below the PBSB (>6cm). This likely indicates a redox boundary that is relatively shallow in the sediment and is consistent with bottom-water oxygen stress. The presence of common, well-preserved *Chondrites* is not consistent with a soupy, softground substrate to account for the absence of larger, well-defined burrows. This interpretation is consistent with the trace metal data whereas Mo values are crustal to slightly enriched, which is congruous with fluctuating conditions under dysoxic bottom waters in modern environments (Crusius et al, 1996; Turgeon and Brumsack, 2006).

The large *Thalassinoides* that pipe down into the Point Gratiot Bed (Upper Kellwasser) at these localities supports a rapid recovery of larger infaunal organisms and a return to fully oxic conditions following the Upper Kellwasser Event. This is in contrast to the sampled black-gray shale intervals stratigraphically below this that are interpreted to preserve continued oxygen stress. Further, this is interpreted to represent a rapid recovery from oxygen stress linked with significant biotic turnover that can provide some insight into the recovery from this bioevent.

This study reports a rapid de-oxygenation event at the PBSB, below what is traditionally interpreted as the Upper Kellwasser anoxic interval. Following this de-oxygenation event, oxygen levels increased, but do not appear to have returned to fully oxygenated conditions. This is an important distinction as fully bioturbated ichnological signals are often interpreted as oxic, but the change in the ichnogeneric diversity and characteristics and size of burrows supports that conditions were stressed, excluding larger burrowing organisms with higher oxygen demands, but not low enough to exclude smaller organisms capable of fully reworking the sediment. Leading directly into the Upper Kellwasser black shale interval, oxygen levels are interpreted to decrease gradually before a long period of persistent oxygen stress, but not persistent anoxia, through this interval. The ichnological signal supports a rapid shift to oxygenated conditions leading out of this interval as indicated by the appearance of large *Thalassinoides*, typical of fully oxygenated conditions.

The ichnological and trace metal data record environmental perturbation in association with an extinction event that was concurrent with neither a slow and continuous reduction in bottom-water oxygen conditions nor an abrupt shift from oxygenated bottom-waters to persistent anoxia leading up to and through this event. Based on the findings from this study, we favor a causal explanation citing long-term environmental perturbation, rather than a geologically instantaneous mechanism, as the driver for the ecological turnover of the F-F extinction at these localities. Other studies through this interval in Europe and Northern Africa record abrupt lithologic shifts that could be interpreted to represent rapid environmental shifts into the base of the Upper Kellwasser interval (Gereke and Schindler, 2012). This is in contrast to the gradual shifts in ichnological and lithological variation seen in these intervals. Previous workers have investigated the role that sea-level change may have had on controlling bottom-water oxygen levels in this broad epeiric sea setting. Bond and Wignall (2008) summarize evidence for transgression and associated anoxia, but the results from this study supports the hypothesis that any sea-level change in the Appalachian Basin was dynamic and likely not a single-flooding event, evidenced in part by numerous black shale depositional events preceding the deposition of the Point Gratiot Bed. As such, it is probable that a series of repeated flooding events of increasing duration resulting in continuous, if not variable, oxygen stress on bottom-water communities, caused the crossing of a biotic threshold, and ultimately resulted in significant diversity loss and ecological turnover. It is significant to note that two successive black shale intervals, the PBSB and the Upper Kellwasser in this study, with similar ichnological and geochemical signals produced in differing thicknesses of sediments, implying differing durations of deposition, recorded environmental conditions with potentially very different impacts on the biota, indicating that tempo is as important as type of environmental perturbation in determining ecological consequences.

CHAPTER 2: MICROBIAL ECOLOGY OF THE LATE DEVONIAN FRASNIAN-FAMENNIAN BOUNDARY: COMPARING THE HIGH-LATITUDE MADRE DE DIOS BASIN AND THE LOW-LATITUDE APPALACHIAN BASIN

Abstract

The pervasiveness of black shale preservation in association with Late Devonian biocrises suggests anoxia played a major role in concurrent ecological perturbations; however, Devonian black shale deposition is still mechanistically poorly-understood, especially on a global scale. This study characterizes the bitumen of Upper Kellwasser equivalent black shales from two foreland basins, the low paleolatitude Appalachian Basin (New York State) and the high paleolatitude Madre de Dios Basin (Bolivia), in order to better understand global environmental conditions during this depositional event. Lipid biomarkers and elemental and stable isotope ratios at high stratigraphic resolution identify non-fossilized primary producers, help constrain changes in relative oxygen levels, and reconstruct biogeochemical cycling in these basins. Hopane/sterane ratio patterns indicate uniformly high eukaryotic contribution to organic matter deposition in both basins, though sterane ratio patterns differ, suggesting the basins contained distinct paleocommunities of primary producers and possibly dissimilar nutrient cycles. All samples contain only very low amounts of aryl isoprenoids, up to several orders of magnitude lower than concentrations reported from other Phanerozoic euxinic basins; these data are consistent with a paleoredox model lacking a persistently shallow sulfidic zone and demonstrate that temporally persistent or spatially pervasive photic zone

euxinia is not associated with all black shale depositional events in the Late Devonian. Importantly, the disparity in paleoecological and redox signals between the two basins highlights the caution that must be employed when extrapolating environmental conditions of one basin to global ocean models.

Introduction

Organic rich sediments preserve exceptional fossil deposits, are abundant hydrocarbon sources, commonly correlate with extinction events throughout the Phanerozoic, and are therefore of central interest to many paleoenvironmental studies (recently: Lenniger et al., 2014; Luo et al., 2015; Rivera et al., 2015; van Helmond et al., 2015); the depositional processes of black shales, however, are among the most poorly understood of any sedimentary depositional process (Tyson and Pearson, 1991; Harris, 2005; Tyson, 2005). The Late Devonian is particularly renowned for its global abundance of organic rich sedimentary facies that are associated with biotic events of varying magnitudes (House, 2002). Reconstructing these depositional environments is of particular value and interest to black shale research: unique continental configurations, with much of the continental masses concentrated near the equator (Golonka et al., 1994), coupled with high sea level stands and active orogenesis (notably the Acadian and Antler orogenies of Laurentia; Averbuch et al., 2005), created the ideal conditions for massive epeiric seaways, the loci for organic carbon burial. These global black shale depositional events characteristically occur in association with elevated extinction rates in marine fauna; the bioevent at the Frasnian/Famennian stage boundary, the Kellwasser Event (Buggisch, 1991; House, 2002), correlative with the deposition of the Upper Kellwasser bituminous limestone in Europe and organic rich facies globally, has been recognized as a mass extinction event (Raup and Sepkoski, 1982; McGhee, 1996; Bambach et al., 2004). Furthermore, recent research on the patterns of extinction and origination and marine ecological restructuring coincident to black shale deposition in the Late Devonian suggest that the fundamental processes driving diversity loss differed fundamentally from those mechanisms forcing mass extinction events in the End-Ordovician, End-Permian, and End-Cretaceous: specifically, the ubiquitous black shale deposition during the Devonian is indicative of significant, unique environmental processes concurrent to the pulses of diversity depletion (Droser et al., 2000; Bambach, 2006; Alroy, 2008).

Because black shale facies are widely characterized as dysoxic or anoxic, Devonian studies have traditionally invoked spatially pervasive and temporally persistent marine anoxia as the likely mechanism for these biological perturbations (Joachimski and Buggisch, 1993; Becker and House, 1994; Levman and von Bitter, 2002; Joachimski et al., 2001; Bond et al., 2004). There is a growing body of literature, however, suggesting a wide range of possible preservation and/or depositional conditions for black shales beyond the traditional interpretation of requiring a persistently anoxic water-column (Arthur and Sageman, 1994; Murphy et al., 2000a; Boyer and Droser, 2011; Boyer et al., 2011; Rivera et al., 2015); indeed, the organic matter composing organic rich facies can be sourced from myriad organisms comprising a variety of ecologies (e.g. Luo et al., 2015). To better understand the diversity of environments in which black shales can be deposited and reconstruct the settings for Devonian ecological perturbations, this study examines the microbial ecology and, to a lesser extent, the oxygen chemistry of two Late Devonian basins preserving end-Frasnian black shale.

Lipid biomarkers can yield valuable information pertaining to the biological origins of source organisms (particularly the assemblages of microbial aquatic primary producers which generally account for a high proportion of the biomarker signals), the thermal maturity of the host organic matter, and the paleoenvironmental conditions (of redox, salinity, etc.) in the water column. The most useful biomarker molecules are those that are thermodynamically-stable, with a limited number of well-defined biological sources and which are relatively straightforward to analyze. Certain lipid compound classes fit all these criteria, and polycyclic terpenoids or highly branched hydrocarbon skeletons, such as hopanoids or steroids, are extremely resistant to degradation and may survive hundreds of millions of years of burial in sedimentary rocks and in their petroleum products.

This study focuses on the proportional relationship of hopanol-synthesizing organisms to sterol-synthesizing organisms in the Late Devonian basins, via their hopane and sterane biomarkers; we are particularly interested in parsing out the various eukaryotic sources of steranes. Schwark and Empt's 2006 biomarker study on both oils and rocks focused on temporal changes in the main eukaryotic primary producers by tracking the C_{28}/C_{29} sterane ratio through the Phanerozoic; following the classic paper by Grantham and Wakefield (1988) who observed a systematic increase in the C_{28}/C_{29} sterane ratio in oils throughout this time period. C_{29} steroids are preferentially produced by green algal clades, which were the major eukaryotic producers in the Paleozoic era, while C_{27} and C_{28} compounds are produced as the main steroids by more-derived algal clades synthesizing chlorophyll a + c that radiated in the oceans after the Permo-Triassic boundary (dinoflagellates and coccolithophores initially, followed much later in the Cretaceous by diatoms; Kodner et al., 2008). Schwark and Empt (2006) found a similar progressive trend through the Phanerozoic as Grantham and Wakefield (1988) but noted C_{28}/C_{29} sterane ratio excursions at Paleozoic extinction events. They identified a persistent shift in sterane compositions after the Hangenberg Devonian/Carboniferous boundary event, represented by a stepwise increase in C_{28}/C_{29} sterane ratios. An important impetus for this study is the possibility that this pivotal turnover in the phytoplanktonic assemblage may have been triggered by the unique accumulation of extinction events in the Late Devonian. The transient spike in C_{28}/C_{29}, however, which Schwark and Empt (2006) observed at the Frasnian/Famennian boundary event, is attributed not to the secular trend towards chlorophyll a + c synthesizing phytoplankton but instead to an increase in the proportion of prasinophytes to total eukaryotic input, because Prasinophyceae is the only class of green algae known to produce abundant C_{28} sterols (Kodner et al., 2008).

We also measured elemental and stable isotope ratios, including C, N, and P, because microorganisms, like the eukaryotic assemblage highlighted by the sterane distributions in the organic matter, are the primary mediators of biogeochemical processes, and the relative abundances of eukaryotes and prokaryotes may drive disruptions to ecosystem functions linked to extinction events. For example, nitrogen cycling will differ significantly in an environment dominated by diazotrophic prokaryotes rather than algal eukaryotes with important implications for primary production, trophic web dynamics, and organic matter preservation.

Secondarily, we investigate the presence and extent of photic zone euxinia in the Late Devonian basins. The aromatic cartenoid pigment molecule produced by green sulfur bacteria Chlorobi, isorenierantene, is well-preserved in sediments as the molecular fossil isorenieratane and its diagenetic fragments, aryl isoprenoids (Summons and Powell, 1986). These molecules indicate that free hydrogen sulfide was present at least episodically up into the photic zone of the water column (Summons and Powell, 1987) during deposition of these strata because Chlorobi are strictly anaerobic, obligate phototrophs using mainly H_2S as an electron donor for photosynthesis. As such, isorenieratane and aryl isoprenoids are considered robust markers for recognizing periods of photic zone euxinia (PZE). Previous biomarker studies at the Frasnian-Famennian boundary have found near-global evidence for photic zone euxinia in epeiric basins at sub-tropical to tropical latitudes (in Europe, western Canada, Australia, and North America; Brown and Kenig 2004). Joachimski et al. (2001) and Marynowski et al. (2011) found Chlorobi biomarkers in all samples across the F/F boundary and into the early Famennian in the Kowala quarry of the Holy Cross Mountains, Poland, including isorenieratane and a series of C_{13}–C_{22} aryl isoprenoids with a 2,3,6-trimethyl substitution pattern on the aromatic ring (Summons and Powell 1986). Brown and Kenig (2004) expanded the scope of Devonian biomarker investigations of low-latitude epeiric seas to the Laurentian Michigan and Illinois Basins; like Joachimski et al. (2001) and Marynowski et al. (2011), Brown and Kenig (2004) found aromatic carotenoid biomarkers for green sulfur bacteria in every analyzed sample of Middle Devonian-Early Mississippian black and green/grey shale, despite explicit signs of bioturbation in the latter samples.

Material and Methods

Geological and sedimentological setting

This study characterizes depositional conditions of black shale deposits from the low-latitude Appalachian Basin of Laurentian (present-day New York State) and the high-latitude Madre de Dios Basin of Godwana (present-day Bolivia). During the Late Devonian, the Appalachian Basin was situated in the sub-tropics (approximately 30^{o}S latitude), while the Madre de Dios Basin was at approximately 60^{o}S latitude (Scotese and McKerrow, 1990; Figure 4), making a comparison between these two basins useful for insights into potential latitudinal effects on depositional environments.

During the Devonian, the Appalachian Basin was a foreland basin associated with the Acadian Orogeny; today, it contains numerous localities with well-exposed, continuous successions that are biostratigraphically well-constrained and paleontologically well-characterized (Thayer, 1974; Woodrow and Isley, 1983; Kirchgasser et al., 1988; Brett et al., 1991; Baird et al., 1999; Sageman et al., 2003). Strata in western New York State preserve the distal expression of the westward thinning package of primarily clastic sediment that was sourced from the Acadian highlands to the west. A thin black shale interval, the Point Gratiot Bed, contained within the Hanover Formation of the Java Group has been identified to correlate with the global Upper Kellwasser Event (Over, 1997, 2002; Over et al., 2013). The Frasnian-Famennian boundary, defined by the contact of the Upper *linguiformis* and Lower *triangularis* conodont chronozones, crops out as a minor disconformity near or at the top of the Point Gratiot Bed.

The four localities sampled for this study are, from most distal to most shoreward, Walnut Creek, Eighteenmile Creek , Irish Gulf, and Beaver Meadow Creek (Figure 4). The Hanover Formation at these localities is underlain by the Pipe Creek Formation, interpreted to represent the Lower Kellwasser Event, overlain by the petroliferous Dunkirk Shale, and is comprised of over 35 meters of alternating gray-green mudstones and laminated black shales with nodular carbonate beds, that has been interpreted as an overall shallowing-upward succession, with the black shales representing episodic deepening events (Over, 2002). Samples from these localities were hand-sampled continuously through the Upper Kellwasser black shale bed; care was taken to collect the least weathered samples, usually along creek beds, and samples were stored in aluminum foil and paper or cloth bags to avoid introducing hydrocarbon contaminants. The Point Gratiot Bed ranges from 19 to 68 cm thick across the basin; for ease of comparison between the four localities, Figures 5-7 show an idealized combined stratigraphy, standardizing stratigraphic biomarker trends at each locality to 25 units. Geochemistry of the Upper Kellwasser interval at Walnut Creek, Irish Gulf and a third site not examined as part of the current study, Perry Farm, are reported in Tuite and Macko (2013).

The Madre de Dios Basin in the Devonian is interpreted to be a deepening prodelta that, because of high organic carbon content and dominant kerogenous facies, was thought to have experienced permanent or intermittent anoxia as a result of restriction or

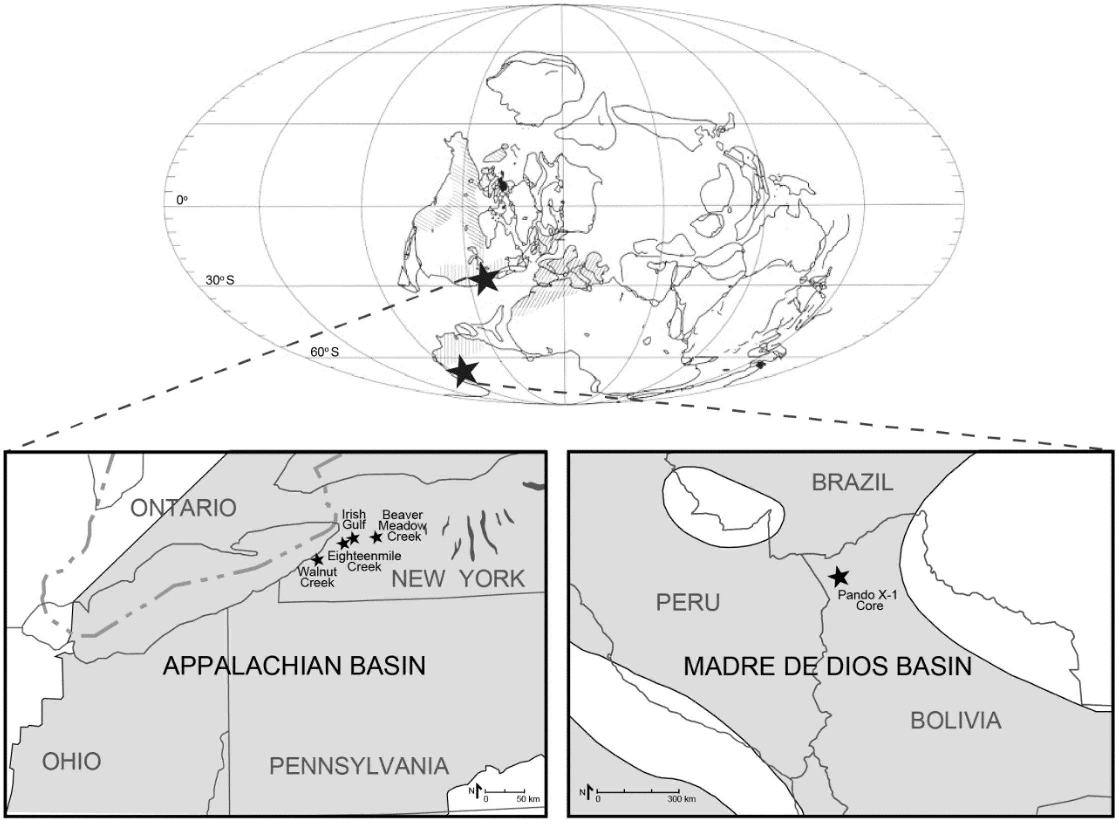

Appalachian Basin (New York) **Pando X-1 Core (Bolivia)**

Figure 4. Locality map: Paleogeography from Scotese and McKerrow (1990). Shaded regions in basinal maps show Devonian extent of the respective epeiric seaways (Appalachian Basin from Swezey, 2002; Madre de Dios Basin from Peters et al., 1997a); non-shaded region is land. Stars indicate sampling localities: in the Appalachian Basin, localities become more distal toward the west.

stratification. The latest Devonian interval from the Madre de Dios basin was sampled from the Pando X-1 core, one of five boreholes drilled into the Bolivian Shield, which recovered a sedimentary succession from Precambrian basement rock to the Tertiary (Peters et al., 1997a). Upper Kellwasser equivalent samples are taken from material from the Tomachi Formation, which is poorly biostratigraphically constrained especially in comparison to Appalachian Basin sections, across a 20 m section spanning the Frasnian-Famennian boundary transition. Attempts to assign the Frasnian-Famennian boundary to a single horizon have proven challenging, and extensive conodont studies have only succeeding in constraining the boundary to a 10 m section (Over, 2009).

Extraction and separation

For biomarker analysis, the two sample sets were extracted and fractionated in separate labs, with the Appalachian Basin samples extracted and fractionated in the Love Lab at UC Riverside, and the Madre de Dios Basin samples extracted and fractionated at the University of Virginia. For each of the Appalachian Basin samples, 5 g of cleaned and crushed rock was extracted in a CEM Microwave Accelerated Reaction System (MARS) at 100°C in a 4:1 dichloromethane (DCM):methanol mixture for 15 minutes. 6–15 g of ground material from the Madre de Dios samples was soxhlet extracted for 48 hours in a mixture of DCM and methanol (7.5:1 by volume). All solvents were distilled prior to use. Saturate hydrocarbon and aromatic fractions for both sample sets were obtained by alumina/silica column chromatography; the saturate fractions were eluted with hexanes and the aromatic fractions with a 1:1 mixture of DCM and hexanes.

GC-MS analyses of the saturate hydrocarbons were performed on a Waters AutoSpec Premier instrument at UC Riverside; sterane and hopane biomarkers were analyzed in detail by metastable reaction monitoring (MRM) GC-MS. The aromatic fractions were analyzed in both full scan and single ion monitoring methods on an Agilent GC-MSD. 200 ng of d14-p-terphenyl standard was added to between 2 and 20 mg of aromatic hydrocarbon fraction to quantify aryl isoprenoids, which were identified based on 134 Da in SIM mode. Aryl isoprenoid abundances are presented in this paper as TOC-normalized yields.

Elemental and stable isotope analyses

Twenty-eight Pando X-1 samples were washed with acetone and ground to < 200 mesh size with a ceramic mortar and pestle, acidified with a 30% HCl solution to remove carbonates, washed to neutrality, and dried at 50° C. The carbonate-free residues were weighed into tin capsules and converted to CO_2 and N_2 for element and isotope analysis using a Costech 4010 elemental analyzer coupled to a Delta V Plus stable isotope ratio mass spectrometer (Thermo Fisher) via a Conflo IV interface (Thermo Fisher). The mean range of values between duplicate samples for both $\%C_{org}$ (TOC) and $\%N_{total}$, (TN) was less than 2% of the measured abundance. Raw carbon and nitrogen isotope values were corrected using a dual point calibration (Coplen et al., 2006): $\delta^{13}C_{org}$ values with NBS19 (limestone, 1.95‰) and LSVEC (lithium carbonate, -46.6‰); $\delta^{15}N_{total}$ values with IAEA-N3 (potassium nitrate, 4.7‰) and USGS34 (potassium nitrate, -1.8‰). The mean range of duplicate samples for $\delta^{13}C_{org}$ was 0.04‰ and 0.18‰ for $\delta^{15}N_{total}$.

Total phosphorus (TP) was determined using the combustion method (Aspila, 1976). Briefly, a 0.5 g aliquot of each sample was combusted at 550°C for two hours, allowed to cool, and shaken overnight in a water bath in a 50 mL 1 N HCl solution at 25°C. The P content of the decanted solution was determined spectrophotometrically using a molybdate colorimetric reagent. The reproducibility for replicate samples and standards was less than 3.5% of the measured abundance.

Results

Maturity Parameters

From the 18 Madre de Dios samples and the 65 Appalachian Basin samples, abundant rock bitumen extract (12-109 mg of total bitumen from 5-15 g of rock powder) was generated and a full complement of linear, branched and polycyclic hydrocarbon biomarkers, such as hopanes and steranes and their methylated homologs, was detected using MRM-GC-MS with high signal/noise ratios. Hopane and sterane maturity ratios are consistent with a mid-oil window stage of thermal maturity (Figure 5); while these biomarker maturity parameters have generally equilibrated, the ratio of Ts to Tm shows that the Pando core is slightly less mature than the NY rocks. Rock-Eval confirms this disparity in maturity – T_{max} values for the Pando core is <435°C (Peters et al., 1997a,b) while Appalachian Basin samples have T_{max} values of 440-444^{o}C and Hydrogen Index (HI) values of 250-380 mg/g TOC – and independently verifies that these units are ideal for biomarker analysis (Peters et al., 2005).

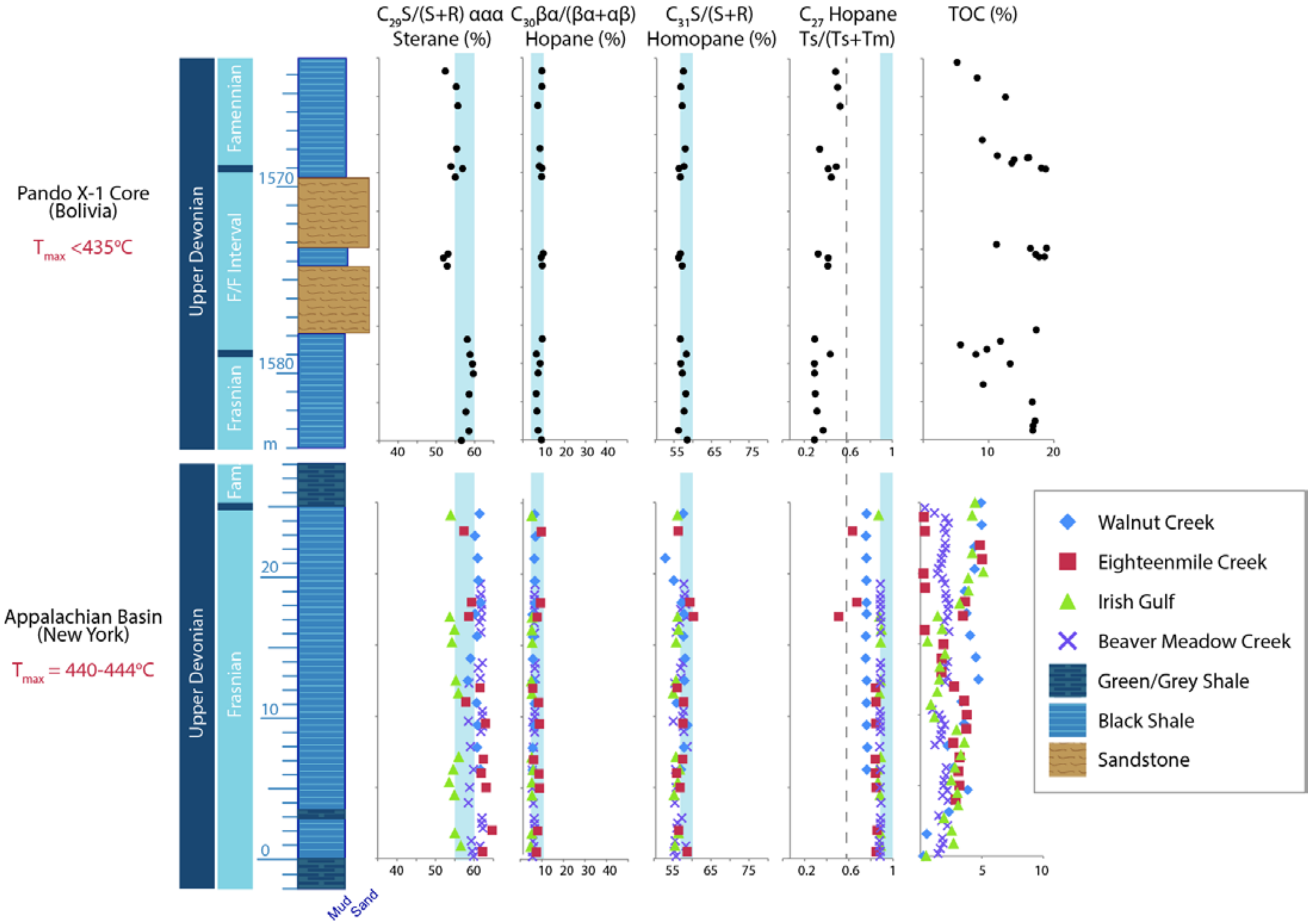

Figure 5. Maturity parameters based on hopane and sterane distributions and total organic carbon (TOC) content in weight percent. T_{max} is maximum pyrolysis temperature. Shaded bars in molecular parameter plots indicate ranges of thermal equilibration for each parameter. Dotted line through Ts/Tm plot indicates disparity in maturity between the two basins.

Ecology from Biomarker Assemblage

Following chromatographic separation, the saturate hydrocarbon fractions produced full complements of linear, branched and polycyclic hydrocarbon biomarkers. Resultant sterane ratios display no strong secular trend through either the Pando core or the Appalachian column (Figure 6). Notable, however, is the offset in the C_{28}/C_{29} sterane ratios between the two basins, which remain consistently high through the Frasnian, F/F, and Famennian intervals of the Pando core, with a max value of 0.70 and a mean value of 0.53, but are significantly lower in each of the Appalachian Basin localities (min = 0.15, max = 0.33, mean = 0.29).

Methylhopane ratios similarly suggest no strong excursions through the Upper Kellwasser interval in either basin, though in the Pando core they show slight variation between the three lithologic packages (Figure 7). 3β-methylhopanes are derived from 3β-methylbacteriohopanepolyols synthesized by both aerobic methanotrophic proteobacteria and acetic acid bacteria (though methanotrophs are the likely dominant contributor to marine source rocks; Farrimond et al., 2004); elevated 3β-methylhopane index (3-MeHI) values in marine rocks are therefore thought to reflect significant environmental methane cycling. In the Madre de Dios samples, 3-MeHI values do not systematically vary from the mean of 1.69%, and all values are within the range of Phanerozoic averages for marine petroleum source rocks (1-3%; Farrimond et al., 2004); in the Appalachian samples, 3-MeHI values average 1.14%. Values are generally lower for both Beaver Meadow Creek (mean = 0.79) and Walnut Creek (mean = 0.82) but are

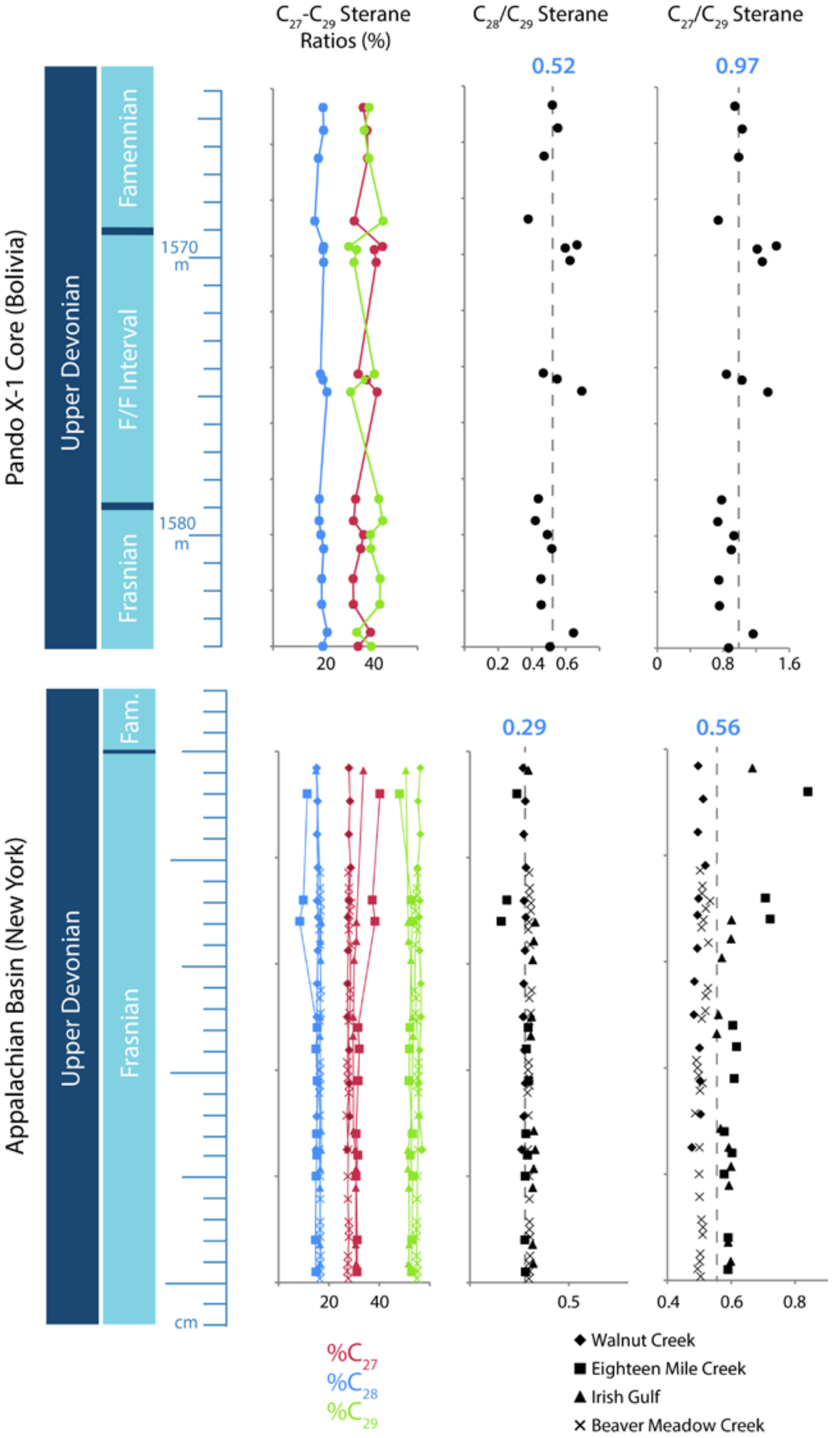

Figure 6. Sterane biomarker plots. %C27 steranes = C27/(C27+C28+C29+C30); %C28 steranes = C28/(C27+C28+C29+C30); %C29 steranes = C29/(C27+C28+C29+C30). Dotted lines through C28/C29 and C27/C29 plots indicate mean stratigraphic values of the sterane ratios.

not exceptional for Phanerozoic assemblages. Indeed, what is exceptional is the Upper Kellwasser shale's divergence in 3-MeHI values from other significant Phanerozoic extinction events: notably, elevated 3-MeHI values have been measured from both Late Ordovician (1.7%>3-MeHI<12%; Rohrssen et al., 2013) and Late Permian-Early Triassic bitumens (1.6%>3-MeHI<7%; Cao et al., 2009), but are not observed in either Late Devonian basin studied here.

The 2α-methylhopane index (2-MeHI) was previously thought to be a robust indicator of cyanobacterial input to organic matter deposition (Summons et al., 1999). Recent research, however, has questioned the taxonomic link between 2-methylhopanoids and cyanobacteria (and by extension, oxygenic photosynthesis) by demonstrating that 2α-methylbacteriohopanepolyols are readily synthesized in anaerobic α-proteobacteria (Rashby, 2007). Additionally, it appears that 2-methylhopanoids may not be mechanistically tied to oxygenic photosynthesis when they are produced in cyanobacterial membranes and are thus further unreliable biomarkers for photosynthesis (Doughty et al., 2009; Welander et al., 2010). 2-MeHI values in the Pando core are low through the F/F interval (mean: 2.14%), and comparatively slightly elevated through the Frasnian (mean: 3.40%) and Famennian (mean: 3.03%) intervals; 2-MeHI values for the Appalachian Basin samples are uniformly higher, with a basinal mean of 4.11%, with the Beaver Meadow Creek locality displaying the lowest values (mean = 2.30%; Figure 7). All 2-MeHI values for the Upper Kellwasser sediments are comparably low and not indicative of unusually high input from 2-methylbacteriohopanepolyol-synthesizing

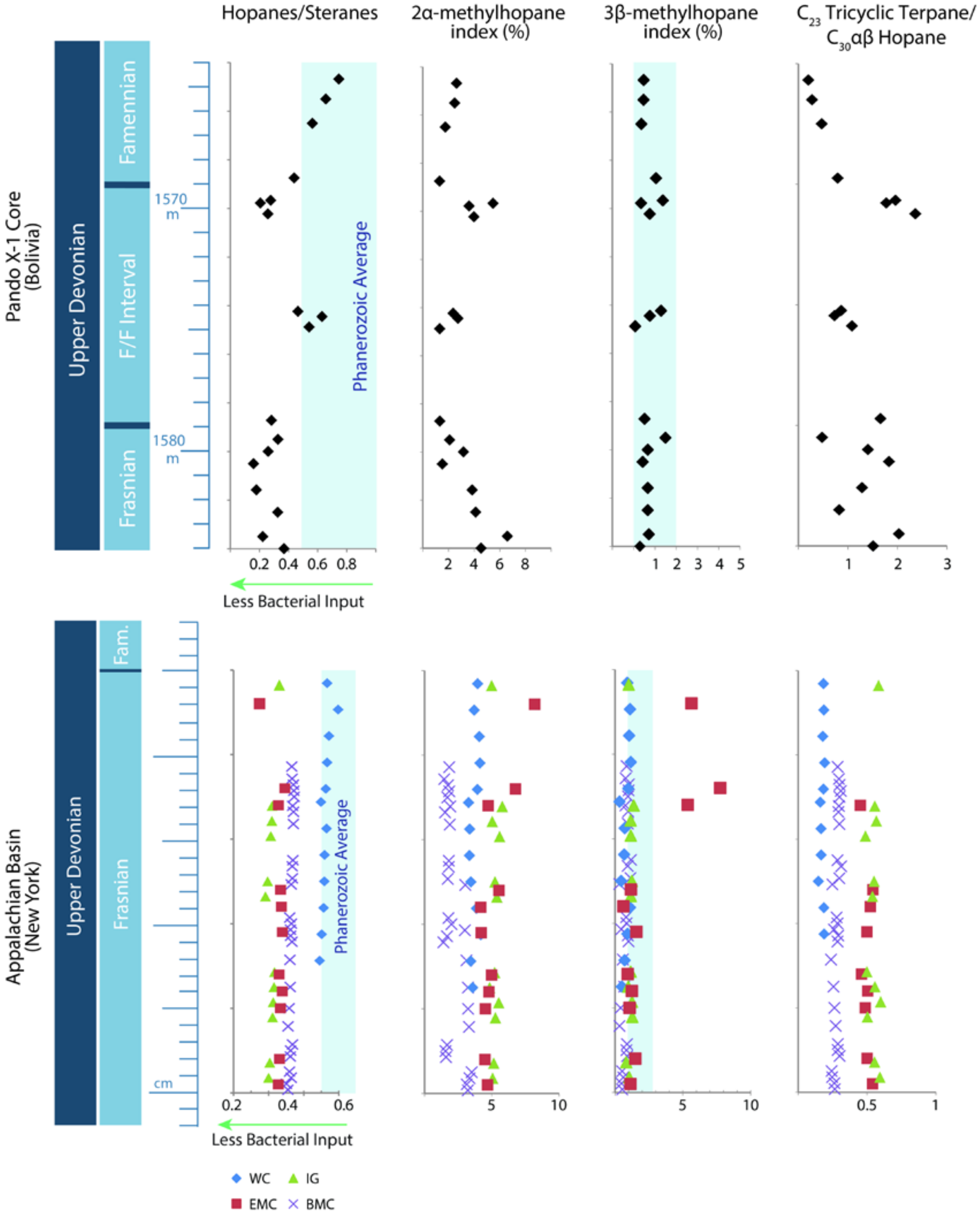

Figure 7. Hopane biomarker plots. Hopanes/Steranes = C_{27}-C_{35} hopanes/C_{27}-C_{30} steranes. 2α-methylhopane index (%) = 2α-methylhopane/C_{30} αβ hopane; 3β-methylhopane index (%) = 3β-methylhopane/C_{30} αβ hopane. Shaded boxes indicate Phanerozoic averages. WC = Walnut Creek, EMC = Eighteenmile Creek, IG = Irish Gulf, BMC = Beaver Meadow Creek.

organisms to either the Appalachian or Madre de Dios Upper Kellwasser organic matter. While this is to our knowledge the first reported 2-MeHI data for Upper Kellwasser-equivalent sediments, Marynowski et al. (2011) reported consistently elevated 2-MeHI values (6.1-13.4%) in early Famennian strata overlying the Upper Kellwasser depositional event at Kowala, Poland. These biomarkers, coupled with microstratigraphic data for cyanobacterial mats, are cited as evidence for increased opportunistic microbial activity following environmental perturbation associated with mass extinction. Lack of elevated 2-MeHI values in Upper Kellwasser black shales contrasts with elevated 2-MeHI values from Cretaceous organic matter-rich depositional events, specifically the early Aptian ocean anoxic event OAE 1a and late Cenomanian OAE 2. Kuypers et al. (2004) report 2-MeHI values up to 20% for both events; Dumitrescu and Brassell (2005) report 2-MeHI values up to 39% for OAE 1a and 45% for OAE 2.

Hopane (C_{27}-C_{35})/sterane (C_{27}-C_{30}) ratios (H/S) in the Pando core show a statistically significant ($p<0.05$) difference between the mean ratio in the Frasnian interval (0.27) and those in the F/F (0.55) and Famennian (0.45) intervals (which do not vary from each other), demonstrating a trend toward higher values in the youngest core samples. All measured H/S values, however, are very low, with the composite average of 0.38 falling below the Phanerozoic average of 0.5-2. The H/S values in the Appalachian Basin localities are similarly and characteristically low, with the three most shoreward localities having a mean H/S of 0.27; Walnut Creek, the most distal locality, displays distinct H/S values (mean = 0.53) and the majority of samples analyzed from this locality fall within the range of Phanerozoic averages. (Figure 7)

Tricyclic terpanes were previously thought to be robust biomarkers diagnostic of *Tasmanites*, a prasinophycean algal genus, due to their consistent occurrence and abundance in Tasmanite oil shales, like that of the Tomachi Formation (Simoneit and Leif 1990; Aquino Neto et al., 1992; Greenwood et al., 2000). The biological affinity of these molecules, however, has been called into question (Dutta et al., 2006) as *Leiosphaeridia* palynomorphs were found to be another source organism of the compounds. Due to extensive microfossil evidence in the Tomachi Formation for an abundance of tricyclic terpane-associated palynomorphs, including *Tasmanites*, *Leiosphaeridia* and other prasinophytes (de la Rue, 2010), we examined the trends of tricylic terpane(C_{23})/17α-hopanes($C_{30}\alpha\beta$) in both basins: the average tricyclics/hopanes ratio in the Pando core is 1.20 (range= 0.20-2.36), while the composite average tricyclics/hopanes ratio from the four Appalachian Basin localities is 0.38 (range= 0.15-0.60; Walnut Creek mean= 0.17; Eighteenmile Creek mean= 0.50; Irish Gulf mean= 0.55; Beaver Meadow Creek mean= 0.29; Figure 7).

Redox Indicators

The aromatic hydrocarbon fractions were analyzed on GC-MS SIM mode; *Chlorobi*-derived biomarkers, aryl isoprenoids, isorenieratane, and Devonian marker paleorenieratane (Maslen et al., 2009; Melendez et al., 2013) were identified using

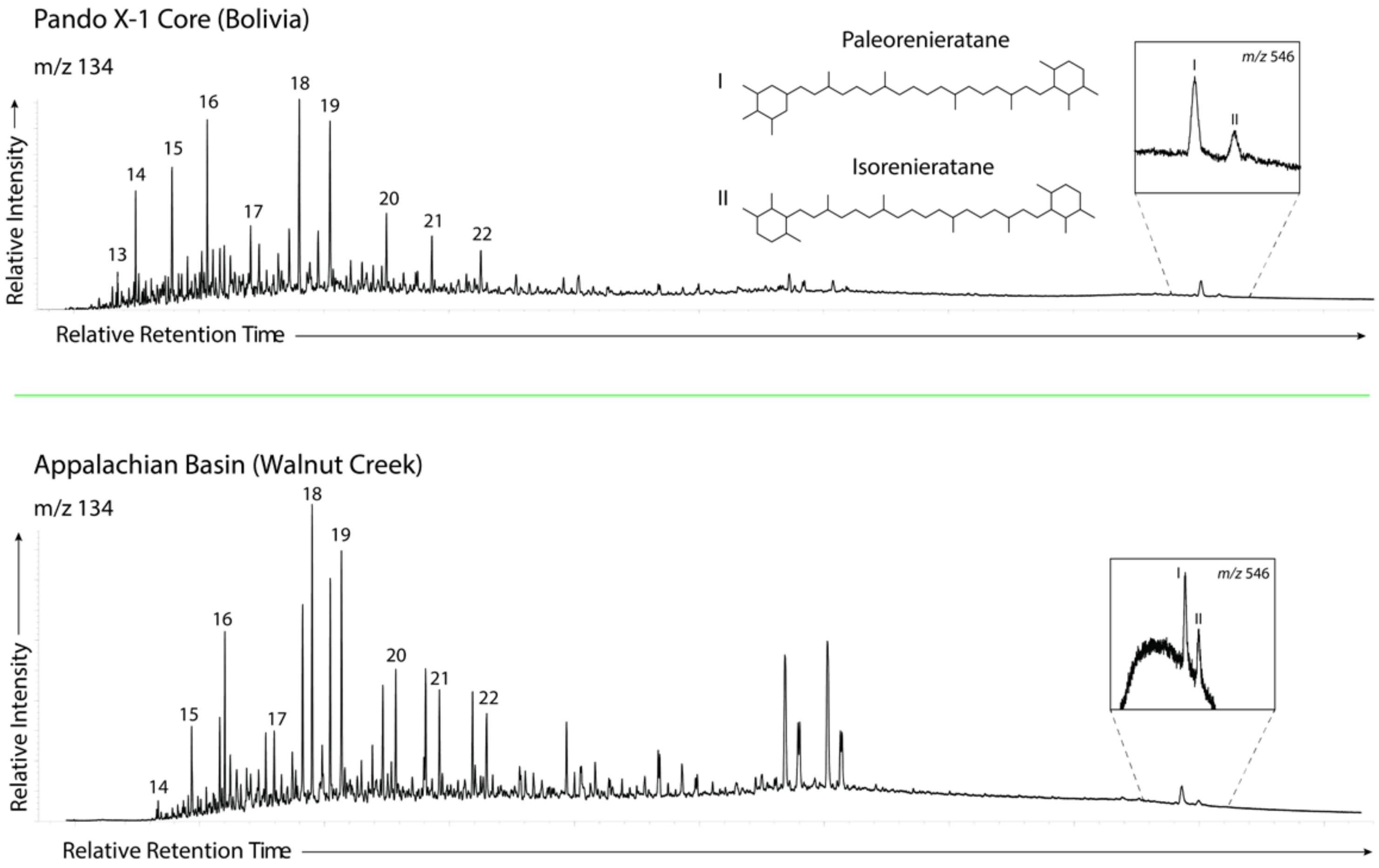

Figure 8. Mass chromatograms (134 Da) of the Pando 25 (Madre de Dios Basin) and Walnut Creek 80 (Appalachian Basin) samples showing the distribution of paleorenieratane (I), isorenieratane (II), and their aryl isoprenoid derivatives (numbers indicate individual carbon number homologues C_{13}-C_{22}). Inset magnifies 546 Da response of the C_{40} isoprenoids.

133/134 Da, with aryl isoprenoid abundances measured from 134 Da and isorenieratane and paleorenieratane verified from 546 Da molecular ion. Isorenieratane and paleorenieratane was detected only in trace amounts in eight samples from the Pando core (20 to 25 and 1 to 3) in the Frasnian and Famennian intervals; no isorenieratane was detectable in the F/F interval. The C_{40} compounds were also detected in three of the Appalachian Basin localities (not at Eighteenmile Creek), but just above detection limits, in even lower amounts than in the Pando core. Both isorenieratane and paleorenieratane were detected in Walnut Creek samples; only paleorenieratane was present in high enough abundances to be detected in Irish Gulf and Beaver Meadow Creek samples. A suite of aryl isoprenoids (C_{13}–C_{22}; Figure 8) was identified in each sample from both basins and quantified to a standard in ppm TOC. Aryl isoprenoid abundances for the Pando core ranged from 0.92 to 6.57 ppm TOC, displaying no significant variation through the core or between the three intervals; aryl isoprenoid abundances for the Appalachian Basin localities are complicated by isomerization, but range from 0.38 to 16.34 ppm TOC across the four localities, with the highest abundances occurring in sediments from the most distal, Walnut Creek, and the most shoreward, Beaver Meadow Creek, localities.

Carbon, Nitrogen, and Phosphorus

Total organic carbon (TOC) content of the Madre de Dios samples ranges from 5% to 19%, with an average TOC of 13.8%; TOC for the Appalachian samples is much lower, with a range from 0.5-5% and the mean TOC for each locality decreasing shoreward

(Walnut Creek = 3.12%; Eighteenmile Creek = 2.51%; Irish Gulf = 2.3%; Beaver Meadow Creek = 1.82%; Figure 5). Because TOC and TN are characteristically well correlated, the molar ratio of organic C to organic N (ON), determined by the slope of a regression of TN and TOC (Calvert 2004), for the Pando samples is 44.5 (Figure 10A). The positive intercept on the TN axis indicates that a consistent 0.084% of each sample is inorganic N, likely in the form of ammonium bound in clay mineral matrices (Muller 1977; Calvert 2004). For the increasingly distal intervals at Perry Farm, Irish Gulf, and Walnut Creek the values of TOC/ON rise systematically from 38.5 to 46.1 to 51.8 (Tuite and Macko, 2013). Similarly, the mean of the ratio TOC/TP within the Upper Kellwasser interval at those sites also rises distally (Perry Farm= 150, Irish Gulf = 194, Walnut Creek= 546) as TP declines exponentially (Tuite and Macko, 2013). TOC/TP among the Pando

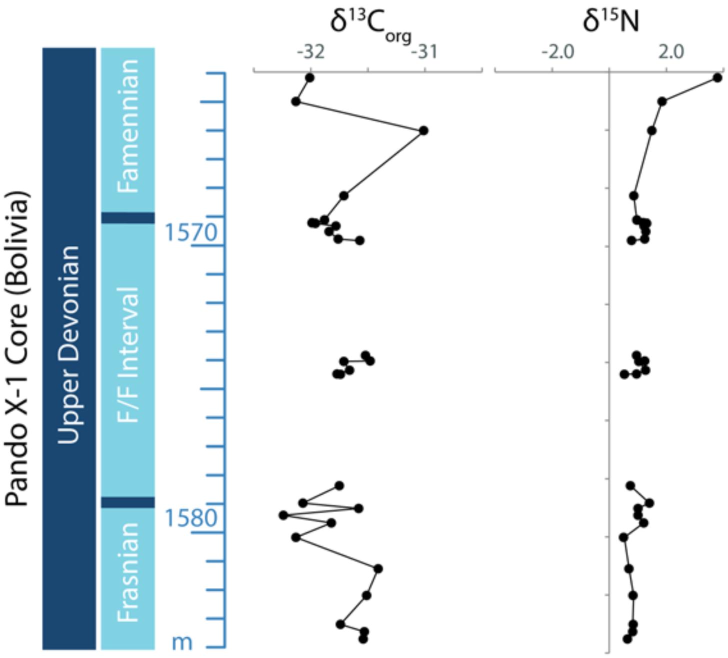

Figure 9. Pando $\delta^{13}C_{org}$ and $\delta^{15}N$. $\delta^{15}N_{total}$ values exhibit little variation with the exception of the uppermost sample which is significantly more ^{15}N-enriched. Variation of $\delta^{13}C_{org}$ values is likewise very limited. The sample at 1566.02 m, however is 0.8‰ more ^{13}C-enriched than the mean $\delta^{13}C_{org}$ and may correlate to a positive 3‰ excursion observed in the earliest *triangularis* zone in the Kowala Upper Kellwasser section in Poland.

samples ranges from 419 to 1813 with a mean value of 1221. The relationship between the ratio of organic N to total P and TOC (Figure 10B) suggests that increasing organic C preservation is correlated with a diminishing relative P abundance. Both crossplots in Figure 10 suggest that with respect to the biogeochemical processes that determine C/N/P relationships, there is significant continuity between the Appalachian and Madre de Dios Basins. In the Appalachian Basin, $\delta^{15}N_{total}$ values at Perry Farm, Irish Gulf, and Walnut Creek are very consistent: -0.2‰ ± 0.5 (n=24), -0.1‰ ± 0.4 (n=9), and -0.1 ± 0.2 (n=5), respectively (Tuite and Macko, 2013). Excluding the uppermost sample in the section, the mean $\delta^{15}N_{total}$ value in the Pando samples is 1.0‰ ± 0.3 (n=27), a ^{15}N enrichment of ~1‰ relative to the Appalachian Basin values. The uppermost sample is significantly more ^{15}N-enriched with a value of 3.8‰.

With a single significant outlier, the range of $\delta^{13}C_{org}$ values along the 20 m Pando interval is 0.8‰. The sample at 1566.02 m is 0.8‰ more ^{13}C-enriched than the mean $\delta^{13}C_{org}$ (Figure 9). We propose that this excursion correlates to a positive 3‰ excursion observed in the earliest *triangularis* zone in the Upper Kellwasser sections of Kowala, Poland (Joachimski et al., 2001) and the Appalachian Basin (Murphy et al., 2000b). The 28 samples analyzed from this interval are thus shown to be temporally correlative to the Upper Kellwasser events at other global localities, even without a tightly constrained Frasnian-Famennian boundary.

Discussion

Eukaryotic vs. Bacterial Contribution

Hopane/sterane ratios (H/S) track the relative contribution of bacteria (hopanoid-producers) and eukaryotes (sterol-synthesizers) to sedimentary organic matter; accordingly, the abnormally low H/S reported here from the Pando X-1 core and the Appalachian Basin localities indicate high relative input of eukaryotes during deposition of the Upper Kellwasser equivalent sediments in both high- and low-latitude basins. These ratios contrast with extremely elevated H/S in epeiric settings during other Phanerozoic extinction events, including the Late Ordovician (Rohrssen et al., 2013 report a Hirnantian excursion of H/S in excess of 12) and the earliest Triassic aftermath of the Permo-Triassic Mass Extinction (Cao et al. 2009 report H/S up to 60 following the extinction boundary in Meishan, China). High H/S values may point to bacterially-dominated assemblages and algal-production limited by denitrification (LaPorte et al., 2009). The low H/S values reported here for the Upper Kellwasser, however, are consistent with an increase in algal production, and are further supported by the anomalously high C28/C29 sterane ratios in the high-latitude Madre de Dios Basin.

C_{28}/C_{29} sterane ratios for the Paleozoic generally lie below a threshold of 0.55 (Schwark and Empt, 2006). Schwark and Empt (2006), however, noted C_{28}/C_{29} sterane ratio excursions at Paleozoic extinction events, specifically the end-Ordovician Hirnantian event, the end-Givetian extinction, the Lower and Upper Kellwasser events, and the Hangenberg extinction event, and attributed these temporary increases in C_{28}/C_{29} sterane values to predominantly C_{28}-synthesizing prasinophytes acting as "disaster taxa." The C_{28}/C_{29} sterane ratios for the Pando X-1 core are consistent with Schwark and Empt's (2006) findings; a maximum C_{28}/C_{29} value of 0.70 in the F/F interval indicates increased contribution from C_{28}-sterol synthesizing organisms during the deposition of this Upper Kellwasser equivalent black shale. An interpretation favoring increased prasinophyte input as an explanation for the C_{28} sterane abundance is consistent with the prasinophyte-dominated palynology of the Pando X-1 core (de la Rue, 2010) and the elevated tricyclics/hopanes ratios we report from the Bolivian samples. Palynological support for an algal assemblage dominated by prasinophytes is lacking in the low-latitude Appalachian Basin, an observation commensurate with both the tricyclics/hopanes ratios and the sterane ratios we measure there: Appalachian Basin samples display normal Paleozoic sterane signals lacking the anonymously inflated C_{28}/C_{29} ratios we see in the Pando X-1 core. This latitudinal difference in primary producer ecology is not unexpected, as *Tasmanites* and other prasinophyte algae have a well-known association with high-latitude marginal marine settings, like that of the Madre de Dios Basin (Revill et al., 1994; Peters et al., 2005).

Photic zone euxinia

While the presence of aryl isoprenoids and trace isorenieratane and paleorenieratane provide evidence for at least intermittent photic zone euxinia in the Madre de Dios Basin during the deposition of the Tomachi Formation and in the Appalachian Basin during the deposition of the Hanover Formation and specifically the Point Gratiot Bed, occurrence of these compounds alone is not as informative of dynamic water column chemistry as the abundance of green sulfur bacteria markers and their relative contribution to organic matter. Both Pando X-1 core samples and Appalachian Basin samples contain very low amounts of C_{13}-C_{22} aryl isoprenoids, in similar concentrations (mean: 3.50 ppm TOC for the Pando X-1 core; mean: 6.68 ppm TOC for the Appalachian Basin) as those reported from the middle Famennian of Poland (C_{13}-C_{22}, mean: 3.70 ppm TOC; Marynowski et al., 2007); these low concentrations in the Holy Cross Mountains of Poland were attributed to only episodic photic zone euxinia, in contrast to persistence of a sulfidic chemocline into the photic zone, and the concentrations in the Pando X-1 core and Appalachian Basin are interpreted similarly.

The aryl isoprenoid concentrations reported here are much lower than concentrations reported at other black shale events in the Late Devonian, including during the Famennian Dasberg event (C_{13}-C_{22}, max: 143.5 ppm TOC; Marynowski et al., 2010) and the end-Famennian Hangenberg event (C_{13}-C_{22}, max: 120 ppm TOC; Marynowski and Filipiak, 2007), both as expressed in the Holy Cross Mountains of Poland. These Devonian events, in turn, track aryl isoprenoid abundances up to several orders of magnitude lower than concentrations reported from other euxinic basins through the Phanerozoic, especially during the Permo-Triassic (P-T) mass extinction. At the Meishan section in South China, Cao et al. (2009) measured C_{14}-C_{27} aryl isoprenoid abundances of 2723 ppm TOC during the Changhsingian leading into the P-T mass extinction event and 2301.4 ppm TOC at the P-T boundary. While most research supports that PZE was widespread during the P-T extinction, it has been observed that local redox and nutrient variations impact green sulfur bacteria production: Grice et al. (2005) reported individual aryl isoprenoid abundances (C_{18}, C_{19}, and C_{20}) at the P-T boundary from the Perth Basin, Western Australia, with single peak values up to 90 ppm TOC though with isorenieratane abundances reaching less than 30 ppm TOC. Further multiproxy work will serve to clarify the significance of the redox biomarkers detected in Frasnian-Famennian sediments and the redox chemistry of the Appalachian and Madre de Dios Basins.

C/N/P biogeochemistry

Sediment ratios of TOC to TP and ON provide an indication of the degree to which the macronutrients N and P have been remineralized relative to the C that was fixed by primary production and subsequently preserved in sediments. Although ON can be differentiated from TN based on the regression of TN against TOC (as in Figure 10A), TP is used as a proxy for organic P because detrital P is typically a minor component of TP in basinal settings (Algeo and Ingall, 2007). Modern prasinophytes exhibit a cellular C:N:P stoichiometry of approximately 200:25:1 (Quigg et al., 2003), suggesting a lower cellular P requirement than modern Redfield-like biomass with an average value of 106:16:1 (Redfield et al., 1963; Sterner and Elser, 2002). Assuming that algal stoichiometry is an evolutionarily conservative trait (Quigg et al., 2003), the Devonian ancestors of this dominant green algal clade were likely similar in their major element compositions. The TOC/ON ratio in the Pando samples, 44.5, is more than five times the cellular C/N of prasinophyte biomass but likely overestimates the bioavailability of

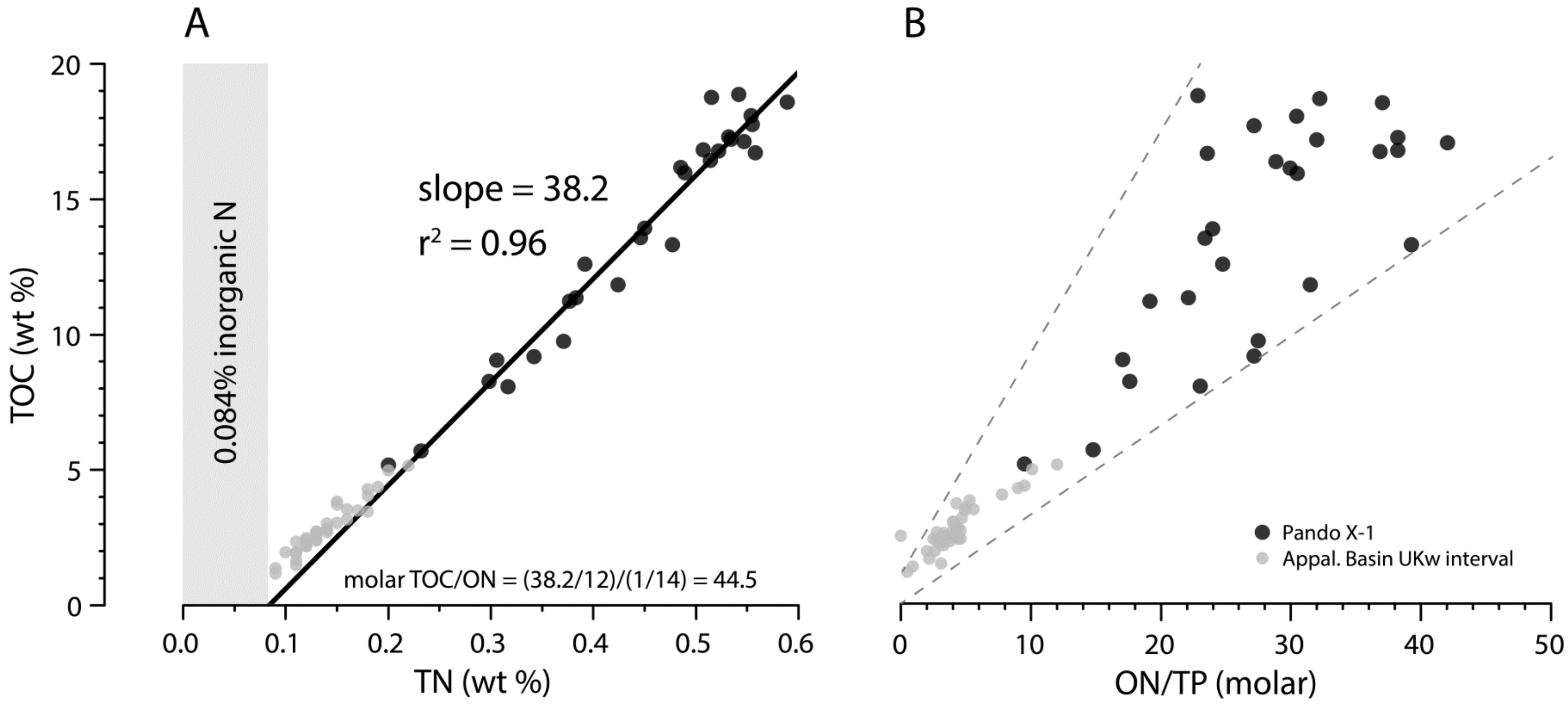

Figure 10. C/N/P relationships. Pando samples are represented by black points. Values for three Upper Kellwasser-equivalent intervals from the Appalachian Basin of western New York detailed in Tuite and Macko (2013) are represented by grey points. Regression line is for Pando samples only. A) TOC and TN are highly correlated and the slope of the regression represents a very consistent ratio of organic C to organic N that is much greater than algal C/N. The positive intercept on the TN axis is a result the incorporation of a consistent mass of NH_4^+ in clay mineral matrices. B) The positive, although not well-constrained, relationship between the ratio of organic N and total P and TOC suggests that greater regeneration of P relative to N is correlated with greater organic C preservation. Together, both crossplots indicate the continuity of biogeochemical processes in the Appalachian and Madre de Dios basins.

recycled N because an undetermined fraction of reactive N was removed from the system as N_2 via denitrification and/or annamox and as NH_4^+ fixed within clay minerals. The mean TOC/TP ratio, 1288, is more than six times the cellular C/P ratio of prasinophytes. Together, these ratios suggest that the upward diffusion of regenerated N and P in the forms of ammonium and phosphate were deficient in N relative to living biomass. Immediately above the sediment water interface beneath an anoxic water column in the Effingham Inlet, British Columbia, Ingall et al. (2005) observed that the ratio of ammonium to phosphate was approximately 6, a fraction of the cellular ratio in primary producers. Because of the importance of recycled nutrients in sustaining production in shallow epeiric seas, the stoichiometrically unbalanced regeneration of P in favor of N suggests that primary production in the Madre de Dios Basin was chronically N-limited. C/N/P ratios suggest that primary production was also N-limited in the Appalachian Basin during deposition of the Upper Kellwasser interval and increased in severity with increasing distance from shore (Tuite and Macko, 2013).

The reservoir of reactive N in marine systems is continuously depleted by losses of organic N to burial and N_2 to the atmosphere. Sources of new reactive N include N fixed in terrestrial soils that is transported by river discharge or atmospheric deposition, upwelling from deeper, nutrient-rich water, and *in situ* N fixation by diazotrophic prokaryotes. Although N limitation may prompt N fixation, there are multiple physical and ecological barriers to ameliorating N limitation via fixation including energetic constraints, limitation by other nutrients, and competition with non-fixing species

(Vitousek and Howarth, 1991). Because of the high energetic cost required to rend triply-bonded N_2, the small isotope fractionation associated with N fixation results in diazotrophic biomass $\delta^{15}N$ that differs little from atmospheric $\delta^{15}N$ (by definition, $\delta^{15}N_{air} = 0‰$) (Macko et al., 1984; Minagawa and Wada, 1986) and is more depleted than typical modern sediment $\delta^{15}N$ values that typically resemble the mean $\delta^{15}N$ of marine nitrate (~+5‰) (Peters et al., 1978; Brandes and Devol, 2002; Robinson et al., 2012). The depleted $\delta^{15}N$ values that are typical of organic-rich marine facies throughout the Phanerozoic have, therefore, often been interpreted as indicating periods of prokaryote-dominated phytoplankton communities (Rau et al., 1987; Sachs and Repeta, 1999; Kuypers et al,. 2004; Meyers, 2006; Higgins et al., 2010). Our data, however, point to biomass dominated by eukaryotic phytoplankton communities in association with depleted sediment $\delta^{15}N$ values in both the Appalachian and Madre de Dios Basins.

There are several mechanisms that contribute to the depletion of sediment $\delta^{15}N$ in low oxygen marine environments like those that obtained during the deposition of Late Devonian black shales. Where water column oxygen levels are sufficiently low to inhibit nitrification and the subsequent $\delta^{15}N$ enrichment associated with denitrification, sediment $\delta^{15}N$ will reflect the small fractionation associated with fixation of atmospheric N_2 (Quan and Falkowski, 2009). Under oxic marine conditions, Mo is the primary metal cofactor incorporated into nitrogenase, the enzyme responsible for diazotrophic N fixation. Under reducing conditions, however, Mo is rapidly scavenged from the water column and nitrogenases incorporate Fe and V in place of Mo. Iron and V nitrogenases, however, produce biomass that is 6-7‰ more depleted than (Mo)-nitrogenase (Zhang et al., 2014). During early diagenesis under anoxic conditions, the $\delta^{15}N$ of algal biomass has been observed to decline by ~3‰ (Lehmann et al., 2002). Finally, Higgins et al. (2012) proposed that the greater assimilation fractionation associated with NH_4^+ versus NO_3^- uptake by eukaryotic algae was sufficient to account for depleted $\delta^{15}N$ values and molecular evidence for eukaryote dominance during Mesozoic ocean anoxic events (Higgins et al., 2012).

Ammonium was likely the dominant reactive N species in epeiric basins of the Late Devonian because oxidation of reduced N (nitrification) at the base of the photic zone would have been inhibited by persistent dysoxic conditions and precluded during periods of photic zone euxinia. The demonstrated proclivity of prasinophytes for ammonium-rich environments (Prauss, 2007) supports a model for Devonian black shale microbial ecology in which eukaryotic algae are the environmentally important phytoplankton component even while sediment $\delta^{15}N$ values preserve the signature of prokaryotic N fixation.

The ~1‰ $\delta^{15}N$ enrichment of the Pando samples with respect to contemporaneous Appalachian Basin samples may reflect latitudinal influences on coupled nitrification/denitrification. Cooler temperatures at high latitude may have increased O_2 solubility thus deepening the surface mixed layer seasonally, permitting more oxidation of ammonium diffusing upward through the chemocline and subsequent loss of depleted

N_2 via denitrification near the base of the photic zone. Likewise, significant seasonal differences in solar insolation at high latitude may have diminished primary production and resulting heterotrophic respiration during winter months, permitting deeper penetration of oxic surface waters.

Conclusions

1. Low hopane/sterane ratios indicate that eukaryotic phytoplankton were the major component of primary production in both the Appalachian and Madre de Dios Basins during the deposition of the Upper Kellwasser equivalent black shales.
2. High C28/C29 sterane ratios in the Madre de Dios Basin, coupled with palynological evidence, suggest that specifically prasinophytes were the most significant contributor to primary productivity and organic matter burial.
3. The very low abundances of aryl isoprenoids and vanishingly low amounts of *Chlorobi*-derived C40 carotenoids, and coincident lack of evidence for persistent photic zone euxinia during deposition of the Upper Kellwasser black shale in the Appalachian Basin, suggests that sulfidic waters, when they existed, largely existed below the photic zone.
4. Because of the Madre de Dios Basin’s high latitude position, we hypothesize that photic zone euxinia supporting green sulfur bacteria production was only sustainable in the summer when solar insolation was high enough to deepen the photic zone to the euxinic water column, thus limiting the isorenieratane, paleorenieratane, and aryl isoprenoid signals in the Pando X-1 core.

5. C/N/P relationships suggest chronic N limitation of primary production that was not ameliorated by N fixation. Although sediment $\delta^{15}N$ values do preserve values consistent with N fixation, the values are a product of the reducing conditions that prevailed in epeiric basins, not the preservation of diazotroph-dominated biomass.

Table 3. Samples for biomarker analysis. TOC (wt%) = total organic carbon content in weight percent. ppm rock = parts per million in bulk rock. UKw = Upper Kellwasser black shale.

Madre de Dios Basin, Pando X-1 Core

Sample Code	**Core Depth (in m)**	**TOC (wt. %)**	**Bitumen Yield (ppm rock)**	**Saturate Fraction (ppm rock)**	**Aromatic Fraction (ppm rock)**
P1	1,564.20	5.61	56.69	3.02	5.52
P2	1,565.02	8.71	56.19	5.62	5.94
P3	1,566.02	13.25	67.41	3.41	9.65
P4	1,568.27	9.53	39.68	2.90	5.08
P5	1,569.10	11.87	n.a.	n.a.	n.a.
P6	1,569.19	16.88	47.42	3.22	9.38
P7	1,569.21	16.93	n.a.	n.a.	n.a.
P8	1,569.30	14.65	50.19	4.03	8.38
P9	1,569.49	14.69	n.a.	n.a.	n.a.
P10	1,569.75	19.00	53.14	3.86	10.36
P11	1,569.80	20.18	n.a.	n.a.	n.a.
P12	1,573.76	11.84	37.79	2.95	6.34
P13	1,573.95	20.19	n.a.	n.a.	n.a.
P14	1,573.97	17.73	52.28	4.41	10.52
P15	1,574.27	17.08	n.a.	n.a.	n.a.
P16	1,574.40	20.11	78.90	8.00	16.05
P17	1,574.41	19.05	n.a.	n.a.	n.a.
P18	1,578.24	18.80	79.90	11.17	18.94
P19	1,578.84	12.22	n.a.	n.a.	n.a.
P20	1,579.02	5.96	34.92	6.20	6.23
P21	1,579.26	10.43	n.a.	n.a.	n.a.
P22	1,579.52	8.92	38.94	3.34	7.94
P23	1,580.02	13.93	50.70	5.70	12.14
P24	1,581.10	9.71	44.80	4.85	9.61
P25	1,582.02	17.34	80.76	8.77	16.06
P26	1,583.02	17.67	52.80	4.00	10.20
P27	1,583.27	17.27	n.a.	n.a.	n.a.
P28	1,583.52	17.66	76.37	9.88	14.88

Appalachian Basin, Beaver Meadow Creek

Sample Code	**Stratigraphic Depth (in cm, top of UKw=0)**	**TOC (wt. %)**	**Bitumen Yield (ppm rock)**	**Saturate Fraction (ppm rock)**	**Aromatic Fraction (ppm rock)**
BMC 0.5	68.5	1.44	33.14	14.92	8.14
BMC 1.5	67.5	1.63	34.68	13.71	8.91
BMC 2.5	66.5	1.86	39.39	18.30	10.34
BMC 3.5	65.5	1.80	37.91	17.19	10.16
BMC 6	63	2.21	41.78	16.19	12.59
BMC 7	62	1.74	30.19	8.40	10.20
BMC 8	61	1.50	30.39	9.00	9.00
BMC 11	58	2.25	49.61	18.56	15.63
BMC 12	57	1.81	37.98	14.39	6.40
BMC 13	56	2.19	52.13	13.18	9.89
BMC 14	55	1.91	47.31	18.35	15.45
BMC 15	54	1.94	44.27	13.71	8.81
BMC 16	53	2.09	42.29	14.16	8.85
BMC 17.5	51.5	2.11	88.67	16.00	21.33
BMC 22	47	1.18	22.99	6.00	7.20
BMC 23	46	1.62	40.94	10.78	8.99
BMC 24	45	1.71	43.55	15.28	10.79
BMC 25	44	1.73	41.78	12.59	8.10
BMC 26	43	1.99	45.16	15.99	12.99
BMC 27	42	1.73	39.33	16.77	15.97
BMC 28	41	1.54	37.78	11.99	11.19
BMC 29	40	0.97	22.99	5.50	7.00
BMC 34.5	34.5	2.02	45.33	16.17	13.48
BMC 35.5	33.5	2.19	41.79	13.50	10.80
BMC 37.5	31.5	2.05	42.60	13.50	11.70
BMC 38.5	30.5	2.23	45.40	15.00	10.00
BMC 44.5	24.5	2.34	44.79	15.30	12.60
BMC 46.5	22.5	1.96	42.19	12.60	9.90
BMC 47.5	21.5	2.22	42.40	13.50	13.50
BMC 49	20	2.25	46.40	12.00	10.00
BMC 50	19	2.32	48.39	15.00	10.00
BMC 51	18	2.11	53.39	13.20	13.20
BMC 52	17	2.07	42.59	13.50	13.50
BMC 54	15	2.01	36.19	12.00	12.00
BMC 55	14	1.80	33.99	11.90	8.40

BMC 56	13	1.39	34.79	9.80	9.80
BMC 57	12	1.48	34.16	9.79	6.99
BMC 58	11	1.71	31.80	9.60	6.00
BMC 59	10	1.72	40.57	12.79	7.99
BMC 60	9	1.84	34.39	11.20	10.50
BMC 61	8	2.06	29.60	7.20	6.60
BMC 62	7	2.02	27.97	10.19	10.19
BMC 64	5	2.07	29.37	10.79	10.79
BMC 65	4	1.94	30.97	8.39	10.49
BMC 66	3	2.29	30.39	10.50	9.10
BMC 67	2	2.05	29.80	10.80	9.00
BMC 68	1	1.15	20.20	6.40	6.00
BMC 69	0	0.37	8.30	2.60	3.40

Appalachian Basin, Eighteenmile Creek

Sample Code	**Stratigraphic Depth (in cm, top of UKw=0)**	**TOC (wt. %)**	**Bitumen Yield (ppm rock)**	**Saturate Fraction (ppm rock)**	**Aromatic Fraction (ppm rock)**
EMC 0.5	24.5	2.60	53.40	12.00	4.80
EMC 2	23	2.87	42.23	12.37	13.32
EMC 5	20	3.18	33.54	6.24	12.48
EMC 6	19	3.09	46.13	8.91	11.88
EMC 7	18	3.19	31.15	13.98	11.88
EMC 9.5	15.5	3.74	39.26	16.02	12.02
EMC 11	14	3.57	45.74	12.82	14.79
EMC 12	13	2.74	45.48	11.81	20.67
EMC 17	8	3.46	7.95	0.99	1.59
EMC 18	7	3.64	9.13	1.19	0.99
EMC 23	2	0.37	6.85	1.17	0.78

Appalachian Basin, Irish Gulf

Sample Code	**Stratigraphic Depth (in cm, top of UKw=0)**	**TOC (wt. %)**	**Bitumen Yield (ppm rock)**	**Saturate Fraction (ppm rock)**	**Aromatic Fraction (ppm rock)**
IG 108	1	4.22	41.22	10.94	10.94
IG 116	9	1.41	41.32	15.03	9.49
IG 117	10	1.77	43.98	13.47	10.30
IG 118	11	0.59	37.53	14.30	10.33
IG 121	14	1.54	28.66	11.27	8.89

IG 122	15	1.38	19.35	6.78	5.19
IG 127	20	3.29	50.91	20.88	14.91
IG 128	21	2.82	45.66	18.62	14.70
IG 129	22	2.51	43.28	23.13	14.36
IG 130	23	3.01	40.82	17.52	14.34
IG 131	24	3.07	37.40	13.25	10.13
IG 133	26	2.55	43.78	18.47	10.55
IG 134	27	2.70	42.11	17.40	10.28

Appalachian Basin, Walnut Creek

Sample Code	**Stratigraphic Depth (in cm, top of UKw=0)**	**TOC (wt. %)**	**Bitumen Yield (ppm rock)**	**Saturate Fraction (ppm rock)**	**Aromatic Fraction (ppm rock)**
WC 74.5	0	5.53	40.00	8.80	8.80
WC 75.5	1	4.94	53.38	14.30	19.79
WC 76.5	2	4.99	56.99	12.00	18.00
WC 77.5	3	4.40	46.78	12.99	13.99
WC 78.5	4	4.42	47.58	12.99	13.99
WC 79.5	5	3.62	46.40	14.00	14.00
WC 80	5.5	3.77	48.62	15.94	16.94
WC 81	6.5	4.05	55.32	16.48	16.48
WC 82	7.5	4.51	52.39	14.00	15.00
WC 83	8.5	4.73	42.50	11.97	15.96
WC 84	9.5	3.36	43.59	11.70	12.60
WC 85	10.5	3.55	43.78	12.59	15.29
WC 86	11.5	2.22	39.19	12.00	11.20
WC 87	12.5	2.70	40.94	15.98	15.98
WC 93	18.5	2.64	47.47	19.78	17.80

CHAPTER 3: A MULTI-PROXY REDOX CHARACTERIZATION OF THE ECOLOGICALLY CRITICAL UPPER KELLWASSER EVENT, NEW YORK STATE

Abstract

Organic-rich deposits coeval with biotic events of varying magnitudes characterize global Devonian sedimentary successions. The Upper Kellwasser (Ukw) black shale depositional event is coincident to the largest pulse of elevated diversity loss comprising the marine Late Devonian Bioevent and has been shown to be an ecologically critical turnover for shallow-water species. Anoxia or euxinia is widely thought to be an important and ubiquitous driver for this biotic crisis, though the duration, intensity, and global extent of marine anoxia/euxinia during the UKw event are not well-constrained or demonstrative of a causal link to biological turnover.

We characterize the redox conditions during the UKw deposition in the northern Appalachian Basin to constrain local temporal variability and relative magnitude of oxygen fluctuations. We use a combination of proxies specific to the bottom waters, water column, and photic zone to create an integrated picture of basinal oxygen dynamics; our multi-disciplinary approach combines trace fossil evidence for faunal activity at the sediment-water interface with inorganic and organic geochemical proxies for anoxia and euxinia in the pelagic zone. Minor biological disruptions to laminated sedimentary fabric indicate at least intermittent oxygenation of the bottom waters during the deposition of the UKw. Trace metal proxies provide compelling evidence for a water column experiencing intermittent anoxic and euxinic conditions. Lipid biomarkers

reinforce the interpretation of variable oxygen conditions with proof for only intermittent to seasonal photic zone euxinia. This integrated dataset provides evidence for local redox variability in UKw deposition and supports a non-global signal for persistent anoxia and euxinia at the Frasnian-Famennian boundary.

Introduction

In global Devonian strata there are numerous organic-rich deposits associated with biotic turnover events of varying magnitude (House, 2002). The diversity crisis at the Frasnian-Famennian stage boundary (376 Ma), correlative with the Upper Kellwasser (UKw) depositional event, has long been characterized as one of the “Big 5” Phanerozoic Mass Extinctions (Raup and Sepkoski, 1982; Jablonski, 1991; McGhee, 1996). Paleontological studies of marine diversity trends have recognized a protracted and unexplained drop in diversity from the Givetian (middle-Devonian) through the Famennian (end-Devonian) correlated with suppressed origination rates and peaks in extinction rates that concentrate diversity losses at the end-Givetian, end-Frasnian, and end-Famennian stage boundaries, most appropriately termed biodiversity crises (Bambach et al., 2004; Bambach, 2006; Alroy, 2008a; 2008b; Stigall, 2011). Though the significance of the Late Devonian bioevents as mass extinction events has been deemphasized based on traditional criteria of magnitude and duration (Foote, 1994; Bambach et al., 2004; Alroy, 2008b), community restructuring resulting from these periods of enhanced extinction rates was ecologically critical (Droser et al., 2000; McGhee et al., 2004) and constituted a turning point at the end-Devonian in the evolutionary history of reef communities, vertebrates, and primary producers (Fagerstrom, 1994; Sallan and Coates, 2010; Schwark and Empt, 2006).

Despite their evolutionary importance, the Late Devonian biocrises remain enigmatic, with little consensus among researchers on mechanisms and associated environmental conditions. Marine anoxia is widely thought to be an important contributing factor to these turnover events, in part because of the pervasiveness of black shale preservation coeval with the diversity depletions (Joachimski and Buggisch, 1993; Becker and House, 1994; Joachimski et al., 2001; Levman and von Bitter, 2002; Bond et al, 2004; Bond and Wignall, 2008). The duration and extent of marine anoxia during each black shale/bituminous limestone depositional event are not well constrained, however, and whether anoxia, or more specifically euxinia (toxic hydrogen sulfide in the water column), can be reasonably evoked as a primary kill mechanism is still unresolved.

This study focuses on understanding the dynamics of water column oxygen during the UKw depositional event at the Frasnian-Famennian boundary and its potential influence on marine life, because, though most researchers agree that oxygen is limited in association with Late Devonian biocrises, it is increasingly recognized that organic-rich facies capture a range of bottom water redox conditions and do not represent homogenous depositional regimes. There is a growing body of literature suggesting a wide range of possible preservation and depositional conditions for black shales, beyond the traditional interpretation of requiring a persistently anoxic water-column (Arthur and

Sageman, 1994; Boyer and Droser, 2011; Boyer et al., 2011; Rivera et al., 2015). The interdependent roles of sedimentation, primary production, and microbial metabolism appear to lead to an observed diversity in types of black shales (Sageman et al., 2003; Murphy et al., 2000a).

Frequently cited systemic mechanisms for widespread anoxia (i.e. eustatic transgression, eutrophication, warming events, oceanic turnover and/or stagnation) invoke additional effects, like habitat loss, temperature stress, and ecosystem collapse, which may serve as drivers of extinction (Berry and Wilde, 1978; Wilde and Berry, 1984; 1986; Johnson et al., 1985; Hallam, 1989; Becker, 1993; Joachimski and Buggisch, 1993; Algeo et al., 1995; Murphy et al., 2000b). Approaching the question of the significance of anoxia in the Late Devonian in binary terms of “presence or absence” fails to capture complex earth-life systems dynamics. Here we contribute a piece of the more complete picture: an integrated ichnological and geochemical dataset from an UKw-equivalent black shale in the Appalachian Basin of New York, USA in an attempt to ascertain the extent and duration of anoxia at the Frasnian-Famennian boundary in this Laurentian basin. This research employs a novel microstratigraphic sampling strategy that has the potential to capture small-scale variations in both biological and geochemical parameters.

We examined continuous sedimentary sequences through the UKw black shale bed at 4 localities across a 60 km transect in western New York state (USA): from most distal to most shoreward, Walnut Creek (WC), Eighteenmile Creek (EMC), Irish Gulf (IG), and

Beaver Meadow Creek (BMC) (Figure 11). The UKw Event is expressed in the Appalachian Basin as the Point Gratiot Bed, a black shale unit in the Hanover Formation of the Java Group (Over et al., 2013); this black shale bed ranges from 19 cm thick at Walnut Creek to almost 70 cm thick at Beaver Meadow Creek. The F/F boundary has been well-constrained at these localities via conodont biostratigraphy (Over 1997, 2002). The Hanover Formation consists of light gray or green, silty shale interbedded with dark gray or black, organic-rich silty shale, and is underlain by the black Pipe Creek Shale Member (interpreted to preserve the Lower Kellwasser event; Over 1997) and overlain by the petroliferous Dunkirk Shale. Total organic carbon (TOC) content of the Point Gratiot Bed averaged across the four localities is 2.62 wt% (min = 0.24 wt%; max = 5.53 wt%).

Investigation of ichnofabric of the UKw-equivalent Point Gratiot Bed (PGB) allows for recognition of subtle variations in reduced but non-zero oxygen levels, while lipid biomarkers and trace metals which are not as sensitive to fluctuations under dysoxic conditions can provide unambiguous evidence of anoxic and/or euxinic conditions during deposition of the PGB. The different proxies used in tandem will help distinguish between competing water column redox models for Devonian epeiric seas (Figure 19), ranging from a high-TOC oxic end member with intermittently suboxic-anoxic bottom waters, to an expanded oxygen minimum zone model (after Murphy et al., 2000a; Marynowski et al., 2011; Algeo et al., 2011), to a deep water anoxic/euxinic end member (after Brown and Kenig, 2004 and Melendez et al., 2012). We test whether the UKw black shale was deposited under a persistently anoxic water column in a stagnant basin to

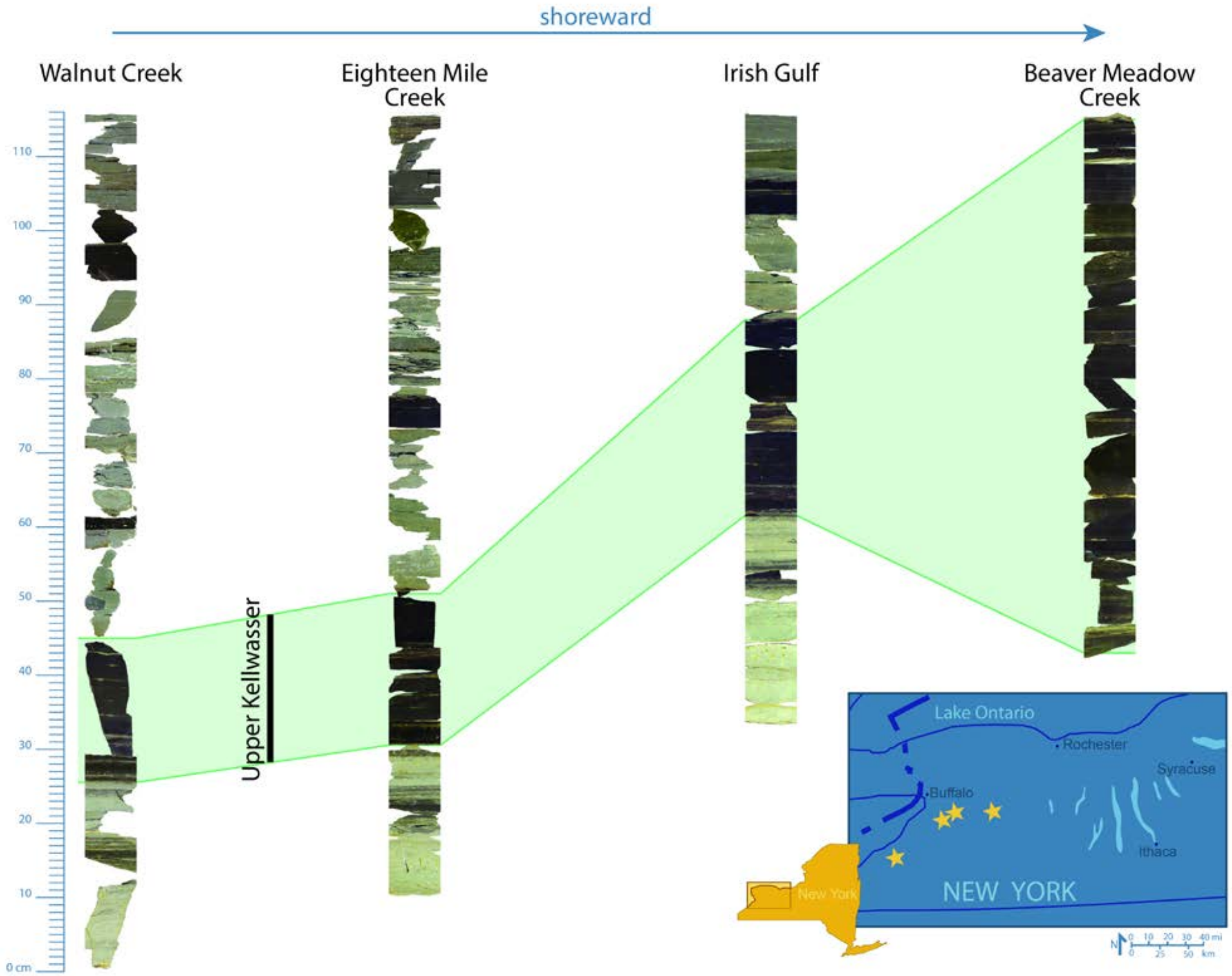

Figure 11. Composite cross-sections of hand samples through the Point Gratiot Bed (UKw-equivalent black shale) in the 4 localities. Inset shows map of western New York; stars from west to east correlate with sedimentary columns from left to right.

address whether the associated biological turnover and ecological change can reasonably be explained by the observed oxygen stress.

Biological signals of episodic bottom-water oxygenation

Devonian traces in shales representing deposition in low oxygen settings are typically horizontal to sub-horizontal, small or diminutive, not distinct, and are recognizable only because they disturb the original sedimentary fabric. It has been demonstrated, however, that trace fossil size, relative amount of bioturbation, and ichnofabric index can be used to infer relative bottom water oxygen on a microstratigraphic scale (Boyer and Droser, 2009; 2011), because the amount of biotic disruption to the original sedimentary fabric can be correlated to a relative oxygen level (Savrda and Bottjer, 1986; Savrda and Bottjer, 1989; Savrda, 1992). Examining ichnofabrics is the best way to characterize the record of bioturbation in the absence of body fossils; ichnofabrics are critical for demonstrating the presence of metazoans and corresponding implications for oxygen chemistry in the water column and for providing an independent test on geochemical redox proxies.

Ichnofabric index values, as a method to quantify the amount of bioturbation, were determined on a cm-scale through each of our measured sections. An ichnofabric index (i.i.) of 1 indicates fully laminated sediments with all original sedimentary structures preserved and i.i. 5 represents a nearly homogenized fabric with completely disturbed bedding though retained discrete burrows (Droser and Bottjer, 1986). Due to the expanded nature of the PGB at BMC (measuring nearly 70 cm thick), we did not collect continuously above and below the UKw event bed there, but the stratigraphy, lithology, and biological traces tracked well across the three more distal localities (WC, EMC, and IG) before, during, and after the deposition of the UKw shale. Preceding the PGB at each of these localities are fully bioturbated silty green-grey shales containing a diverse assemblage of ichnogenera, commonly preserved as pyritized burrows, including *Skolithos, Thalassinoides,* and *Chondrites,* but predominantly *Planolites*. These ichnogenera, in association with an ichnofabric index of 5, indicate fully oxygenated bottom water conditions. Immediately preceding the PGB is a 2-3 cm thick precursor black shale bed (PBSB), which has been interpreted as a rapid shift from fully oxygenated to anoxic bottom water conditions because of the abrupt termination of the pyritized burrows without evidence for an erosional contact. Following this PBSB, and leading into the PGB, is 10 cm of fully mottled, though sparsely populated with discrete larger burrows, ichnofabric, which is interpreted to represent an already-oxygen-stressed dysoxic facies leading into the more anoxic UKw event (Boyer et al., 2014; see Chapter 1 for an expanded discussion).

The PGB black shale units do not preserve consistent ii values of 1, however, as would be expected for deposition under a persistently anoxic water column, but rather fluctuate between i.i. 1 and i.i. 3; at Beaver Meadow Creek, i.i. values reach 4, indicating biological disturbance of up to 60% of the original sedimentary fabric (Figure 12). These occurrences of i.i. 4 are interpreted to represent the highest relative oxygen levels in the

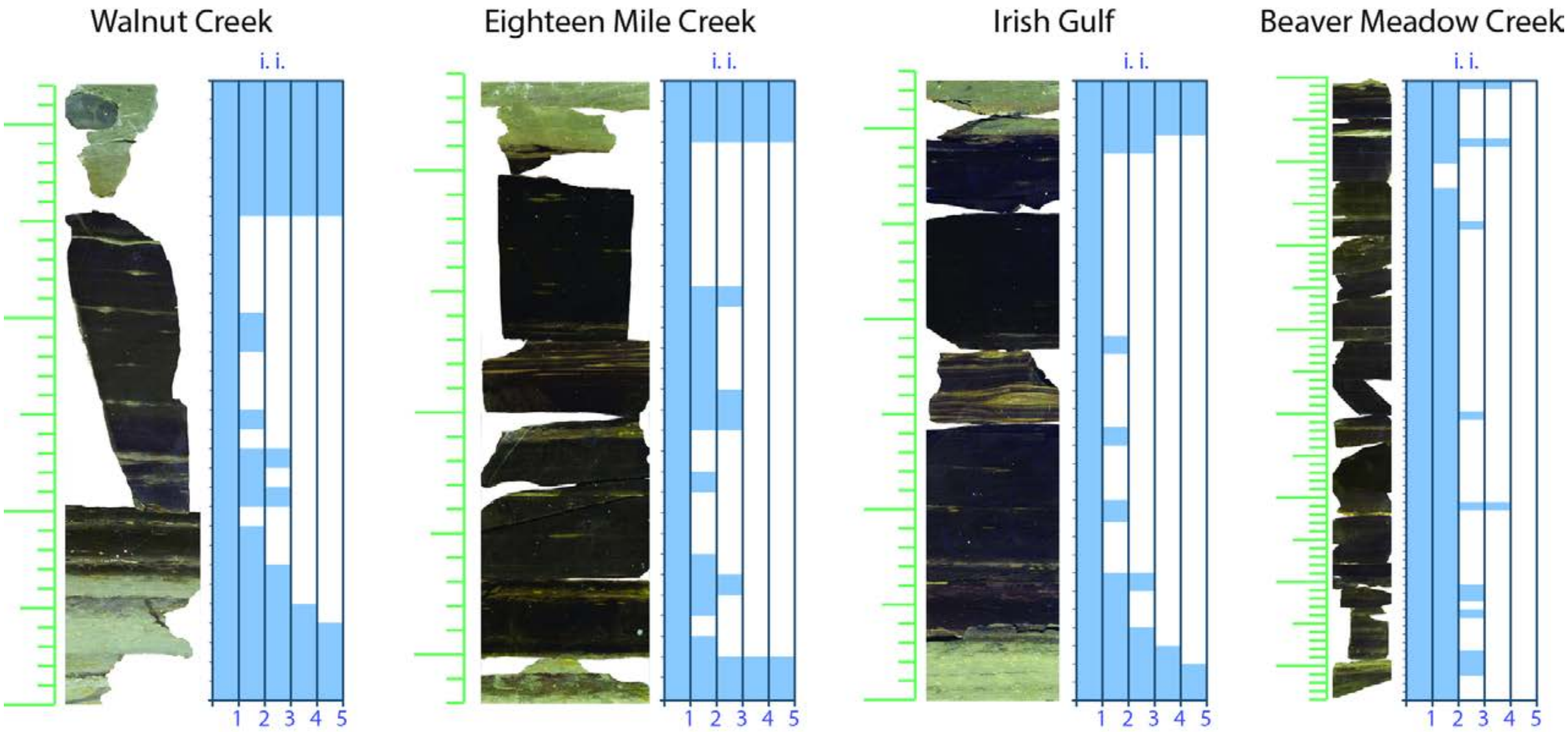

Figure 12. Ichnofabric index (i.i.) values through the Point Gratiot Bed (black shale as indicated by the cross-section of composite hand samples) at the 4 localities. Mean i.i. values are as follows: Walnut Creek = 2, Eighteenmile Creek = 1.64, Irish Gulf = 1.33, Beaver Meadow Creek = 2.15. i.i. 1 indicates all original sedimentary structures are preserved; i.i. 2 captures discrete, isolated trace fossils with less than 10% of the sedimentary fabric disturbed; i.i. 3 represents sedimentary disturbance of between 10-40% of the fabric; i.i. 4 indicates bedding is still discernible, but between 40 and 60% of the original sedimentary fabric is disturbed; i.i. 5 represents a nearly homogenized fabric with completely disturbed bedding but a possibility of discrete burrows. (Droser and Bottjer, 1986)

PGB. Few discrete trace fossils are captured in the PGB. Where they are recognized, they are identified as likely *Planolites*, measuring no more than a few mm in width and depth; no *Skolithos* or *Chondrites* are recognized in the UKw-equivalent interval. At the top of the PGB at each locality are large, >1 cm wide *Thalassanoides* burrows, penetrating up to 5 cm from the overlying green-grey shale with which the burrows are in-filled. These burrows mark a return to fully oxygenated conditions and are interpreted to represent a rapid re-oxygenation event based on erosional surfaces indicative of soupy substrates and active bottom currents.

Heterolithic, somewhat gradational bedding, facilitated by variable organic carbon and silt content, characterizes the PGB at each locality; within the first 10 cm of UKw-equivalent deposition are cm-thick bioturbated green-grey shale laminae with i.i. values of 3. Several sedimentary structures are common to each locality, including lenticular bedding, where increased silt input produced abundant silt laminae, and starved ripples at EMC, IG, and BMC, capped by a cm-thick cross-bedding at BMC (Figure 13). Lenticular bedding, starved ripples, and cross-stratification are most likely to have been formed by clear-water bottom currents rather than by turbidity currents (Shanmugam et al., 1993). These structures, products of traction and suspension deposition, are therefore interpreted to reflect episodic enhancement in bottom current energy and possible concomitant increases in benthic dissolved oxygen levels, especially in light of the ichnofabric evidence for intermittent colonization of the seafloor during the deposition of the UKw.

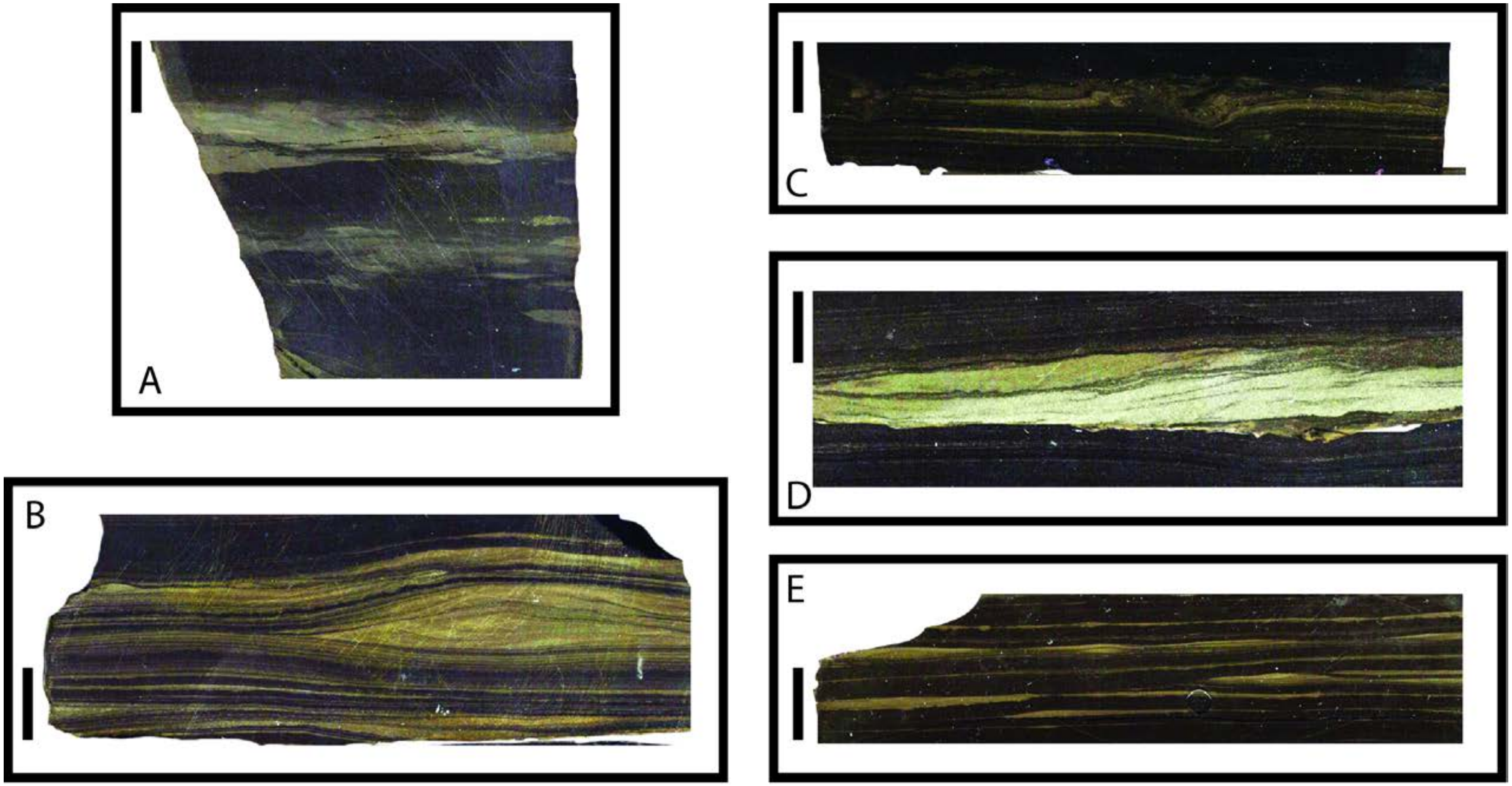

Figure 13. Diversity of sedimentary structures as displayed in cross-sections of polished hand samples of the Point Gratiot Bed. A) Bioturbated green-grey shale laminae within the first 10 cm of the PGB at each locality, example from Walnut Creek; B) Lenticular bedding or starved ripples at Irish Gulf; C) Rippling at Eighteenmile Creek; D) Cm-thick cross-bedding at Beaver Meadow Creek; E) Silt laminae common to each locality, example from Eighteenmile Creek. Scale bar indicates 1 cm.

Biological sedimentary disruption evinced by i.i. 2 does not suggest fully oxygenated conditions or colonization by larger macrofauna (indicated by the paucity of large, discrete burrows). Bioturbation of i.i. 3 or 4, however, especially in conjunction with interbedded grey-green shale, was most likely caused by autochthonous macrofauna because of lack of evidence for turbidity currents which may have brought in allochthonous benthic fauna from shallower waters (Ozalas et al., 1994). As the alternating sequences of black and green-grey shale are attributable to transgressive-regressive cycles, it is probable that the oxygenation events within the UKw were a result of shorter-term changes in oceanic circulation. Occurrences of i.i. 2 may indicate seasonal or event-induced fluctuations in bottom water oxygen, whereas the periods of greater oxygenation, as indicated by i.i. 3 or 4 and with an implication of short-term recolonization, was presumably facilitated by oxygenation events on a longer time-scale than subannual (Wetzel and Uchmann, 1998).

Geochemical signals of intermittent euxinia

Trace metals (e.g. Mo, V, U, Zn, Ni, Pb, Cu, Co, and Cr) have demonstrated variable utility as redox proxies, and their concentrations are often used to infer variations in bottom water oxygen and, more specifically, variations in the concentration of sulfide in the water column (Arthur and Sageman, 1994; Wignall, 1994; Rimmer, 2004; Algeo and Maynard, 2004; Tribovillard et al., 2006). Mo has specifically been demonstrated to reflect variations in bottom water oxygen levels in Devonian black shales from New

York state, and high-resolution fluctuations in Mo concentrations have been shown to be useful for extrapolating relative paleo-oxygen levels on a cm scale (Boyer et al., 2011).

Mo levels are enriched under persistently low oxygen settings (Morford and Emerson, 1999; Scott et al., 2008) and typically highly enriched in euxinic sediments (Calvert and Pederson, 1993; Lyons et al., 2003); however, Mo values between ~2 and 30 ppm are recognized beneath dysoxic waters (McManus et al., 2006; Scott and Lyons, 2012). Intermittent or seasonal euxinia can result in similarly enriched values or higher depending on water column Mo availability and the persistence of euxinia (Murphy et al., 2000a; Lyons et al., 2009). Greatly enriched Mo values (in excess of 100 ppm) are interpreted to represent permanent euxinia in Mo-replete settings (Werne et al., 2002; Sageman et al., 2003; Gordon et al., 2009; Scott and Lyons, 2012; Figure 14).

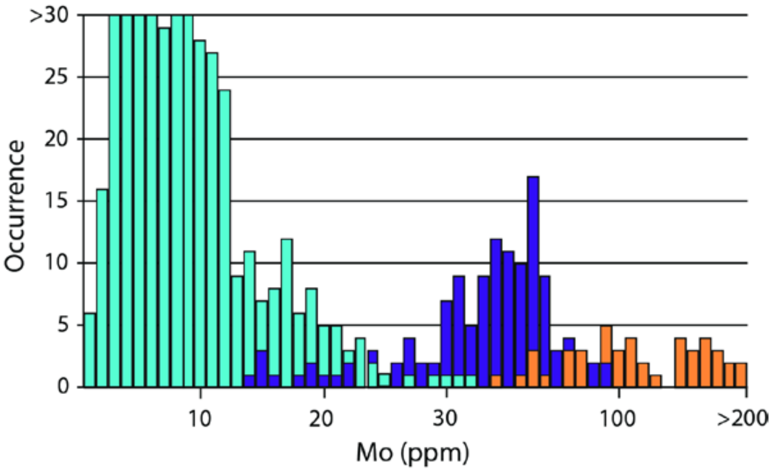

Figure 14. Mo concentrations in modern sulfidic environments, from Scott and Lyons (2012). Teal bars are non-euxinic settings where sulfide is restricted to pore waters throughout the year. Orange bars are permanently euxinic, Mo-replete settings. Purple bars are intermittently/seasonally euxinic settings and the Mo-depleted Black Sea.

Mo enrichments in the PGB at these four localities average 17 ppm (min = 1 ppm; max = 72 ppm; mean crustal value = 2 ppm; Figure 15). Irish Gulf and Walnut Creek, the first and third most distal localities, share a distinctive stratigraphic pattern, with Mo values enriched up to 55 ppm in the bottom half of the UKw depositional sequence, and depleted to between 4 and 20 ppm in the top half. Enrichment of Mo in sediments is dependent on the reservoir of Mo in the water column, which may be finite in a restricted basinal setting (Algeo and Lyons, 2006); the muted and declining concentrations of Mo measured at our localities could be attributed to a depletion of the Mo basinal reservoir, depending on the paleo-configuration and degree of restriction of the Appalachian Basin. A different stratigraphic pattern is displayed in the expanded section at Beaver Meadow Creek, however, where Mo concentrations remain low (mean = 9 ppm; max = 29 ppm) for the first 45 cm of UKw deposition, and then spike to maxima of 72 ppm and 62 ppm in two excursions in the top 20 cm of deposition (Figure 15). This stratigraphic progression suggests that the PGB at BMC was deposited under a Mo-replete water column, assuming the subpycnoclinal watermasses at each locality were connected (probable, as BMC and IG are separated by only 25 km). The muted enrichments at all four localities then are likely reflecting local redox conditions and are not artifacts of the basin reservoir effect and a lack of available Mo. Furthermore, very high (>200 ppm) Mo values found in correlative strata in the Madre de Dios Basin, Bolivia, imply that the global dissolved Mo inventory remained high throughout the UKw deposition (Figure 15). While the Appalachian Basin may have remained semi-restricted during the black shale event, the sea level high-stand of transgression coupled with an 800 ka residence

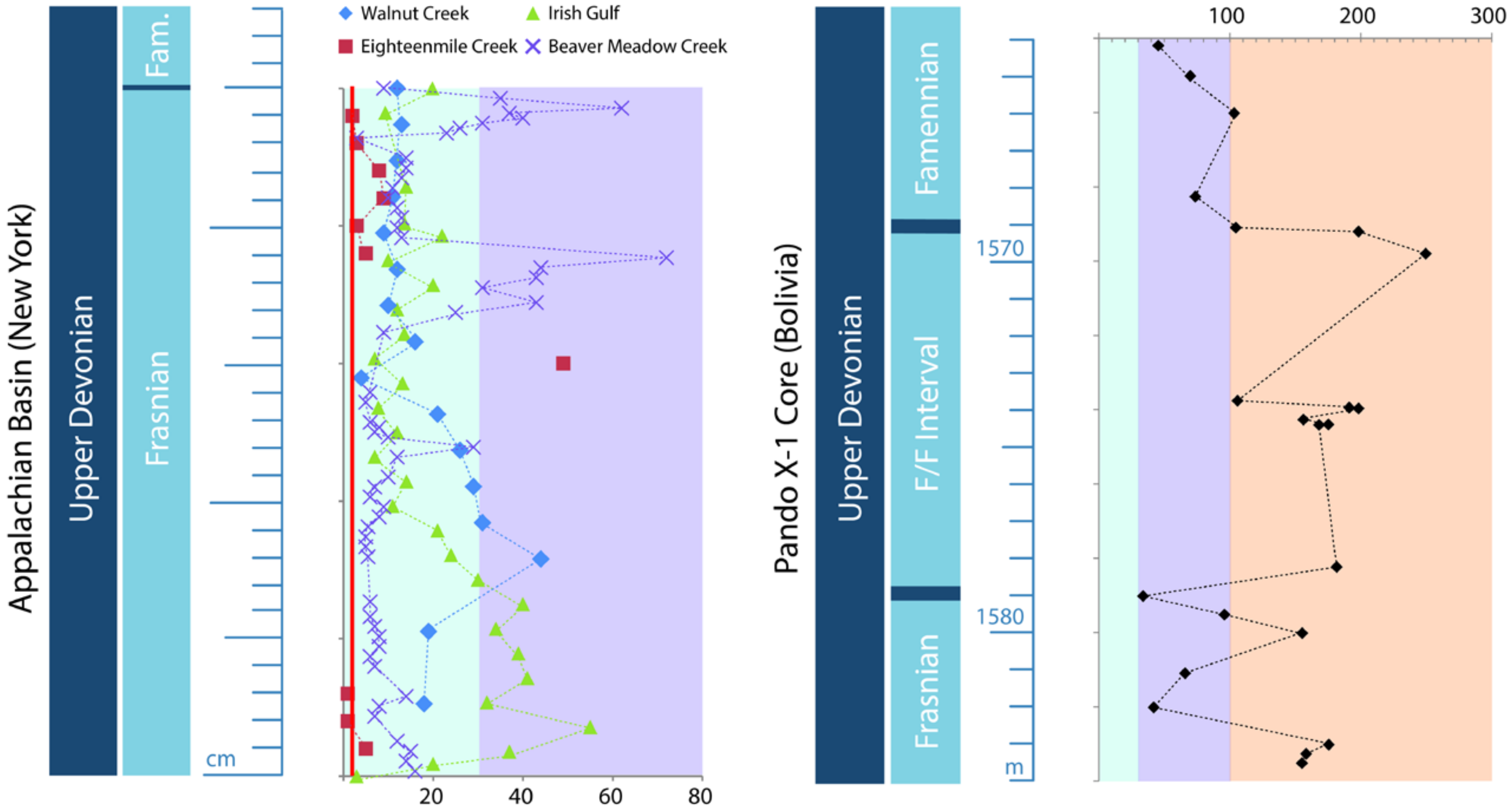

Figure 15. Mo concentrations from the Appalachian Basin (left) and the Madre de Dios Basin (right). The four Appalachian Basin localities are standardized to a 25 unit (cm-scale) stratigraphic column for ease of comparison. Blue background indicates dysoxic/suboxic range, purple background is intermittently euxinic range, orange background is permanently euxinic (corresponds with Figure 14). X-axis is ppm Mo.

time for Mo (Algeo and Lyons, 2006) suggest that muted Mo signals in New York may not be attributable to localized depletion.

These patterns indicate that Mo concentrations do not remain consistently enriched throughout the deposition of the UKw-equivalent black shale in the Appalachian Basin, but rather fluctuate dramatically on a cm-scale. This demonstrates the utility of a high-resolution scope for this investigation as such a sampling scheme has enabled us to capture variability and a range of trace metal concentrations that dm- or m-scale sampling would miss. Furthermore, the levels of Mo enrichment do not correspond to average values for stagnant, permanently euxinic basins, like the Black Sea (Table 4); the majority of Mo values fall well within the range for deposition under a dysoxic/suboxic water column (i.e. lacking large concentrations of dissolved sulfide), and excursions in Mo enrichment suggest only intermittent or seasonal euxinic conditions during deposition of the UKw. Additionally, the uniformly low TOC values measured in our sections (0.24-5.53 wt%), which are exceptionally organic-lean for Devonian black shales and do not correlate significantly with measured sedimentary Mo concentrations, are further evidence for fluctuating redox conditions (Sageman, 2003; Algeo et al., 2007).

The relational enrichment of various trace metals, specifically U, V, and Mo, may shed further light on coeval bottom water redox conditions, because U and V can accumulate under only anoxic conditions while Mo requires free H_2S. Enrichment in only U and V to the exclusion of Mo suggests deposition under suboxic to anoxic conditions, whereas enrichment of U, V, and Mo necessarily reflects sulfidic conditions in the sediments or overlying water column (Algeo and Maynard, 2004). At all four localities, V is enriched to slightly higher than average shale values, comparable to Black Sea sediment enrichments (PGB average = 183 ppm; Figure 16; Table 4); however, U is barely enriched above average shale and crustal values (PGB average = 4 ppm; Figure 16; Table 4), while Mo, as discussed above, is moderately enriched in the PGB across western New

Table 4. Comparative trace metal and minor element data, modified from Brumsack, 2006. Minor elements in µg/g (parts per million); average shale data from Wedepohl (1971, 1991); Black Sea data from Lüschen (2004); n.d. = not determined.

Element	**Average shale**	**Gulf of California (modern)**	**Black Sea (modern)**	**Cenomanian/ Turonian mean (ancient)**	**Point Gratiot Bed mean (this study)**
Ba	580	566	1171	895	557
Cr	90	44	60	179	133
Cu	45	27	106	194	93
Mn	850	193	270	557	513
Mo	1	12	117	316	16
Ni	68	38	110	267	96
Pb	22	17	17	26	41
Re	0.01	n.d.	0.054	0.21	0.004
U	3.7	5.7	14.8	28	4.1
V	130	101	196	1016	184
Zn	95	88	83	2056	127

York. Secondary loss of trace element enrichment is possible via post-depositional reoxygenation, mobilizing authigenic elements and decreasing original enrichments in preserved sediments, especially in environments where conditions vary relatively rapidly (Tribovillard et al., 2006). U is particularly sensitive to reoxidation and remobilization (Morford et al., 2001; McManus et al., 2005); even if U accumulated under reducing conditions initially, the absence of U enrichment in the UKw-equivalent shales of the Appalachian Basin could imply post-depositional oxygen replenishment to the bottom waters on a rapid temporal scale.

V/Cr and V/(V+Ni) have also been used as redox indicators for black shale formation; each relate a redox-sensitive element (V) to an element that is not expected to fluctuate with redox because of its strong association with the detrital fraction (Jones and Manning, 1994; Tribovillard et al., 2006). Threshold values of these ratios have been described and are interpreted to correlate with oxic, dysoxic, and anoxic conditions (Hatch and Leventhal, 1992; Jones and Manning, 1994; Wignall, 1994; Rimmer, 2004). Joachimski et al. (2001) measured V/Cr and V/(V+Ni) ratios across the Frasnian-Fammenian boundary in the Polish Kowala section; they reported V/Cr ratios consistently above 4.25 (the anoxic threshold) and up to 18 and V/(V+Ni) ratios around 0.8 (near the 0.85 suboxic/anoxic transition proposed by Hatch and Leventhal, 1992) through the UKw. These data support an interpretation for clearly anoxic conditions during UKw deposition at Kowala; our data for the Appalachian Basin is more ambiguous. V/Cr values for our Appalachian Basin localities range from 0.18 (well within what would be interpreted as

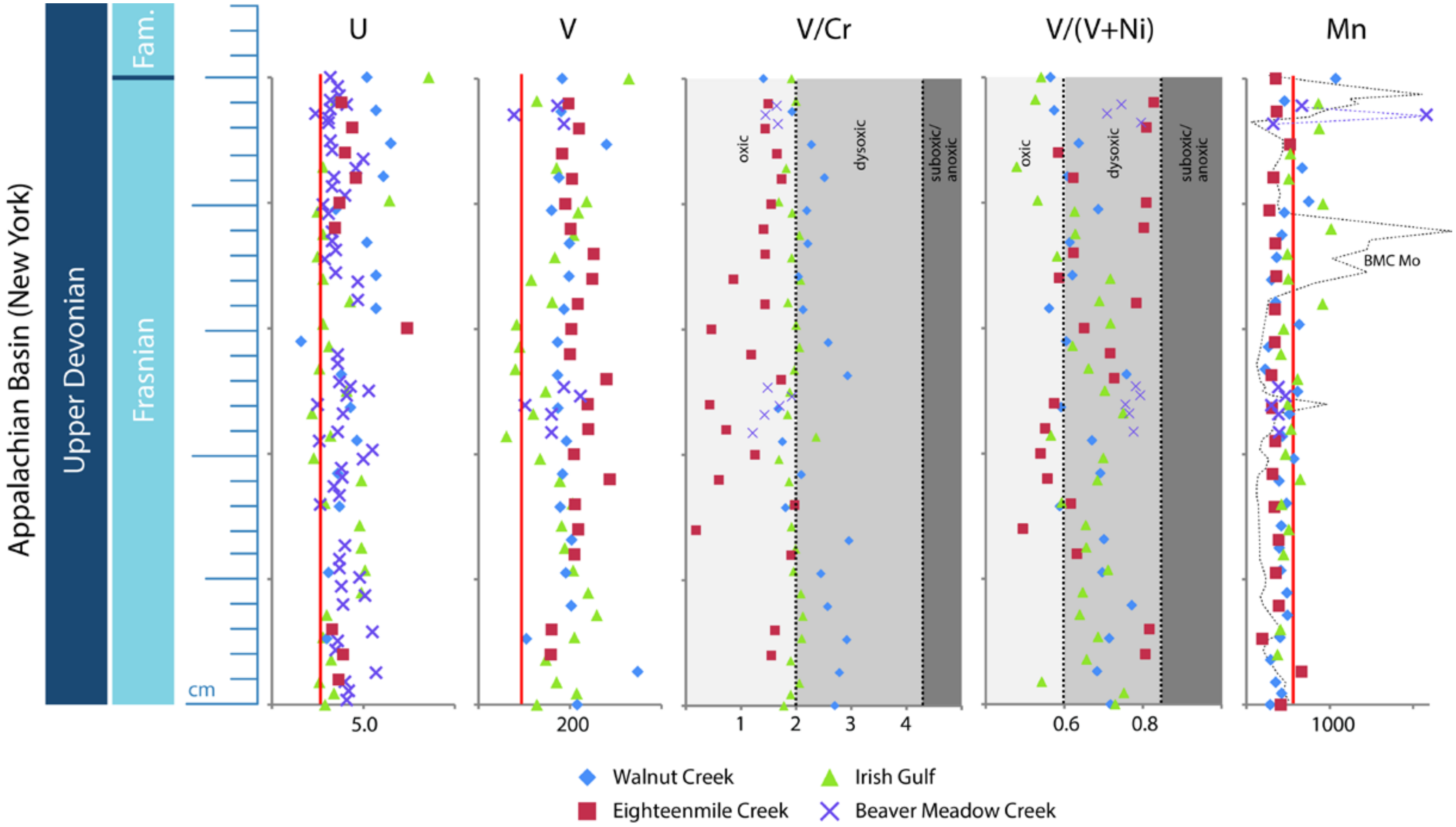

Figure 16. Trace metal concentrations. From left to right: U (ppm whole rock), V (ppm whole rock), V/Cr, V/(V + Ni), and Mn (ppm whole rock). The four localities are standardized to a 25 unit (cm-scale) stratigraphic column. Red lines indicate average crustal values: U = 2.7 ppm; V = 93 ppm; Mn = 600 ppm (Rudnick and Gao, 2003; Tribovillard et al., 2006). V/Cr thresholds: oxic-dysoxic = 2, dysoxic-suboxic/anoxic = 4.25 (Jones and Manning, 1994); V/(V + Ni) thresholds: oxic-dysoxic = 0.6, dysoxic-suboxic/anoxic = 0.85. Black dotted line on Mn chart is Beaver Meadow Creek Mo trends, overlain to show relationship to Mn trend.

oxic levels) at Eighteenmile Creek to 2.96 (still below the 4.25 dysoxic/anoxic transition threshold) at Walnut Creek (Figure 16). V/(V+Ni) values display a similar range, from oxic values (min = 0.48) to values at the dysoxic/suboxic transition (max = 0.83; Figure 16). The contrast in these redox indicators between the European and North American basins highlights the variable redox regimes in play during the global UKw deposition.

Mn is enriched in oxic settings as it has a strongly adsorptive affinity for organic matter in the presence of oxygen and is reported at values greater than crustal average (600 ppm) under oxygenated bottom waters (Calvert and Pederson, 1993). Enrichments of Mn have been interpreted to be a result of variation in the position of the chemocline in the Black Sea (Lyons et al., 1993), providing evidence for a meaningful Mn signal in the rock record. While Mn values at WC, the most distal locality and condensed section, remain unenriched throughout the UKw sequence, Mn concentrations increase to values much greater than crustal values, and even greater than average shale values, in the top half of the PGB at EMC (max = 1018 ppm), IG (max = 1072 ppm), and BMC (max = 2161 ppm) (Figure 16). Interestingly, the maximum at BMC, the most shoreward locality, occurs between and within cms of the two peaks in Mo concentrations toward the end of the deposition of the UKw-equivalent black shales, suggesting a rapidly fluctuating chemocline and reinforcing the dramatic redox variability we interpret from our proxies.

Biomarker record of photic zone euxinia

While the inorganic proxies capture redox variability at the sediment-water interface and in the bottom waters, lipid biomarkers can determine the extent of sulfidic watermass pervasion into the upper water column. Specifically, the aromatic cartenoid pigment molecule produced by green sulfur bacteria (GSB), isorenierantene, is well-preserved in sediments as the molecular fossil isorenieratane and is a biomarker for euxinia in the photic zone of ancient bodies of water (Summons and Powell, 1986). Isorenieratane and its diagenetic products, aryl isoprenoids, indicate that free hydrogen sulfide was present at least episodically up into the photic zone of the water column (Summons and Powell, 1987) during deposition of these strata because GSB are strictly anaerobic, obligate phototrophs using mainly H_2S as an electron donor for photosynthesis. While global-scale photic zone euxinia has been implied by previous biomarker studies of Frasnian-Famennian boundary sediments in Europe, western Canada, Australia, and North America (Brown and Kenig, 2004), this interpretation has not been adequately constrained due to the localized nature of these studies and the tendency to concentrate on the most organic-rich strata in the respective epeiric basins.

GSB-derived biomarkers were identified at each locality at cm-scale, quantified to a standard, and normalized to TOC. Isorenieratane and Devonian marker paleorenieratane (Maslen et al., 2009; Melendez et al., 2013) were detected in three localities (WC, IG, and BMC), but just above detection limits (0-0.73 ppm TOC; Figure 18), and a suite of aryl isoprenoids (C_{13}–C_{22}; Figure 17) was identified in each PGB sample and quantified.

While the presence of aryl isoprenoids and trace isorenieratane and paleorenieratane provide evidence for at least intermittent photic zone euxinia in the Appalachian Basin during the deposition of the Point Gratiot Bed, occurrence of these compounds alone is not as informative of dynamic water column chemistry as the abundance of GSB markers and their relative contribution to organic matter. Aryl isoprenoid abundances range from 0.43 to 17.28 ppm TOC across the four localities; the highest abundances occurring in sediments from the most distal locality, WC (mean = 12.45 ppm TOC, max = 16.47 ppm TOC) and the most shoreward locality, BMC (mean = 9.63 ppm TOC, max = 17.28 ppm TOC), though the widest range of abundances also comes from BMC (1.60-17.28 ppm TOC, > 2 standard deviations).

While all abundances are roughly within the same order of magnitude through the deposition of the PGB at the four localities, there is clear and possibly systematic variability on the cm-scale through the PGB. This is particularly evident at BMC, where pre-PGB aryl isoprenoid abundances exceed 10 ppm TOC, and decrease to <2 ppm TOC in the first 5 cm of PGB deposition; this crash in apparent abundance of GSB-biomarkers is not due to lower TOC values before the PGB, as TOC is roughly unchanging before and after PGB deposition begins, but reflects an actual decrease in molecular quantity (~240 ng aryl isoprenoids/5 g sediment to ~40 ng aryl isoprenoids/5 g sediment; Figure 17).

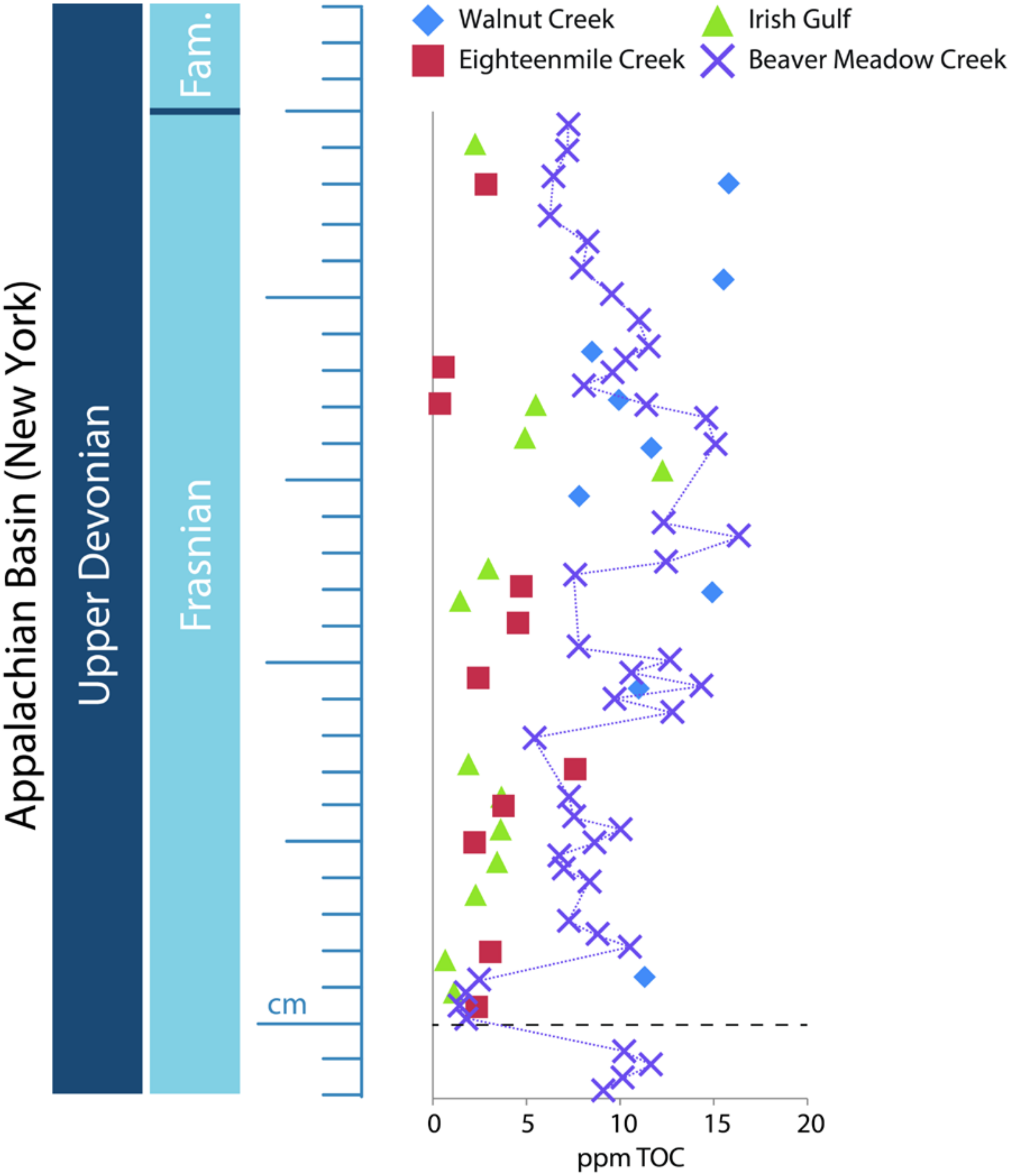

Figure 17. Aryl isoprenoid abundances in ppm TOC. The four localities are standardized to a 25 unit (cm-scale) stratigraphic column. Dotted horizontal line indicates the beginning of UKw deposition.

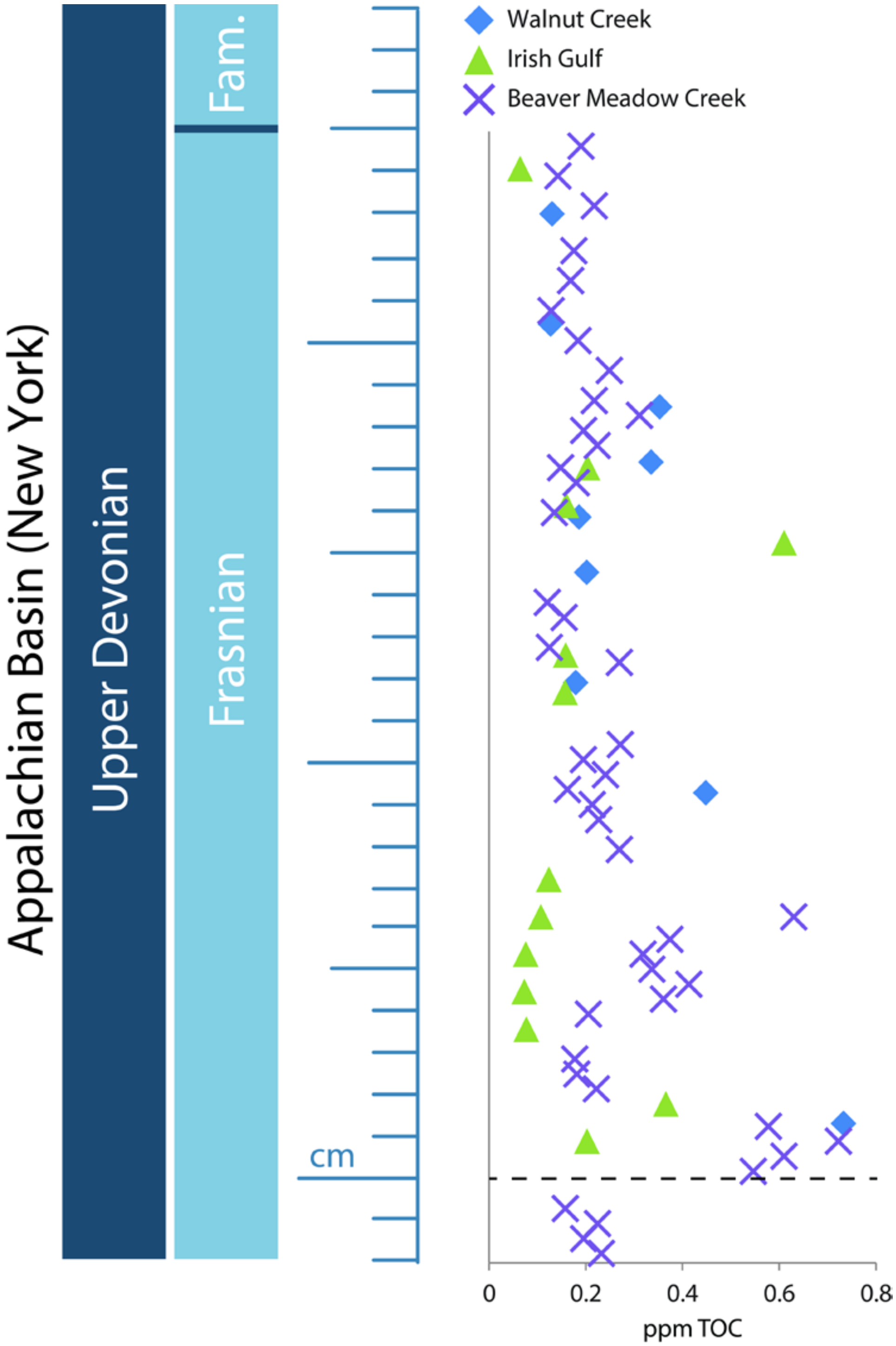

Figure 18. Summed paleorenieratane and isorenieratane abundances in ppm TOC. The three localities are standardized to a 25 unit (cm-scale) stratigraphic column. Dotted horizontal line indicates beginning of UKw deposition.

The low abundances of aryl isoprenoids detected in the PGB of New York are similar in concentration to those reported from the middle Famennian of Poland (max: 5.2 ppm TOC; Marynowski et al., 2007), from a succession that does not correlate with a significant bioevent. The low aryl isoprenoid concentrations in these Polish strata were attributed to only episodic photic zone euxinia, in contrast to persistence of hydrogen sulfide into the photic zone; we interpret the origin of the low concentrations of isorenieratane, paleorenieratane, and aryl isoprenoids in the Appalachian Basin similarly. Furthermore, the aryl isoprenoid concentrations reported here are much lower than concentrations reported at other black shale events in the Late Devonian, including during the Famennian Dasberg event (max: 143.5 ppm TOC; Marynowski et al., 2010) and the end-Famennian Hangenberg event (max: 120 ppm TOC; Marynowski and Filipiak, 2007), both as expressed in the Holy Cross Mountains of Poland. While the Hangenberg event has been acknowledged as a bioevent nearly equivalent to the Frasnian-Famennian extinction in terms of magnitude and ecological impact (Bambach, 2006; Sallan and Coates, 2010), the Dasberg event is not recognized as an extinction but is instead characterized by the radiation of an ammonoid suborder (House, 2002). The aryl isoprenoid abundances from these Devonian sediments are up to several orders of magnitude lower than concentrations reported in other euxinic basins through the Phanerozoic (e.g. Cao et al. (2009) reported an aryl isoprenoid abundance of 2723 ppm TOC during the Changhsingian leading into the Permo-Triassic mass extinction event, unquestionably the largest perturbation and ecological turnover in the Phanerozoic).

Discussion and Conclusions

That the black shales deposited in the Appalachian Basin contemporaneously with the UKw bituminous limestones of Europe record oxygen-poor conditions is not contested here; presence of laminated sediments at the Frasnian-Famennian boundary, lack of intensive bioturbation and body fossils, elevated organic carbon content, pyrite formation, and trace metal indicators all point to restricted oxygen during deposition of the Point Gratiot Bed in New York. We find, however, that the intensity and relative duration of anoxia in the Appalachian Basin at the end-Frasnian are neither exceptional for the Phanerozoic nor extreme relative to other contemporaneous basins: sedimentological and geochemical evidence for intermittent oxygenation events, possible dysoxic bottom water conditions, and only sporadic photic zone euxinia point to a basin not characterized by persistent and pervasive anoxia. It is reasonable to question whether the oxygen stress was severe enough to have been the controlling kill mechanism for the coeval biological turnover at the Frasnian-Famennian boundary in the Appalachian Basin, especially given the lack of correlation between the magnitude and extent of anoxia/euxinia and biodiversity crises at other times in the Phanerozoic.

There are at least 20 global occurrences of increased organic carbon burial during the Devonian (House, 2002), in addition to 16 major oceanic anoxic events (OAEs) recorded throughout the Phanerozoic, including notable events in the Mesozoic (Khain and Polyakova, 2010). Only some of these black shale and bituminous limestone depositional events correlate with significant signals of marine extinction (i.e. the Late Devonian, Permo-Triassic, and Triassic-Jurassic extinction events), while many more express sulfur, carbon, and trace metal signals indicating biogeochemical cycles potentially far more perturbing to ecosystems than the chemical signals recorded during the UKw Frasnian-Famennian event. Specifically, the Cretaceous OAEs, with rates of proportional genus loss much lower than the end-Frasnian (Bambach, 2006), display what have been interpreted as pervasive signals of global anoxia and euxinia. Models based on $\delta^{34}S_{CAS}$, however, suggest that these "global signals" correlate to only ~5% of the seafloor being overlain by euxinic bottom waters, challenging the assumption that well-characterized organic carbon burial events are necessarily defined by ubiquitous euxinia (Owens et al., 2013). Additionally, there is evidence for more protracted and more intensely anoxic events in the Appalachian Basin which preceded the deposition of the Point Gratiot Bed, including the Frasnian Rhinestreet Shale, a black shale unit reaching a maximum of over 365 m thickness in New York state (Hill et al., 2002) and the famous Middle Devonian Marcellus oil shale, which displays extreme anoxic and euxinic signals (e.g. Mo values in excess of 100; Werne, 2002; Algeo et al., 2007).

Furthermore, evidence from different basins has provided mixed, often conflicting isotopic records of the UKw event and Frasnian-Famennian extinction. Positive $\delta^{13}C$ excursions at the Frasnian-Famennian boundary have been reported from European sections (McGhee et al., 1986; Buggisch, 1991; Schindler, 1990; Joachimski and Buggisch, 1993; Chen et al., 2005) while negative $\delta^{13}C$ excursions from (presumably) correlative strata have been reported from Canada, France, and China (Geldsetzer et al., 1987; Goodfellow, et al., 1988; Wang, et al., 1991; 1996; Chen et al., 2005). Different studies have suggested both ocean warming (e.g. Thompson and Newton, 1988; Brand, 1989; Becker and House, 1994) and cooling (e.g. Joachimski and Buggisch, 2002; Copper, 1986; van Geldern, et al., 2006) events as perturbation mechanisms based on contrary $\delta^{18}O$ trends. Positive $\delta^{34}S$ signatures have been measured in epeiric basins at the F/F in Canada (Geldsetzer et al., 1987), the Kowala section in Poland (Joachimski, et al., 2001), South China (Chen et al., 2013), the Michigan Basin (Formolo et al., 2014), Great Basin (Sim et al., 2015), but John et al. (2010) submit evidence from $\delta^{34}S_{CAS}$ values that these signals were restricted to low-latitude, basinal settings and not significant for the global marine sulfate reservoir.

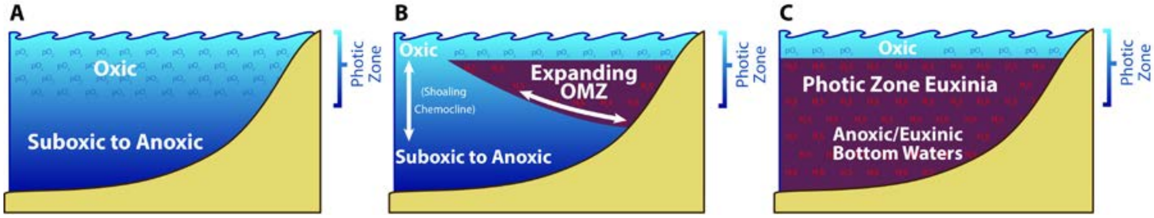

Figure 19. Possible ocean models for ancient epeiric seas. A) Oxic end member: an oxic setting with sub-oxic bottom waters and sulfide productions confined to sedimentary porewaters. B) Expanding OMZ (oxygen minimum zone) model: an expanding and contracting OMZ with highly stratified marine redox column and with only intermittent or seasonal photic zone euxinia (after Murphy et al., 2000a, Marynowksi et al., 2011, and Algeo et al., 2011). C) Anoxic end member: a permanently oxygen stressed setting with a persistent euxinic water column extending up into the photic zone (after Brown and Kenig, 2004 and Melendez et al., 2012).

While very extreme local chemistry has been reported from other Late Devonian basins, the data we present here for the northern Appalachian Basin suggests a non-global signal for widespread and persistent anoxia and euxinia at the Frasnian-Famennian boundary. Similar to the model described by Murphy et al. (2000a) for the deposition of the Geneseo black shale in the Appalachian Basin, the PGB in the same basin was not deposited under a stably stratified water column invoking protracted formation of sulfidic bottom waters (Figure 19). Rather, the UKw-equivalent black shale in the Appalachian Basin was deposited under a complex and variable redox regime, involving suboxic to anoxic conditions and a fluctuating chemocline existing for extended periods below the photic zone (contributing to only intermittent photic zone euxinia, after Marynowski et al., 2011). This study supports on-going research suggesting that organic-rich facies can be deposited under a variety of redox conditions and cautions against extrapolating conditions from a single basin to a global ocean model.

CONCLUSIONS

Summary and Significance

The research detailed herein has provided new and further insight into the environment and ecology of the Late Devonian world, specifically the conditions concurrent to biological upheaval at the Frasnian-Famennian boundary and perturbation associated with the deposition of the Upper Kellwasser black shale. Despite evidence of strongly reducing and toxic environments in multiple epeiric basins at this time, the geochemical and ichnological data presented from the Appalachian Basin show that the onset of anoxia denoted by the organic-rich Upper Kellwasser was not sudden (i.e. representing a dramatic shift from oxic to fully anoxic conditions) but rather gradual, resulting from a series of transgressive events building to increased but variable oxygen stress. The lithology and trace fossil assemblage across the New York localities are consistent with each other and this interpretation of the paleoenvironment preceding the deposition of the Point Gratiot (Upper Kellwasser equivalent) Bed.

Once prevailing conditions of low to no oxygen were established in the bottom waters of the Appalachian Basin, indicated by the beginning of black shale deposition, ichnofabric and sedimentological data suggest that relative oxygen levels fluctuated rapidly; these fluctuations were captured stratigraphically on a cm scale. Trace Mo concentrations and aryl isoprenoid abundances provide supplementary evidence that sulfidic conditions indicative of anoxia were intermittent throughout the water column and transient, perhaps even seasonal, in the photic zone. These data are significant because they supply reasonable doubt that anoxia was the sole and/or most important driving mechanism of increased extinction at the Frasnian/Famennian, at least in the Appalachian Basin. The Appalachian Basin is therefore shown to have a distinct geochemical and sedimentological record of the Upper Kellwasser horizon from those deposited in other low-latitude epicontinental seas; this observation coupled with the data contest the assumption of a global signal of persistent anoxia and euxinia.

Compounding this point is the new lipid biomarker data presented from the high-latitude Madre de Dios Basin. While the Upper Kellwasser black shale in this sub-arctic Gondwanan basin was deposited under a strongly reducing environment, as evidenced by Mo data, we find muted signals for photic zone euxinia similar to those measured in the Appalachian Basin. We posit that seasonal variations in solar insolation tempered the photosynthetic green sulfur bacterial community and its subsequent contribution to organic matter burial; furthermore, the aryl isoprenoid data supporting this interpretation is the first high-latitude record of photic zone euxinia for the Devonian.

The lipid biomarker data from both the Madre de Dios and Appalachian Basins reveal a microbial ecology unique in its signature from other Paleozoic records and certainly from other records of periods of major environmental and biological perturbation. In both basins, regardless of latitudinal differences, the phytoplankton biomass is dominated by a eukaryotic signal, as indicated by anomalously low hopane/sterane ratios. The eukaryotic assemblage in the high-latitude Madre de Dios Basin, in turn, is dominated by C_{28} sterol synthesizing green algae, which is notable for these mid-Paleozoic successions, and sets the Late Devonian apart from the Late Ordovician and End Permian in its extinction-associated biomarker profile.

Further Questions and Future Work

While the relative fluctuations in basin chemistry for the Appalachian Basin have been described, absolute rate of oxygen variability and euxinic poisoning ideally should be established to better constrain the plausible lethality of such conditions on the variety of marine fauna present in the Late Devonian. This will rely on better constraints of sedimentation rate of the Upper Kellwasser and of Devonian faunal oxygen tolerances via modern studies of appropriate analog organisms. Corollary to this, the timing and taxonomic and ecologic selectivity of these diversity crises need to be better characterized. Given the evidence for extreme oxygen stress in some basins, it is probable that anoxia was the main perturbator for some genera, but it is also probable, given the pulsed timing of extinction of disparate clades, that other environmental conditions played an equal or more important role in the extinction of other genera. These possible conditions, some of which were outlined in the Introduction, need to be identified and their relative impacts assessed. Furthermore, the various clades’ extinctions ought to be treated separately with regards to environmental drivers, as some may merely represent extirpation from specific basins. The key to understanding the biological signature of the Late Devonian biocrises may come from recognizing the keystone taxa in an ecosystem and characterizing the restructuring and collapse of the ecosystem in reference to the extinction or extirpation of that taxon.

Proposing alternative extinction mechanisms is not straightforward, and the scope of this dissertation was not to identify new mechanisms but to test the plausibility of permanent and widespread anoxia as the key cause of biological turnover at the Frasnian/Famennian. While I postulate that the oxygen stress and euxinia were not exceptional enough to explain the total manifested diversity loss at the Frasnian/Famennian boundary, these conditions assuredly still played a central role in driving the biotic crises. It is unclear, however, whether it was the accumulative threshold-crossing effect of repeated deoxygenation events that drove ecosystem collapse at varying rates, or whether different clades were affected by different anoxia-associated drivers, like temperature stress. As discussed in the Introduction, myriad explanations have been put forth to explain the rock and fossil record of the Late Devonian, but the complicated pattern will inevitably track back to an integrated series of processes from biological (invasive species dynamics, food web collapse, keystone taxa extinction), chemical (anoxia, euxinia, changing nutrient fluxes, acid dissolution), and physical (warming, habitat loss, stratification) perturbation mechanisms. Further studies combining these disciplines, and especially exploring the causal relationships between various drivers and their respective plausibilities given extinction selectivity data, will help illuminate the yet enigmatic Late Devonian world.

REFERENCES

Alberti, H., 1979. Devonian trilobite biostratigraphy. In: House, M. R., Scrutton, C.T., Bassett, M.G. (Eds.), The Devonian System. Special Papers in Palaeontology 23, 313-324.

Aldridge, R.J., 1988. Extinction and survival in the Conodonta. In Larwood, G.P. (Ed.), Extinction and Survival in the Fossil Record. Systematics Association Special Volume 34, 231-256.

Algeo, T.J., Maynard, J.B., 2004. Trace-element behavior and redox facies in core shales of Upper Pennsylvanian Kansas-type cyclothems. Chemical Geology 206, 289-318.

Algeo, T.J., Lyons, T.W., 2006. Mo-total organic carbon covariation in modern anoxic marine environments: Implications for analysis of paleoredox and paleohydrographic conditions. Paleoceanography 21, PA1016, 1-23.

Algeo, T.J., Ingall, E., 2007. Sedimentary C_{org}:P ratios, paleocean ventilation, and Phanerozoic atmospheric pO_2. Palaeogeography, Palaeoclimatology, Palaeoecology 256, 130-55.

Algeo, T.J., Berner, R.A., Maynard, J.B., Scheckler, S.E., 1995. Late Devonian oceanic anoxic events and biotic crises: “Rooted” in the evolution of vascular land plants. GSA Today 5, 64-66.

Algeo, T.J., Lyons, T.W., Blakey, R.C., Over, D.J., 2007. Hydrographic conditions of the Devono-Carboniferous North American Seaway inferred from sedimentary Mo–TOC relationships. Palaeogeography Palaeoclimatology Palaeoecology 256, 204–230.

Algeo, T.J., Chen, Z.Q., Fraiser, M.L., Twitchett, R.J., 2011. Terrestrial-marine teleconnections in the collapse and rebuilding of Early Triassic marine ecosystems. Palaeogeography, Palaeoclimatology, Palaeoecology 308, 1-11.

Alroy, J., 2008a. Dynamics of origination and extinction in the marine fossil record. Proceedings of the National Academy of Sciences of the United States of America 105, 11536–11542.

Alroy, J., 2008b. Phanerozoic Trends in the Global Diversity of Marine Invertebrates. Science 321, 97-100.

Aquino Neto, F.R., Trigüis, J., Azevedo, D.A., Rodrigues, R., Simoneit, B.R.T., 1992. Organic geochemistry of geographically unrelated tasmanites. Organic Geochemistry 18, 791-803.

Arthur, M.A., Sageman, B.B., 1994. Marine black shales: depositional mechanisms and environments of ancient deposits. Annual Review of Earth and Planetary Sciences 22, 499–551.

Aspila, K.I., Agemian, H.,Chau, A.S.Y., 1976. A Semi-automated Method for the Determination of Inorganic, Organic and Total Phosphate in Sediments. Analyst 101, 187-97.

Averbuch, O., Tribovillard, N., Devleeschouwer, X., Riquier, L., Mistiaen, B., van Vliet-Lanoe, B., 2005. Mountain building-enhanced continental weathering and organic carbon burial as major casues for climatic cooling at the Frasnian-Famennian boundary (c. 376 Ma)? Terra Nova 17, 25-34.

Baird G.C., Brett. C.E., Ver Straeten, C.A., 1999. The first great Devonian flooding episodes in western New York: reexamination of Union Springs, Oatka Creek and Skateateles Formation successions (Latest Eifelian-Lower Givetian) in the Buffalo-Seneca Lake region. New York State Geological Association Field Trip Guide Book 71, 1-444.

Bambach, R.K., Knoll, A.H., Wang, S.C., 2004. Origination, extinction, and mass depletions of marine diversity. Paleobiology 30, 522–542.

Bambach, R.K., 2006. Phanerozoic Biodiversity Mass Extinctions. The Annual Review of Earth and Planetary Science 34, 127-155.

Becker, R.T., 1993. Anoxia, eustatic changes, and Upper Devonian to lowermost Carboniferous global ammonoid diversity. In: House, M.R. (Ed.), The Ammonoidea: Environment, Ecology, and Evolutionary Change. Systematics Association Special Volume 47, 115-163.

Becker, R.T., House, M.R., 1994. Kellwasser events and goniatite successions in the Devonian of the Montagne Noire with comments on possible causations. Courier-Forschung-Institut Senckenberg, 16, 45–77.

Becker, R.T., Feist, R., Flajs, G., House, M.R., Klapper, G., 1989. Frasnian-Famennian extinction events in the Devonian at Coumiac, southern France. Proceedings of the Academy of Sciences. Series 2, Mechanics-physics, chemistry, space sciences, earth sciences 309, 259-266.

Berry, W.B.H., Wilde, P., 1978. Progressive ventilation of the oceans – an explanation for the distribution of the Lower Paleozoic black shales. American Journal of Science 278, 257-275.

Bigey, F.P., 1986. Biogeography of Devonian Bryozoa. In Nielson, C., Larwood, G.P. (Eds.), Bryozoa: Ordovician to Recent. Olsen & Olsen, Fredensborg, Denmark, pp. 9-23.

Bond, D., Wignall, P.B., Racki, G., 2004. Extent and duration of marine anoxia during the Frasnian–Famennian (Late Devonian) mass extinction in Poland, Germany, Austria and France. Geological Magazine 141, 173–193.

Bond, D., Wignall, P.B., 2008. The role of sea-level change and marine anoxia in the Frasnian-Famennian (Late Devonian) mass extinction. Palaeogeography, Palaeoclimatology, Palaeoecology 263, 107-118.

Boucot, A.J., 1975. Evolution and Extinction Rate Controls. Elsevier, Amsterdam.

Boyer, D.L., Droser, M.L., 2009. Palaeoecological patterns within the dysaerobic biofacies: Examples from Devonian black shales of New York state. Palaeogeography, Palaeoclimatology, Palaeoecology 276, 206-216.

Boyer, D.L., Droser, M.L., 2011. A Combined Trace- and Body- Fossil Approach Reveals High-Resolution Record of Oxygen Fluctuations in Devonian Seas. Palaios 26, 500-508.

Boyer, D.L., Owens, J.D., Lyons, T.W., and Droser, M.L., 2011. Joining Forces: Combined biological and geochemical proxies reveal a complex but refined high-resolution palaeo-oxygen history in Devonian epeiric seas. Palaeogeography, Palaeoclimatology, Palaeoecology 308, 134-146.

Boyer, D.L., Haddad, E.E., Seeger, E.S., 2014. The Last Gasp: Trace Fossils Track Deoxygenation Leading into the Frasnian-Famennian Extinction Event. Palaios 29, 646-651.

Brand, U., 1989. Global climatic changes during the Devonian-Mississippian: Stable isotope biogeochemistry of brachiopods. Palaeogeography, Palaeoclimatology, Palaeoecology 75, 311-329.

Brandes, J.A., Devol, A.H., 2002. A global marine-fixed nitrogen isotopic budget: Implications for Holocene nitrogen cycling. Global Biogeochemical Cycles 16, 67-1-67-14.

Brasier, M.D., 1988. Foraminiferal extinction and ecological collapse during global biological events. In: Larwood, G.P. (Ed.), Extinction and Survival in the Fossil Record. Systematics Association Special Volume 34, 37-64.

Brett, C.E., Dick, V.B., Baird, G.C., 1991. Comparative taphonomy and paleoecology of Middle Devonian dark gray and black shale facies from western New York. In: Landing, E., Brett, C.E. (Eds.), Dynamic stratigraphy and depositional environments of the Hamilton Group (Middle Devonian) in New York State, part II. Bulletin, New York State Museum, pp. 5-36.

Briggs, D.E.G, Fortey, R.A., Clarkson, E.N.K., 1988. Extinction and fossil record of the arthropods. In: Larwood, G.P. (Ed.), Extinction and Survival in the Fossil Record. Systematics Association Special Volume 34, 171-209.

Bromley, R.G., 1996. Trace Fossils: Biology, Taphonomy and Applications, second ed. Chapman and Hall, London.

Brown, T.C., Kenig, F., 2004. Water column structure during deposition of Middle Devonian–Lower Mississippian black and green/gray shales of the Illinois and Michigan Basins: a biomarker approach. Palaeogeography, Palaeoclimatology, Palaeoecology 215, 59-85.

Brumsack, H-J., 2006. The trace metal content of recent organic carbon-rich sediments: Implications for Cretaceous black shale formation. Palaeogeography, Palaeoclimatology, Palaeoecology 232, 344-361.

Buggisch, W., 1991. The global Frasnian-Famennian "Kellwasser Event". Geologische Rundschau 80, 49-72.

Calvert, S.E., 2004. Beware intercepts: interpreting compositional ratios in multi-component sediments and sedimentary rocks. Organic Geochemistry 35, 981-987.

Calvert, S.E., Pederson, T.F., 1993. Geochemistry of Recent oxic and anoxic marine sediments: Implications for the geological record. Marine Geology 113, 67-88.

Casier, J.G., Lethiers, F., Claeys, P., 1996. Ostracod evidence for an abrupt mass extinction at the Frasnian/Famennian boundary. C.R. Acad. Sci. Paris. t. série II a 322, 415-422.

Cao, C., Love, G.D., Hays, L.E., Bowring, S.A., Wang, W., Shen, S., Summons, R.E., 2009. Biogeochemical evidence for euxinic oceans and ecological disturbance presaging the end Permian Mass Extinction Event. Earth and Planetary Science Letters 281, 188-201.

Caplan, M.L., Bustin, R.M., 1999. Devonian-Carboniferous Hangenberg mass extinction event, widespread organic-rich mudrock and anoxia: causes and consequences. Palaeogeography, Palaeoclimatology, Palaeoecology 148, 187-207.

Caputo, M.V., 1985. Late Devonian glaciation in South America. Palaeogeography, Palaeoclimatology, Palaeoecology 51, 291-317.

Caputo, M.V., Crowell, J.C., 1985. Migration of glacial centers across Gondwana during the Paleozoic era. Geological Society of America Bulletin 96, 1020-1036.

Chen, D., Qing, H., Li, R., 2005. The Late Devonian Frasnian-Famennian (F/F) biotic crisis: Insights from $\delta^{13}C_{carb}$, $\delta^{13}C_{org}$ and $^{87}Sr/^{86}Sr$ isotopic systematics. Earth and Planetary Science Letters 235, 151-166.

Chen, D., Wang, J., Racki, G., Li, H., Wang, C., Ma, X., Whalen, M.T., 2013. Large sulphur isotopic perturbations and oceanic changes during the Frasnian-Famennian transition of the Late Devonian. Journal of the Geological Society 170, 465-476.

Coplen, T.B., Brand, W.A., Gehre, M., Groning, M., Meijer, H.A.J., Toman, B., Verkouteren, R.M., 2006. New guidelines for delta C-13 measurements. Analytical Chemistry 78, 2439-2441.

Copper, P., 1977. Paleolatitudes in the Devonian of Brazil and the Frasnian-Famennian mass extinction. Palaeogeography, Palaeoclimatology, Palaeoecology 21, 165-207.

Copper, P.,1986. Frasnian/Famennian mass extinction and cold-water oceans. Geology 14, 835-839.

Copper, P., 2002. Reef development at the Frasnian/Famennian mass extinction boundary. Palaeogeography, Palaeoclimatology, Palaeoecology 181, 27-65.

Courtillot, V., Kravchinsky, V.A., Quidelleur, X., Renne, P.R., Gladkochub, D.P., 2010. Preliminary dating of the Viluy traps (Eastern Siberia): Eruption at the time of Late Devonian extinction events? Earth and Planetary Science Letters 300, 239-245.

Cuffey, R.J., McKinney, F.K., 1979. Devonian Bryozoa. In: House, M.R., Scrutton, C.T., Bassett, M.G. (Eds.), The Devonian System. Special Papers in Palaeontology 23, 307-311.

Crusius, J., Calvert, S. E., Pedersen, T., Sage, D., 1996. Rhenium and molybdenum enrichments in sediments as indicators of oxic, suboxic and sulfidic conditions of deposition. Earth and Planetary Science Letters 145, 65-78.

De la Rue, S.R., 2010. Implications for an Anoxia-Related Control on Green Algal Distributions at the Late Devonian Frasnian/Famennian Boundary. Doctoral Dissertation, University of Idaho.

Dennison, R., 1978. Placodermi. In: Schultze, H.P. (Ed.), Handbook of Paleoichthyology, Vol. 2. Gustav Fisher Verlag, Stuttgart.

Dennison, R., 1979. Acanthodii. In: Schultze, H.P. (Ed.), Handbook of Paleoichthyology, Vol. 2. Gustav Fisher Verlag, Stuttgart.

Diaz, R.J., Rosenberg, R., 2008. Spreading Dead Zones and Consequences for Marine Ecosystems. Science 321, 926-929.

Dineley, D.L., 1984. Aspects of a Stratigraphic System: The Devonian. John Wiley, New York.

Doughty, D.M., Hunter, R.C., Summons, R.E., Newman, D.K., 2009. 2-Methylhopanoids are maximally produced in akinetes of Nostoc punctiforme: geobiological implications. Geobiology 7, 524-532.

Droser, M.L., Bottjer, D.J., 1986. A semiquantitative field classification of ichnofabric. Journal of Sedimentary Petrology 56, 558-559.

Droser, M.L., Bottjer, D.J., Sheehan, P.M., McGhee, G.R., Jr., 2000. Decoupling of taxonomic and ecologic severity of Phanerozoic marine mass extinctions. Geology 28, 675–678.

Dumitrescu, M., Brassell, S.C., 2005. Biogeochemical assessment of sources of organic matter and paleoproductivity during the early Aptian Oceanic Anoxic Event at Shatsky Rise, ODP Leg 198. Organic Geochemistry 36, 1002-1022.

Dutta, S., Greenwood, P.F., Brocke, R., Schaefer, R.G., Mann, U., 2006. New insights into the relationship between Tasmanites and tricyclic terpenoids. Organic Geochemistry 37, 117-127.

Fagerstrom, J.A., 1994. The History of Devonian-Carboniferous Reef Communities: Extinctions, Effects, Recovery. Facies 30, 177-192.

Farrimond, P., Talbot, H.M., Watson, D.F., Schulz, L.K., Wilhelms, A., 2004. Methylhopanoids: Molecular indicators of ancient bacteria and a petroleum correlation tool. Geochimica et Cosmochimica Acta 68, 3873–3882.

Fischer, A.G., Arthur, M.A. 1977. Secular variations in the pelagic realm. Society of Economic Paleontologists and Mineralogists Special Publication 25, 19-50.

Foote, M. 1994. Temporal Variation in Extinction Risk and Temporal Scaling of Extinction Metrics. Paleobiology 20, 424-444.

Formolo, M.J., Riedinger, N., Gill, B.C., 2014. Geochemical evidence for euxinia during the Late Devonian extinction events in the Michigan Basin (U.S.A.). Palaeogeography, Palaeoclimatology, Palaeoecology 414, 146-154.

Geldsetzer, H. H. J., Goodfellow, W. D., McLaren, D. J., Orchard, M. J., 1987. Sulfur-isotope anomaly associated with the Frasnian-Famennian extinction, Medicine Lake, Alberta, Canada. Geology 15, 393-396.

Geldsetzer, H.H.J., Goodfellow, W.D., McLaren, D.J., 1993. The Frasnian-Famennian extinction event in a stable cratonic shelf setting: Trout Rivers, Northwest Territories, Canada. Palaeogeography, Palaeoclimatology, Palaeoecology 104, 81-95.

Gereke, M., Schindler, E., 2012. “Time-specific Facies” and biological crises – The Kellwasser Event interval near the Frasnian/Famennian boundary (Late Devonian). Palaeogeography, Palaeoclimatology, Palaeoecology 367-368, 19-29.

Golonka, J., Ross, M.I., Scotese, C.R., 1994. Phanerozoic paleogeographic and paleoclimatic modeling maps. In: Pangea: Global Environments and Resources. (A. F. Embry, B. Beauchamp, D. J. Glass, eds). Canadian Society of Petroleum Geology 17, 1–47.

Goodfellow, W.D., Geldsetzer, H.H.J, McLaren, D.J., Orchard, M.J., Klapper, G., 1988. The Frasnian-Famennian extinction: Current results and possible causes. In: McMillan, N.J., Embry, A.F., Glass, D.J. (Eds.), Devonian of the World. Canadian Society of Petroleum Geologists Memoir 14, 9-21.

Gordon G.W., Lyons, T.W., Arnold, G.L., Roe, J., Sageman, B.B., Anbar, A.D., 2009. When do black shales tell molybdenum isotope tales? Geology 37, 535-538.

Grantham, P.J., Wakefield, L.L., 1988. Variations in the sterane carbon number pattern distributions of marine source rock derived crude oils through geological times. Organic Geochemistry 12, 61-77.

Greenwood, P.F., Arouri, K.R., George, S.C., 2000. Tricyclic terpenoids composition of Tasmanites kerogen as determined by pyrolysis GC-MS. Geochimica et Cosmochimica Acta 64, 1249-1263.

Grice, K., Cao, C, Love, G.D., Böttcher, M.E., Twitchett, R.J., Grosjean, E., Summons, R.E., Turgeon S.C., Dunning W., Jin Y., 2005. Photic zone euxinia during the Permian-Triassic Superanoxic Event. Science 307, 706-709.

Hallam, A., 1989. The case for sea-level change as a dominant causal factor in mass extinction of marine invertebrates. Philosophical Transactions of the Royal Society of London B325, 437-455.

Hallam, A., Miller, A.I., 1988. Extinction and survival in the Bivalvia. In: Larwood, G.P. (Ed.), Extinction and Survival in the Fossil Record, Systematics Association Special Volume 34, 121-138.

Halstead, L.B., 1988. Extinction and survival of the jawless vertebrates, the Agnatha. In: Larwood, G.P. (Ed.), Extinction and Survival in the Fossil Record. Systematics Association Special Volume 34, 257-267.

Harnik, P.G., Lockwood, R., 2011. Part N, Revised, Volume 1, Chapter 24: Extinction in the Marine Bivalvia. Treatise Online 29, 1-24.

Harris, N.B., 2005. The Deposition of Organic-Carbon-Rich Sediments: Models, Mechanisms, and Consequences. The Society for Sedimentary Geology (SEPM) Special Publication 82, 1-5.

Hatch, J.R., Leventhal, J.S., 1992. Relationship between inferred redox potential of the depositional environment and geochemistry of the Upper Pennsylvanian (Missourian) stark shale member of the Dennis Limestone, Wabaunsee County, Kansas, USA. Chemical Geology 99, 65-82.

Higgins, M.B., Robinson, R.S., Carter, S.J., Pearson, A., 2010. Evidence from chlorin nitrogen isotopes for alternating nutrient regimes in the Eastern Mediterranean Sea. Earth and Planetary Science Letters 290, 102-107.

Higgins, M.B., Robinson, R.S., Husson, J.M., Carter, S.J., Pearson, A., 2012. Dominant eukaryotic export production during ocean anoxic events reflects the importance of recycled NH_4^+. Proceedings of the National Academy of Sciences of the United States of America 109, 2269-2274.

Hill, D., 1981. Rugosa and Tabulata. In: Teichert, C. (Ed.), Treatise on Invertebrate Paleontology, Part F, Suppl. 1. Geological Society of America and the University of Kansas Press, Boulder, Colorado, and Lawrence, Kansas pp. 1-762.

Hill, D.G., Lombardi, T.E., Martin, J.P., 2002. Fractured Shale Gas Potential in New York. New York State Energy Research and Development Authority, Project 5012 Report.

Horowitz, A.S., Pachut, J.F., 1993. Specific, generic, and familial diversity of Devonian bryozoans. Journal of Paleontology 67, 42-52.

House, M.R., 1985. Correlation of mid-Palaeozoic ammonoid evolutionary events with global sedimentary perturbations. Nature 313, 17-22.

House, M.R., 2002. Strength, timing, setting and cause of mid-Palaeozoic extinctions. Palaeogeography, Palaeoclimatology, Palaeoecology 181, 5–25.

House, M.R., Kirchgasser, W.T., 1993. Devonian goniatite biostratigraphy and timing of facies movements in the Frasnian of eastern North American. In: Hailwood, E.A., Kidd, R.B. (Eds.), High Resolution Stratigraphy. Geological Society Special Publication 70, 267-292.

Ingall, E., Kolowith, L., Lyons, T., Hurtgen, M., 2005. Sediment carbon, nitrogen and phosphorus cycling in an anoxic fjord, Effingham Inlet British Columbia. American Journal of Science 305, 240-258.

Jablonski, D., 1991. Extinctions: A paleontological perspective. Science 253, 754-757.

Joachimski, M.M., Buggisch, W., 1993. Anoxic events in the late Frasnian: Causes of the Frasnian Famennian faunal crisis? Geology 21, 675–678.

Joachimski, M.M., Buggisch, W., 2002. Conodont apatite del18O signatures indicate climatic cooling as a trigger of the Late Devonian mass extinction. Geology 30, 711-714.

Joachimski, M.M., Ostertag-Henning, C., Pancost, R.D., Strauss, H., Freeman, K.H., Littke, R., Sinninghe Damsté, J.S., Racki, G., 2001. Water column anoxia, enhanced productivity and concomitant changes in δ^{13}C and δ^{34}S across the Frasnian–Famennian boundary (Kowala - Holy Cross Mountains, Poland). Chemical Geology 175, 109-131.

Joachimski, M.M., Pancost, R.D., Freeman, K.H., Ostertag-Hennig, C., Buggisch, W., 2002. Carbon isotope geochemistry of the Frasnian-Famennian transition. Palaeogeography, Palaeoclimatology, Palaeoecology 181, 91-109.

John, E.H., Wignall, P.B., Newton, R.J., Bottrell, S.H., 2010. $\delta^{34}S_{CAS}$ and $\delta^{18}O_{CAS}$ records during the Frasnian-Famennian (Late Devonian) transition and their bearing on mass extinction models. Chemical Geology 275, 221-234.

Johnson, J.G., 1974. Extinction of perched faunas. Geology 2, 479-482.

Johnson, J.G., Klapper, G., Sandberg, C.A., 1985. Devonian eustatic fluctuations in Euramerica. Geological Society of America Bulletin. 96:567-587.

Jones, B., Manning, D.A.C., 1994. Comparison of geochemical indices used for the interpretation of palaeoredox conditions in ancient mudstones. Chemical Geology 111, 111-129.

Kaufmann, B., 2006. Calibrating the Devonian Time Scale: a synthesis of U-Pb ID-TIMS ages and conodont stratigraphy. Earth-Science Reviews 76, 175-190.

Khain, V.E., Polyakova, I.D., 2010. Oceanic Anoxic Events and Global Rhythms of Endogenic Activity during the Phanerozoic History of the Earth. Doklady Earth Sciences 432, 722-725.

Kirchgasser, W.T., Baird, G.C., Brett, C.E., 1988. Regional placement of Middle/Upper Devonian (Givetian–Frasnian) boundary in western New York State, In: McMillan, N.J., Embry, A.F., Glass, D.J. (Eds.), Devonian of the World. Canadian Society of Petroleum Geologists, Memoir 14, pp. 113–117.

Knoll, A.H., Bambach, R.K., Payne, J.L., Pruss, S., Fischer, W.W., 2007. Paleophysiology and end-Permian mass extinction. Earth and Planetary Science Letters 256, 295-313.

Kodner, R.B., Pearson, A., Summons, R.E., Knoll, A.H., 2008. Sterols in red and green algae: quantification, phylogeny, and relevance for the interpretation of geologic steranes. Geobiology 6, 411-420.

Kuypers, M.M.M., Van Breugel, Y., Schouten, S., Erba, E., Sinninghe Damsté, J.S., 2004. N_2-fixing cyanobacteria supplied nutrient N for Cretaceous oceanic anoxic events. Geology 32, 853-856.

LaPorte, D.F., Holmden, C., Patterson, W.P., Loxton, J.D., Melchin, M.J., Mitchell, C.E., Finney, S.C., Sheets, H.D., 2009. Local and global perspectives on carbon and nitrogen cycling during the Hirnantian glaciation. Palaeogeography, Palaeoclimatology, Palaeoecology 276, 182–195.

Lehmann, M.F., Bernasconi, S.M., Barbieri, A., McKenzie, J.A., 2002. Preservation of organic matter and alteration of its carbon and nitrogen isotope composition during simulated and in situ early sedimentary diagenesis. Geochimica et Cosmochimica Acta 66, 3573-3584.

Lenniger, M., Nøhr-Hansen, H., Hills, L.V., Bjerrum, C.J., 2014. Arctic black shale formation during Cretaceous Oceanic Anoxic Event 2. Geology 42, 799-802.

Levman, B.G., Von Bitter, P.H., 2002. The Frasnian–Famennian (mid-Late Devonian) boundary in the type section of the Long Rapids Formation, James Bay Lowlands, northern Ontario, Canada. Canadian Journal of Earth Sciences 39, 1795–1818.

Luo, G., Hallmann, C., Xie, S., Xiaoyan, R., Summons, R.E., 2015. Comparative microbial diversity and redox environments of black shale and stromatolite facies in the Mesoproterozoic Xiamaling Formation. Geochimica et Cosmochimica Acta 151, 150-167.

Lüschen, H., 2004. Vergleichende anorganisch geochemische Untersuchungen an phanerozoischen Corg.-reichen Sedimenten: Ein Beitrag zur Charakterisierung ihrer Fazies. PhD-Thesis, University of Oldenburg, 186 pp and suppl.

Lyons, T.W., Berner, R.A., Anderson, R.F., 1993. Evidence for large pre-industrial perturbations of the Black Sea chemocline. Nature 365, 538-540.

Lyons, T.W., Werne, J.P., Hollander, D.J., Murray, R.W., 2003. Contrasting sulfur geochemistry and Fe/Al and Mo/Al ratios across the last oxic-to-anoxic transition in the Cariaco Basin, Venezuela. Chemical Geology 195, 131-157.

Lyons, T.W., Anbar, A.D., Severmann, S., Scott, C., Gill, B.C., 2009. Tracking Euxinia in the Ancient Ocean: A Multiproxy Perspective and Proterozoic Case Study. Annual Review of Earth and Planetary Sciences 37, 507-534.

Macko, S.A., Entzeroth, L., Parker, P.L., 1984. Regional Differences in Nitrogen and Carbon Isotopes on the Continental-Shelf of The Gulf of Mexico. Naturwissenschaften 71, 374-375.

Marynowski, L., Filipiak, P., 2007. Water column euxinia and wildfire evidence during deposition of the Upper Famennian Hangenberg event horizon from the Holy Cross Mountains (central Poland). Geological Magazine 144, 569-595.

Marynowski, L., Rakociński, M., Zatoń, M., 2007. Middle Famennian (Late Devonian) interval with pyritized fauna from the Holy Cross Mountains (Poland): Organic geochemistry and pyrite framboid diameter study. Geochemical Journal 41, 187-200.

Marynowski, L., Filipiak, P., Zatoń, M., 2010. Geochemical and palynological study of the Upper Famennian Dasberg event horizon from the Holy Cross Mountains (central Poland). Geological Magazine 147, 527-550.

Marynowski, L., Rakociński, M., Borcuch, E., Kremer, B., Schubert, B.A., Jahren, A.H., 2011. Molecular and petrographic indicators of redox conditions and bacterial communities after the F/F mass extinction (Kowala, Holy Cross Mountains, Poland). Palaeogeography, Palaeoclimatology, Palaeoecology 306, 1-14.

Martin, K.D., 2004. A re-evaluation of the relationship between trace fossils and dysoxia, In McIlroy, D. (Ed.), The application of ichnology to palaeoenvironmental and stratigraphic analysis, Geological Society Special Publications, pp. 141-156.

Maslen, E., Grice, K., Gale, J.D., Hallmann, C., Horsfield, B., 2009. Crocetane: A potential marker of photic zone euxinia in thermally mature sediments and crude oils of Devonian age. Organic Geochemistry 40, 1-11.

McGhee, G.R., Jr. 1981. The Frasnian-Famennian extinctions: A search for extraterrestrial causes. Bulletin of the Field Museum of Natural History 52, 3-5.

McGhee, G.R., Jr., 1996. The Late Devonian Mass Extinction: The Frasnian/Famennian Crisis. Columbia University Press, New York.

McGhee, G.R., Jr., Orth, C.J., Quintana, L.R., Gilmore, J.S., Olsen, E.J., 1986. Late Devonian “Kellwasser Event” mass-extinction horizon in Germany: No geochemical evidence for a large-body impact. Geology 14, 776-779.

McGhee, G.R., Jr., Sheehan, P.M., Bottjer, D.J., Droser, M.L., 2004. Ecological ranking of Phanerozoic biodiversity crises: ecological and taxonomic severities are decoupled. Palaeogeography, Palaeoclimatology, Palaeoecology 211, 289-297.

McGhee, G.R., Jr., Clapham, M.E., Sheehan, P.M., Bottjer, D.J., Droser, M.L., 2013. A new ecological-severity ranking of major Phanerozoic biodiversity crises. Palaeogeography, Palaeoclimatology, Palaeoecology 370, 260-270.

McKinney, M.L., 1985. Mass extinction patterns of marine invertebrate groups and some implications for a causal phenomenon. Paleobiology 11, 227-233.

McManus, J., Berelson, W.M., Klinkhammer, G.P., Hammond, D.E., Holm, C., 2005. Authigenic uranium: relationship to oxygen penetration depth and organic carbon rain. Geochimica et Cosmochimica Acta 69, 95–108.

McManus, J., Berelson, W.M., Severmann, S., Poulson, R.L., Hammond, D.E., Klinkhammer, G.P., Holm, C., 2006. Molybdenum and uranium geochemistry in continental margin sediments: Paleoproxy potential. Geochimica et Cosmochimica Acta 70, 4643-4662.

Melendez, I., Grice, K., Trinajstic, K., Ladjavardi, M., Greenwood, P., Thompson, K., 2012. Biomarkers reveal the role of photic zone euxinia in exceptional fossil preservation: An organic geochemical perspective. Geology 41, 123-126.

Melendez, I., Grice, K., Schwark, L., 2013. Exceptional preservation of Palaeozoic steroids in a diagenetic continuum. Scientific Reports 3, 2768.

Meyer, K.M., Kump, L.R., 2008. Oceanic Euxinia in Earth History: Causes and Consequences. Annual Review of Earth and Planetary Sciences 36, 251-288.

Meyers, P.A., 2006. Paleoceanographic and paleoclimatic similarities between Mediterranean sapropels and Cretaceous black shales. Palaeogeography, Palaeoclimatology, Palaeoecology 235, 305-320.

Minagawa, M., Wada, E., 1986. Nitrogen Isotope Ratios of Red Tide Organisms in the East-China-Sea - A Characterization of Biological Nitrogen-Fixation. Marine Chemistry 19, 245-259.

Morford J. L., Emerson S., 1999. The geochemistry of redox sensitive trace metals in sediments. Geochimica et Cosmochimica Acta 63, 1735–1750.

Morford, J.L., Russell, A.D., Emerson, S., 2001. Trace metal evidence for changes in the redox environment assocoated with the transition from terrigenous clay to diatomaceous sediments, Saanich Inlet, BC. Marine Geology 174, 355–369.

Muller, P.J., 1977. C-N Ratios in Pacific Deep-Sea Sediments - Effect of Inorganic Ammonium and Organic Nitrogen-Compounds Sorbed by Clays. Geochimica et Cosmochimica Acta 41, 765-776.

Murphy, A.E., Sageman, B.B., Hollander, D.J., Lyons, T.W., Brett, C.E., 2000a. Black shale deposition and faunal overturn in the Devonian Appalachian basin: clastic starvation, seasonal water-column mixing, and efficient biolimiting nutrient recycling. Paleoceanography 15, 280–291.

Murphy, A.E., Sageman, B.B., Hollander, D.J., 2000b. Eutrophication by decoupling of the marine biogeochemical cycles of C, N, and P: A mechanism for the Late Devonian mass extinction. Geology 28, 427-430.

Nitecki, M.H., 1969. Redescription of *Ischadites koenigii* Murchinson 1839. Fieldiana Geology 16, 241-359.

Nitecki, M.H., Webby, B.D., Spjeldnaes, N., Yong-Yi, Z., 2004. Receptaculitids and algae. In: Webby, B.D., Paris, F., Droser, M.L., Percival, I.G. (Eds.), The Great Ordovician Biodiversification Event. Columbia University Press, New York, pp. 336-347.

Oliver, W.A., Jr., Pedder, A.E.H., 1994. Crises in the Devonian History of the Rugose Corals. Paleobiology 20, 178-190.

Over, D.J., 1997. Conodont biostratigraphy of the Java Formation (Upper Devonian) and the Frasnian–Famennian boundary in western New York State. Geological Society of America Special Paper 321, 161–177.

Over, D.J., 2002. The Frasnian–Famennian boundary in central and eastern United States. Palaeogeography, Palaeoclimatology, Palaeoecology 181, 153–169.

Over, D.J., De la Rue, S., Isaacson, P., Ellwood, B., 2009. Upper Devonian conodonts from black shales of the high latitude Tomachi Formation, Madre de Dios Basin, northern Bolivia. Palaeontographica Americana 62, 89-99.

Over, D.J., Baird, G.C., Kirchgasser, W.T., 2013. Middle-Upper Devonian strata along the Lake Erie Shore, Western New York. New York State Geological Association Field Trip Guidebook, 85th annual meeting, 182–219.

Owens, J.D., Gill, B.C., Jenkyns, H.C., Bates, S.M., Severmann, S., Kuypers, M.M.M., Woodfine, R.G., Lyons, T.W., 2013. Sulfur isotopes track the global extent and dynamics of euxinia during Cretaceous Oceanic Anoxic Event 2. Proceedings of the National Academy of Sciences of the United States of America 110, 18407-18412.

Ozalas, K., Savrda, C.E., Fullerton, R., 1994. Bioturbated oxygenation-event beds in siliceous facies: Monterey Formation (Miocene), California. Palaeogeography, Palaeoclimatology, Palaeoecology 112, 63–83.

Pepper, J.F., De Witt, W., Jr., 1950. Stratigraphy of the Upper Devonian Wiscoy Sandstone and the Equivalent Hanover Shale in Western and Central New York. U.S. Geological Survey Oil and Gas Investigations Chart OC-37, scale 1:253,440, 2 sheets.

Peters, K.E., Sweeney, R.E., Kaplan, I.R., 1978. Correlation of Carbon and Nitrogen Stable Isotope Ratios in Sedimentary Organic-Matter. Limnology and Oceanography 23, 598-604.

Peters, K.E., Wagner, J.B., Carpenter, D.G., Conrad, K.T., 1997a. World class Devonian potential seen in eastern Madre de Dios basin. Part I. Oil & Gas Journal 95, 61-65.

Peters, K.E., Wagner, J.B., Carpenter, D.G., Conrad, K.T., 1997b. World class Devonian potential seen in eastern Madre de Dios basin. Part II. Oil & Gas Journal 95, 84-87.

Peters, K. E., Walters, C.C., Moldowan, J.M., 2005. Petroleum Systems through Time: Devonian Source Rocks. In: Peters, K. E., Walters, C.C., Moldowan, J.M ., (Eds.), The Biomarker Guide: Biomarkers and Isotopes in Petroleum Exploration and Earth History, vol. 2. Cambridge University Press, Cambridge, pp. 794-807.

Prauss, M.L., 2007. Availability of reduced nitrogen chemospecies in photic-zone waters as the ultimate cause for fossil prasinophyte prosperity. Palaios 22, 489-499.

Quan, T.M., Falkowski, P.G., 2009. Redox control of N:P ratios in aquatic ecosystems. Geobiology 7, 124-139.

Quigg, A., Finkel, Z.V., Irwin, A.J., Rosenthal, Y., Ho, T.Y., Reinfelder, J.R., Schofield, O., Morel, F.M.M., Falkowski, P.G., 2003. The evolutionary inheritance of elemental stoichiometry in marine phytoplankton. Nature 425, 291-294.

Racki, G., 1990. Frasnian/Famennian event in the Holy Cross Mts, central Poland: Stratigraphic and ecological aspects. In: Kauffman, E.G., Walliser, O.H. (Eds.), Extinction Events in Earth History. Lecture Notes in Earth Sciences, Vol. 30, Springer-Verlag, Berlin, pp. 169-181.

Rashby, S.E., Sessions, A.L., Summons, R.E., Newman, D.K., 2007. Biosynthesis of 2-methylbacteriohopanepolyols by an anoxygenic phototroph. Proceedings of the National Academy of Sciences of the United States of America 104, 15099-15104.

Rau, G.H., Arthur, M.A., Dean, W.E., 1987. N_{15}/N_{14} Variations In Cretaceous Atlantic Sedimentary Sequences - Implication For Past Changes In Marine Nitrogen Biogeochemistry. Earth and Planetary Science Letters 82, 269-279.

Raup, D.M., Sepkoski, J.J., Jr., 1982. Mass extinctions in the marine fossil record. Science 215, 1501-1503.

Redfield, A.C., Ketchum, B.H., Richards, F.A., 1963. The influence of organisms on the composition of seawater, In: Hill, M.N. (Ed.), The Sea. Interscience Press, New York, pp. 26-77.

Revill, A.T., Volkman, J.K., O'Leary, T., Summons, R.E., Boreham, C.J., Banks, M.R., Denwar, K., 1994. Hydrocarbon biomarkers, thermal maturity, and depositional setting of tasmanite oil shales from Tasmania, Australia. Geochimica et Cosmochimica Acta 58, 3803-3822.

Rhoads, D.C., Morse, J. W., 1971. Evolutionary and ecologic significance of oxygen-deficient marine basins. Lethaia 4, 413-428.

Rigby, J.K., 1979. Patterns in Devonian sponge distribution. In: House, M.R., Scrutton, C.T., Bassett, M.G. (Eds.), The Devonian System. Special Papers in Palaeontology 23, 141-144.

Rimmer, S.M., 2004. Geochemical paleoredox indicators in Devonian-Mississippian black shales, Central Appalachian Basin (USA). Chemical Geology 206, 373-391.

Rivera, K.T., Puckette, J., Quan, T.M., 2015. Evaluation of redox versus thermal maturity controls on $\delta^{15}N$ in organic rich shales: A case study of the Woodford Shale, Anadarko Basin, Oklahoma, USA. Organic Geochemistry 83, 127-139.

Robinson, R.S., Kienast, M., Albuquerque, A.L., Altabet, M., Contreras, S., Holz, R.D., Dubois, N., Francois, R., Galbraith, E., Hsu, T.C., Ivanochko, T., Jaccard, S., Kao, S.J., Kiefer, T., Kienast, S., Lehmann, M.F., Martinez, P., McCarthy, M., Mobius, J., Pedersen, T., Quan, T.M., Ryabenko, E., Schmittner, A., Schneider, R., Schneider-Mor, A., Shigemitsu, M., Sinclair, D., Somes, D., C., Studer, A., Thunell, R., Yang, J.Y., 2012. A review of nitrogen isotopic alteration in marine sediments. Paleoceanography 27, 13.

Rode, A.L., Lieberman, B.S., 2004. Using GIS to unlock the interactions between biogeography, environment, and evolution in Middle and Late Devonian brachiopods and bivalves. Palaeogeography, Palaeoclimatology, Palaeoecology 211, 345-359.

Rode, A.L., Lieberman, B.S., 2005. Using environmental niche modeling to study the Late Devonian biodiversity crisis. In: Over, D.J., Morrow, J.R., Wignall, P.B. (Eds.), Understanding Late Devonian and Permian-Triassic Biotic and Climatic Events: Towards an Integrated Approach, pp. 93-179.

Rodrìguez-Tovar, F.J., Uchman, A., Agustìn, M-A., 2009. Oceanic Anoxic Event at the Cenomanian-Turonian boundary interval (OAE-2): ichnological approach from the Betic Cordillera, southern Spain. Lethaia 42, 407-417.

Rohrssen, M., Love, G., Fisher, W., Finnegan, S., Fike, D.A., 2013. Lipid biomarkers record fundamental changes in microbial community structure of tropical seas during the Late Ordovician Hirnantian Glaciation. Geology 41, 127-130.

Rudnick, R.L., Gao, S., 2003. Composition of the Continental Crust. In: Holland, H.D., Turekian, K.K. (Eds.), Treatise on Geochemistry, Vol. 3., pp.1-64.

Sachs, J.P., Repeta, D.J., 1999. Oligotrophy and nitrogen fixation during eastern Mediterranean sapropel events. Science 286, 2485-2488.

Sageman, B.B., Murphy, A.E., Werne, J.P., ver Straeten, C.A., Hollander, D.J., Lyons, T.W., 2003. A tale of shales: the relative roles of production, decomposition, and dilution in the accumulation of organic-rich strata, Middle-Upper Devonian, Appalachian Basin. Chemical Geology 195, 229-273.

Sallan, L.C., Coates, M.I., 2010. End-Devonian extinction and a bottleneck in the early evolution of modern jawed vertebrates. Proceedings of the National Academy of Sciences of the United States of America 107, 10131-10135.

Savrda, C.E., 1992. Trace fossils and benthic oxygenation, In Maples, C.G., and West, R.R., (Eds.), Trace Fossils: Short Courses in The Paleontological Society, pp. 172-196.

Savrda, C.E., Bottjer, D.J., 1986. Trace fossil model for reconstruction of paleo-oxygenation in bottom waters. Geology 14, 3-6.

Savrda, C.E., Bottjer, D.J., 1987. The exaerobic zone, a new oxygen-deficient marine biofacies. Nature 327, 54-56.

Savrda, C.E., Bottjer, D.J., 1989. Trace fossil model for reconstructing oxygenation histories of ancient marine bottom-waters: application to Upper Cretaceous Niobrara Formation, Colorado. Palaeogeography, Palaeoclimatology, Palaeoecology 74, 49-74.

Schindler, E., 1990. The Late Frasnian (Upper Devonian) Kellwasser Crisis. Lecture Notes in Earth Sciences 30, 151-159.

Schwark, L., Empt, P., 2006. Sterane biomarkers as indicators of Palaeozoic algal evolution. Palaeogeography, Palaeoclimatology, Palaeoecology 240, 225-236.

Scotese, C.R., McKerrow, W.S., 1990. Revised World maps and introduction, In: McKerrow, W.S., Scotese, C.R. (Eds.), Palaeozoic Palaeogeography and Biogeography. Geological Society Memoir 12, pp. 1-21.

Scott, C., Lyons, T.W., Bekker, A., Shen, Y., Poulton, S.W., Chu, X., Anbar, A.D., 2008. Tracing the stepwise oxygenation of the Proterozoic ocean. Nature 452, 456-459.

Scott, C., Lyons, T.W., 2012. Contrasting molybdenum cycling and isotopic properties in euxinic versus non-euxinic sediments and sedimentary rocks: Refining the paleoproxies. Chemical Geology 324–325, 19–27.

Sepkoski, J.J., Jr., 1981. A factor analysis description of the Phanerozoic marine fossil record. Paleobiology 7, 3–53.

Sepkoski, J.J., Jr., 1982. A compendium of fossil marine families. Milwaukee Public Museum Contributions to Biology and Geology 51, 1-125.

Sepkoski, J.J., Jr., 1986. Phanerozoic overview of mass extinctions, In Raup, D.M., and Jablonski, D., (Eds.), Patterns and Processes in the History of Life. Springer-Verlag, Berlin, pp. 277-295.

Shanmugam, G., Spalding, T.D., Rofheart, D.H., 1993. Traction structures in deep-marine bottom-current reworked sands in the Pliocene and Pleistocene, Gulf of Mexico. Geology 21, 929–932.

Sim, M.S., Ono, S., Hurtgen, M.T., 2015. Sulfur isotope evidence for low and fluctuating sulfate levels in the Late Devonian ocean and the potential link with the mass extinction event. Earth and Planetary Science Letters 419, 52-62.

Simoneit, B.R.T., Leif, R.N., 1990. On the Presence of Tricyclic Terpane Hydrocarbons in Permian Tasmanite Algae. Naturwissenschaften 77, 380-383.

Stearn, C.W., 1987. Effect of the Frasnian-Famennian extinction event on the Stromatoporoids. Geology 15, 677-679.

Sterner, R.W., Elser, J.J., 2002, Ecological Stoichiometry. Princeton University Press, Princeton, New Jersey.

Stigall, A.L., 2011. Speciation collapse and invasive species dynamics during the Late Devonian “Mass Extinction”. GSA Today 22, 4-9.

Streel, M., 1986. Miospore contribution to the upper Famennian-Strunian event stratigraphy. Annales de la Société géologique de Belgique 109, 75-92.

Summons, R.E., Powell, T.G., 1986. Chlorobiaceae in Palaeozoic seas- Combined evidence from biological markers, isotopes and geology. Nature 319, 763-765.

Summons, R.E., Powell, T.G., 1987. Identification of aryl isoprenoids in source rocks and crude oils: biological markers for the green sulphur bacteria. Geochimica et Cosmochimica Acta 51, 557–566.

Summons, R.E., Jahnke, L.L., Hope, J.M., Logan, G.A., 1999. 2-Methylhopanoids as biomarkers for cyanobacterial oxygenic photosynthesis. Nature 400, 554-557.

Swezey, C.S., 2002. Regional Stratigraphy and Petroleum Systems of the Appalachian Basin, North America. United States Geological Survey, Geologic Investigations Series, Map I-2768.

Thayer, C.W., 1974. Marine paleoecology in the Upper Devonian of New York. Lethaia 7, 121-155.

Thompson, J.B., Mullins, H.T., Newton, C.R., Vercoutere, T.L., 1985. Alternative biofacies model for dysaerobic communities. Lethaia 18, 167-179.

Thompson, J.B., Newton, C.R., 1988. Late Devonian mass extinction: Episodic climatic cooling or warming? In: McMillan, N.J., Embry, A.F., Glass, D.J. (Eds.), Devonian of the World. Canadian Society of Petroleum Geologists Memoir 14, 29-34.

Toomey, D., Mamet, B.L., 1979. Devonian Protozoa. In: House, M.R., Scrutton, C.T., Bassett, M.G. (Eds.), The Devonian System. Special Papers in Palaeontology 23, 189-192.

Tribovillard, N., Algeo, T.J., Lyons, T., Riboulleau, A., 2006. Trace metals as paleoredox and paleoproductivity proxies: An update. Chemical Geology 232, 12-32.

Tuite, M.L, Jr., Macko, S.A., 2013. Basinward nitrogen limitation demonstrates role of terrestrial nitrogen and redox control of $\delta^{15}N$ in a Late Devonian black shale. Geology 41, 1079-1082.

Turgeon, S., Brumsack, H-J., 2006. Anoxic vs dysoxic events reflected in sediment geochemistry during the Cenomanian–Turonian Boundary Event (Cretaceous) in the Umbria–Marche Basin of central Italy. Chemical Geology 234, 321-339.

Tyson, R.V., 1987. The genesis and palynofacies characteristics of marine petroleum source rocks, In: Brooks, J., and Fleet, A.J., (Eds.), Marine petroleum source rocks. Geological Society of London Special Publication 26, 47–67.

Tyson, R.V., 2005. The “Productivity Versus Preservation” Controversy: Cause, Flaws, and Resolution. The Society for Sedimentary Geology (SEPM) Special Publication 82, 17-33.

Tyson, R.V., Pearson, T.H., 1991. Modern and ancient continental shelf anoxia: an overview, In: Tyson, R.V., Pearson, T.H. (Eds.), Modern and Ancient Continental Shelf Anoxia. Geological Society Special Publication, pp. 1–26.

Van Geldern, R., Joachimski, M.M., Day J., Jansen, U., Alvarez, F., Yolkin, E.A., Ma, X.-P., 2006. Carbon, oxygen and strontium isotope records of Devonian brachiopod shell calcite. Palaeogeography, Palaeoclimatology, Palaeoecology 240, 47-67.

Van Helmond, N.A.G.M., Sluijs, A., Sinninghe Damsté, J.S., Reichart, G.-J., Voigt, S., Erbacher, J., Pross, J., Brinkhuis, H., 2015. Freshwater discharge controlled deposition of Cenomanian-Turonian black shales on the NW European epicontinental shelf (Wunstorf, northern Germany). Climate of the Past 11, 495-508.

Vaquer-Sunyer, R., Duarte, C.M., 2008, Thresholds of hypoxia for marine biodiversity. Proceedings of the National Academy of Sciences of the United States of America 105, 15452-15457.

Vitousek, P.M., Howarth, R.W., 1991. Nitrogen Limitation on Land and in the Sea - How Can it Occur? Biogeochemistry 13, 87-115.

Wang, K., Orth, C.J., Attrep, M., Jr., Chatterton, B.D.E., Hou, H., Geldsetzer, H.H.J., 1991. Geochemical evidence for a catastrophic biotic event at the Frasnian/Famennian boundary in south China. Geology 19, 776-779.

Wang, K., Geldsetzer, H.H.J., Goodfellow, W.D., Krouse, H.R., 1996. Carbon and sulfur isotope anomalies across the Frasnian-Famennian extinction boundary, Alberta, Canada. Geology 24, 187-191.

Wedepohl, K.H., 1971. Environmental influences on the chemical composition of shales and clays. In: Ahrens, L.H., Press, F., Runcorn, S.K., Urey, H.C. (Eds.), Physics and Chemistry of the Earth, vol. 8. Pergamon, Oxford, pp. 305-333.

Wedepohl, K.H., 1991. The composition of the upper earth's crust and the natural cycles of selected metals. Metals in natural raw materials. Natural Resources. In: Merian, E. (Ed.), Metals and Their Compounds in the Environment. VCH, Weinheim, pp. 3-17.

Welander, P.V., Coleman, M.L., Sessions, A.L., Summons, R.E., Newman, D.K., 2010. Identification of a methylase required for 2-methylhopanoid production and implications the interpretation of sedimentary hopanes. Proceedings of the National Academy of Sciences of the United States of America 107, 8537-8542.

Werne, J.P., Sageman, B.B., Lyons, T.W., Hollander, D.J., 2002. An integrated assessment of a "type euxinic" deposit: Evidence for multiple controls on black shale deposition in the Middle Devonian Oatka Creek Formation. American Journal of Science 302, 110-143.

Wetzel, A., Uchmann, A., 1998. Biogenic Sedimentary Structures in Mudstones – an Overview. In: Schieber, J., Zimmerle, W., Sethi, P. (Eds.), Shales and Mudstones I. E. Schweizerbart'sche Verlagsbuchhandlung (Nägele u. Obermiller), Stuttgart, pp. 351-369.

Wignall, P.B., 1994. Black Shales. Oxford Monographs on Geology and Geophysics, 30. Oxford Science Publications, Oxford.

Wilde, P., Berry, W.B.N., 1984. Destabilization of the oceanic density structure and its significance to marine "extinction" events. Palaeogeography, Palaeoclimatology, Palaeoecology 48, 143-162.

Wilde, P., Berry, W.B.N., 1986. The role of oceanographic factors in the generation of global bio-events. In: Walliser, O.H. (Ed.), Global Bio-events. Lecture Notes in Earth Sciences, Vol. 9, Springer-Verlag, Berlin, pp. 75-91.

Woodrow, D.L., Isley, A.M., 1983. Facies, topography, and sedimentary processes in the Catskill Sea (Devonian), New York and Pennsylvania. Geological Society of America Bulletin 4, 459-470.

Zhang, X.N., Sigman, D.M., Morel, F.M.M., Kraepiel, A.M.L., 2014. Nitrogen isotope fractionation by alternative nitrogenases and past ocean anoxia. Proceedings of the National Academy of Sciences of the United States of America 111, 4782-4787.